MECHANISM AND FUNCTION OF THE CYTOPLASMIC SERINE HYDROXYMETHYLTRANSFERASE INTERNAL RIBOSOME ENTRY SITE THAT REGULATES FOLATE-MEDIATED ONE-CARBON METABOLISM

A Dissertation

Presented to the Faculty of the Graduate School

of Cornell University

In Partial Fulfillment of the Requirements for the Degree of

Doctor of Philosophy

by

Jennifer Theresa Fox

August 2009

MECHANISM AND FUNCTION OF THE CYTOPLASMIC SERINE HYDROXYMETHYLTRANSFERASE INTERNAL RIBOSOME ENTRY SITE THAT REGULATES FOLATE-MEDIATED ONE-CARBON METABOLISM

Jennifer Theresa Fox, Ph. D.

Cornell University 2009

Folate-mediated one-carbon metabolism is a network of interdependent pathways in which single carbon units derived from serine or glycine are activated and used for the biosynthesis of purines, thymidylate, and methionine. Folate-mediated one-carbon metabolism plays essential roles in development, DNA replication, the maintenance of genome stability, and gene expression. Consequently, impairments in this network are associated with an increased incidence of neural tube defects, cardiovascular disease, and cancer.

Cytoplasmic serine hydroxymethyltransferase (cSHMT) serves as a source of folate-activated one-carbon units by catalyzing the conversion of serine and tetrahydrofolate (THF) to glycine and 5,10-methyleneTHF, the one-carbon donor in the thymidylate biosynthesis reaction. cSHMT is regulated by several factors at both the transcriptional and translational levels. At the translational level, cSHMT expression is enhanced through an internal ribosome entry site (IRES) located in the 5'untranslated region (UTR) of the transcript.

IRESes are *cis*-acting regulatory elements that permit 5'-cap-independent translation by interacting with IRES *trans*-acting factors (ITAFs) and recruiting the 40S ribosomal subunit. IRESes permit protein synthesis when cap-mediated ribosome scanning is impaired. Although it had previously been reported that the 3'UTR of the

cSHMT transcript and the proteins CUG-Binding Protein 1 (CUGBP1) and heavy chain ferritin (H ferritin) influence the IRES-mediated translation of cSHMT, the mechanism by which they act and the physiological conditions that stimulate cSHMT IRES activity had not been determined. The results of the current studies reveal that by interacting with both the 3'UTR and a novel ITAF heterogeneous nuclear ribonucleoprotein H2 (hnRNP H2), CUGBP1 circularizes the cSHMT transcript, thereby enhancing translation rates. Although H ferritin does not play a direct role in the IRES-mediated translation of cSHMT, it may stimulate IRES activity by facilitating the interaction between CUGBP1 and hnRNP H2. The results of the current studies also reveal that the cSHMT IRES functions to enhance rates of cSHMT protein expression in response to UV-induced cellular stress. Following exposure to UV radiation, CUGBP1, hnRNP H2, and H ferritin protein levels increase in the cytoplasm. This stimulates cSHMT IRES activity, increases cSHMT protein levels, and allows for the production of thymidylate necessary for DNA repair.

BIOGRAPHICAL SKETCH

Jennifer Fox was born to Tom and Donna Fox on June 23, 1982 in Baltimore, Maryland. She was the first of three children. Her sister Christina was born in 1985, and her brother Greg was born in 1988. From 1996-2000 Jennifer attended Notre Dame Preparatory School in Towson, Maryland, and then went to the University of Maryland, Baltimore County (UMBC) to study Biochemistry and Molecular Biology. While an undergraduate, she had the opportunity to conduct research in the Laboratory of Molecular Gerontology at the National Institute on Aging, and to work in the laboratory of Dr. Mordecai Blaustein at the University of Maryland, School of Medicine. Upon receiving her Bachelor's of Science degree from UMBC in 2004, Jennifer entered the Biochemistry, Molecular, and Cell Biology graduate program at Cornell University. She eventually joined the laboratory of Dr. Patrick Stover in the Division of Nutritional Sciences, where she conducted her Ph.D. research on the translational regulation of cytoplasmic serine hydroxymethyltransferase.

ACKNOWLEDGMENTS

I would like to thank my PI, Dr. Patrick Stover; my committee members, Drs. Eric Alani, Volker Vogt, and Tom Fox (no relation); and all the other great scientists I have met over the years whose advice helped shape my research and career-path. I would like to thank my labmates who made each day entertaining, and my friends who were always there for me and who encouraged me to never give up. Lastly, and most importantly, I would like to thank my family, especially my parents. Although you don't understand folate-mediated one-carbon metabolism (or in some cases "biochemistry"), your constant love, support, and sacrifice made all of this work possible. I really appreciate the many calls, e-mails, cards, and care packages you sent during my time in Ithaca. I love you all.

TABLE OF CONTENTS

LIST OF FIGURES

LIST OF TABLES

LIST OF ABBREVIATIONS

AdoHcy: S-adenosylhomocysteine

AdoMet: S-adenosylmethionine

AICARFT: phosphoribosylaminoimidazolecarboxamide formyltransferase

ALL: acute lymphocytic leukemia

AMT: aminomethyltransferase

BiP: immunoglobulin heavy-chain binding protein

cSHMT: cytoplasmic serine hydroxymethyltransferase

CUGBP1: CUG-binding protein 1

DFO: deferoxamine

DHFR: dihydrofolate reductase

DMGDH: dimethylglycine dehydrogenase

dTMP: deoxythymidine monophosphate

dUMP: deoxyuridine monophosphate

eIF: eukaryotic initiation factor

EMSA: electrophoretic mobility shift assay

FDH: 10-formylTHF dehydrogenase

Fluc: Firefly luciferase

FTHFS: 10-formylTHF synthetase

ΔG: Gibb's free energy

GARFT: phosphoribosylglycinamide formyltransferase

GCS: glycine cleavage system

GNMT: glycine N-methyltransferase

H ferritin: heavy chain ferritin

HCV: hepatitis C virus

hnRNP: heterogeneous nuclear ribonucleoprotein

IRES: internal ribosome entry site

ITAF: IRES *trans*-acting factor

K_d: dissociation constant

MCF-7: mammary adenocarcinoma

MFT: methionyl-$tRNA_f^{Met}$ formyltransferase

MS: methionine synthase

MTHFC: 5,10-methenylTHF cyclohydrolase

MTHFD: 5,10-methyleneTHF dehydrogenase

MTHFR: methylene tetrahydrofolate reductase

MTHFS: 5,10-methenylTHF synthetase

NER: nucleotide excision repair

NTD: neural tube defect

ORF: open reading frame

PABP: poly(A) binding protein

PCBP1: poly r(C) binding protein 1

PCNA: proliferating cell nuclear antigen

PLP: pyridoxal phosphate

RevUTR: reverse complement of the cSHMT 5'UTR

Rluc: Renilla luciferase

SDH: sarcosine dehydrogenase

SHMT2: mitochondrial serine hydroxymethyltransferase

SNP: single nucleotide polymorphism

siRNA: small interference RNA

SUMO: small ubiquitin-like modifier

TfR: transferrin receptor

THF: tetrahydrofolate

TS: thymidylate synthase

UTR: untranslated region

WT: wildtype

CHAPTER 1[1]

INTRODUCTION TO FOLATE-MEDIATED ONE-CARBON METABOLISM

Part I: Abstract

Tetrahydrofolate polyglutamates are a family of cofactors that carry and chemically activate one-carbon units for biosynthesis. Tetrahydrofolate-mediated one-carbon metabolism is a metabolic network of interdependent biosynthetic pathways that is compartmentalized in the cytoplasm, mitochondria and nucleus. One-carbon metabolism in the cytoplasm is required for the synthesis of purines and thymidylate and the remethylation of homocysteine to methionine. One-carbon metabolism in the mitochondria is required for the synthesis of formylated methionyl-tRNA, the catabolism of choline, purines, and histidine, and the interconversion of serine and glycine. Mitochondria are also the primary source of one-carbon units for cytoplasmic metabolism. Increasing evidence indicates that folate-dependent *de novo* thymidylate biosynthesis occurs in the nucleus of certain cell types. Disruption of folate-mediated one-carbon metabolism is associated with many pathologies and developmental anomalies, yet the biochemical mechanisms and causal metabolic pathways responsible for the initiation and/or progression of folate-associated pathologies have yet to be established. This review focuses on our current understanding of mammalian folate-mediated one-carbon metabolism, its cellular compartmentation, and knowledge gaps that limit our understanding of one-carbon metabolism and its regulation.

[1] Reprinted from *Vitamins and Hormones, Volume 79*, Jennifer T. Fox and Patrick J. Stover, Chapter 1: Folate-Mediated One-Carbon Metabolism, p. 1-44, Copyright (2008), with permission from Elsevier.

Part II: Overview

The reduced tetrahydrofolates (THF) serve as a family of enzyme cofactors that chemically activate and carry one-carbon units on the N-5 and/or N-10 of THF at the oxidation level of formate (e.g. 10-formylTHF), formaldehyde (e.g. 5,10-methyleneTHF) or methanol (e.g. 5-methylTHF) (1-4). Folate derivatives also contain a covalently-bound polyglutamate peptide of varying length. Serum folates contain a single glutamate residue, whereas intracellular folates contain a polyglutamate peptide usually consisting of 5 to 8 glutamate residues that are polymerized through unusual γ-linked peptide bonds (5,6). The polyglutamate peptide increases the affinity of THF cofactors for folate-dependent enzymes and binding proteins, and prevents their efflux from the cell and intracellular organelles (3). Tetrahydrofolate polyglutamates are coenzymes that donate or accept one-carbon units in a network of reactions known as one-carbon metabolism, which occurs in three specific and isolated cellular compartments: the mitochondria, nucleus and cytoplasm (Figure 1.1) (7-9). The one-carbon forms of THF can be interconverted enzymatically (Figure 1.1), although each cofactor form is specific to a particular biosynthetic pathway. The formyl group of 10-formylTHF is incorporated into the C2 and C8 of the purine ring in the cytoplasm and is used to synthesize formylated methionyl-tRNA in mitochondria (Figure 1.1). The one-carbon moiety of 5,10-methyleneTHF is required to convert uridylate to thymidylate, and the one carbon carried by 5-methylTHF is required to remethylate homocysteine to methionine. The cellular concentration of folate-binding proteins (50 μM) exceeds that of folate derivatives (20-35 μM). Given that the dissociation constant (K_d) of polyglutamated folates for many folate-binding proteins is typically in the 100 nM range, the concentration of free folate in the cell is negligible (3,10,11). This implies that each folate-dependent biosynthetic pathway competes for a limiting pool of folate cofactors (11,12).

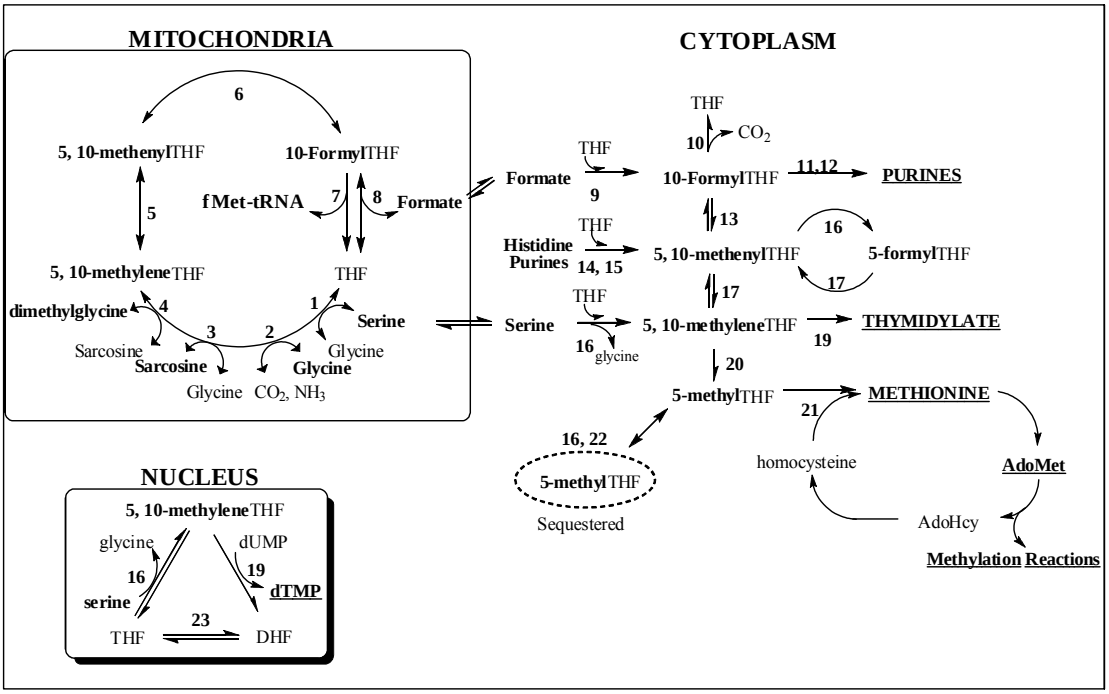

Figure 1.1. Compartmentation of folate-mediated one-carbon metabolism in the cytoplasm, mitochondria and nucleus. One-carbon metabolism in the cytoplasm is required for the de novo synthesis of purines and thymidylate, and for the remethylation of homocysteine to methionine. One-carbon metabolism in mitochondria generates one-carbon units for cytoplasmic one-carbon metabolism by generating formate from serine, glycine, sarcosine and dimethylglycine. One-carbon metabolism in the nucleus synthesizes dTMP from dUMP and serine. 1, Mitochondrial serine hydroxymethyltransferase; 2, Aminomethyltransferase; 3, Sarcosine dehydrogenase; 4, Dimethylglycine dehydrogenase; 5, 5,10-Methylenetetrahydrofolate dehydrogenase (NAD dependent); 6, 5,10-Methenyltetrahydrofolate cyclohydrolase; 7, Methionyl-tRNA formyltransferase; 8, 10-Formyltetrahydrofolate synthetase; 9, 10-Formyltetrahydrofolate synthetase; 10, 10-Formyltetrahydofolate dehydrogenase; 11-12, Phosphoribosylglycinamide formyltransferase & Phosphoribosylaminoimidazolecarboxamide formyltransferase; 13, 5,10-Methenyltetrahydrofolate cyclohydrolase; 14-15, Glycine formiminotransferase/ formimidoyltetrahydrofolate cyclodeaminase & Glutamate formiminotransferase/ formimidoyltetrahydrofolate cyclodeaminase; 16, Cytoplasmic serine hydroxymethyltransferase; 17, Methenyltetrahydrofolate synthetase; 18, 5,10-Methylenetetrahydrofolate dehydrogenase (NADP dependent); 19, Thymidylate synthase; 20, Methylenetetrahydrofolate reductase; 21, Methionine synthase; 22, Glycine N-methyltransferase; 23, Dihydrofolate reductase.

Epidemiological studies implicate impaired folate metabolism in several pathologies and developmental anomalies including neural tube defects (NTDs) (13,14), cardiovascular disease (15-17) and cancer (18-22). One-carbon metabolism can be impaired by folate and other B-vitamin deficiencies and/or common, penetrant genetic mutations and polymorphisms (13,23-25). However, the biochemical mechanisms and causal metabolic pathways responsible for the initiation and/or progression of folate-associated pathologies have yet to be established. In fact, there are still major gaps in our fundamental understanding of one-carbon metabolism and its regulation. There is also the potential for identifying putative "missing" enzymes and their associated genes whose discovery may be necessary to complete the assembly of the folate-dependent metabolic network. This review focuses on our current understanding of mammalian folate-mediated one-carbon metabolism, its cellular compartmentation, and knowledge gaps that limit our understanding of folate metabolism and its regulation.

Part III: Introduction to Cytoplasmic One-Carbon Metabolism

Folate-mediated one-carbon metabolism in the cytoplasm is a metabolic network of interdependent biosynthetic pathways that are required for the biosynthesis of purines and thymidylate, and the remethylation of homocysteine to methionine (Figure 1.1). Methionine can be adenosylated to *S*-adenosylmethionine (AdoMet), a cofactor and methyl group donor for numerous methylation reactions including the methylation of neurotransmitters and other small molecules, phospholipids, proteins including histones, RNA and cytosine bases within CpG islands in DNA. Many AdoMet-dependent methylation reactions, including those involved in chromatin methylation, serve regulatory functions by affecting gene transcription (26), protein localization (27), and the catabolism of small molecules (28). The sources of one-

carbon moieties for cytoplasmic one-carbon metabolism include formate, serine, histidine and purines.

Proteins involved in folate metabolism can be classified into four functional categories, although many folate-dependent enzymes exhibit two or more of these activities: 1) One-carbon generating enzymes, 2) THF one-carbon interconverting enzymes, 3) THF-dependent biosynthetic enzymes and 4) non-catalytic THF binding proteins. This section details the mechanisms, regulation, and physiological functions of the enzymes involved in cytoplasmic one-carbon metabolism, as well as common genetic variants that affect enzyme function and the one-carbon network.

A. Enzymes that Generate One-Carbon Units

1. Cytoplasmic Serine Hydroxymethyltransferase (cSHMT)

Reaction – Serine hydroxymethyltransferase (SHMT) catalyzes the reversible and PLP-dependent interconversion of serine and glycine. Mammals express cytoplasmic (SHMT1 or cSHMT) and mitochondrial (SHMT2) SHMT isozymes; the human isozymes share 63% amino acid sequence identity and are encoded on separate genes (29). When catalyzing serine cleavage, cSHMT transfers the C3 of serine to THF generating glycine and 5,10-methyleneTHF, the cofactor required for thymidylate biosynthesis. The one-carbon moiety of 5,10-methyleneTHF can also support homocysteine remethylation when converted to 5-methylTHF by methylenetetrahydrofolate reductase (MTHFR) (Figure 1.1). cSHMT-derived one-carbons are not believed to make significant contributions to purine biosynthesis, because the reductive environment (NADPH/NADP+ ratio) in the cytoplasm does not support the conversion of 5,10-methyleneTHF to 10-formylTHF (30). When catalyzing serine synthesis, cSHMT depletes methyleneTHF pools for AdoMet

synthesis and regenerates unsubstituted THF for purine biosynthesis (31,32). cSHMT may also play a role in gluconeogenesis; glycine is a glucogenic amino acid through its conversion to serine, although it is not known which SHMT isozyme functions in this capacity (33).

Mechanism - The cSHMT protein is a homotetramer consisting of two obligate dimers. Residues from each subunit of the obligate dimer contribute to the formation of a single active site on each subunit, where Lys257 is covalently bound to the pyridoxal phosphate (PLP) cofactor (34-36). The definitive mechanism for the reaction is still subject to debate (35). The proposed retroaldol cleavage mechanism involves a base-catalyzed proton abstraction from the C3-hydroxyl group of serine to form glycine and a formaldehyde intermediate. The SHMT-bound formaldehyde then condenses with THF to form 5,10-methyleneTHF through an N-5 iminium cation intermediate. However, this mechanism is not consistent with the structure of the *Bacillus stearothermophilus* SHMT (bsSHMT)-serine complex (37) and metabolic labeling experiments (38), both of which indicate that the C3-hydroxyl group of serine is oriented in the synperiplanar configuration rather than the antiperiplanar configuration required for a retroaldol mechanism. In addition, the catalytic base has never been identified. A second putative "direct displacement" mechanism was revealed from the structures of bsSHMT complexed with serine and with 5-formylTHF and glycine (37). This proposed mechanism proceeds with the N5 of THF displacing the C3 hydroxyl of serine to form a covalent intermediate. However, Szebenyi *et al* (39) provide evidence that the reverse reaction could not proceed by direct displacement and that the position of N5 of THF is unfavorable for nucleophilic attack. Rather, they propose a third mechanism whereby the N5 of THF attacks the C3-hydroxy group of serine to form N5-hydroxymethyleneTHF, glycine, and possibly a transient formaldehyde intermediate (35,39).

Regulation – In addition to their primary catalytic function, both SHMT isozymes catalyze the irreversible conversion of 5,10-methenylTHF to 5-formylTHF (Figure 1.1). 5-formylTHF is not a cofactor for folate-dependent one-carbon transfer reactions, but rather is an inhibitor of several folate-dependent reactions including SHMT (40,41). The SHMT isozymes may also play roles as a folate binding proteins (42). Both 5-formylTHF and 5-methylTHF polyglutamates are tight-binding SHMT inhibitors.

Unlike many enzymes involved in cytoplasmic folate-mediated one-carbon metabolism, cSHMT is not ubiquitously expressed in tissues; but it is abundant in the liver, kidney, and colon and is also found in the brain (43). Its expression and/or activity are regulated by several nutrients and metabolic factors including pyridoxal phosphate (vitamin B6), retinoic acid, zinc, and ferritin. Vitamin B6 deficiency was shown to decrease cSHMT activity in rat liver (44) and protein levels in cultured cells (45). Retinoic acid, which inhibits proliferation and induces differentiation during vertebrate development, greatly reduces cSHMT mRNA levels (46). In contrast, zinc induces cSHMT transcription by acting through a metal regulatory element present within the promoter (47). The heavy chain subunit of the iron-storage protein ferritin was also shown to increase cSHMT protein levels (48) by stimulating the cap-independent translation of the transcript (49).

Physiological Function/Gene Variants – Although the cSHMT and SHMT2 isozymes exhibit similar catalytic and physical properties, they have distinct physiological functions. Loss of the mitochondrial SHMT2 isozyme creates a glycine auxotrophy in Chinese hamster ovary cells (50), indicating that cSHMT is not a primary source of glycine and that cSHMT cannot substitute for SHMT2 function. Stable isotope tracer studies using cultured cells indicate that cSHMT-derived 5,10-methyleneTHF is preferentially directed to thymidylate biosynthesis relative to

homocysteine remethylation (31,48). This preferential partitioning of cSHMT-derived one-carbons to thymidylate synthesis may be achieved through the cell cycle-dependent partitioning of the thymidylate synthesis pathway in the nucleus (51) (Figure 1.1) (see Nuclear Folate Metabolism below). The cSHMT protein has also been demonstrated to be a 5-methylTHF tight-binding protein in cultured cells; increased expression of cSHMT increased cellular levels of 5-methylTHF at the expense of other one-carbon forms of folate while depleting AdoMet levels (31). This latter observation is consistent with cSHMT serving as a 5-methylTHF-binding protein in the cytoplasm and thereby limiting the availability of 5-methylTHF for homocysteine remethylation (Figure 1.1) (31).

A common cSHMT single nucleotide polymorphism (SNP), C1420T, has been shown to be protective against adult acute lymphocytic leukemia (ALL) (52) and malignant lymphoma (53). This SNP results in an amino acid substitution of leucine to phenylalanine at position 474 of the protein (L474F) and prevents cSHMT SUMOylation (9). The cSHMT C1420T gene variant has also been shown to be associated with elevated plasma and red cell folate levels (54), and some studies report that it protects against neural tube defects (55,56). When present in combination with the MTHFR C677T polymorphism (see below), cSHMT C1420T is a risk factor for cardiovascular disease (57).

2. 10-FormylTHF Synthetase (FTHFS)

Reaction – 10-formylTHF synthetase is a formate-activating enzyme found in a wide variety of organisms, including bacteria, plants, insects, nematodoes, yeast, and mammals. In eukaryotes, 10-formylTHF synthetase activity is found on the C-terminal domain of the trifunctional enzyme, C_1-THF synthase, which also contains 5,10-methenylTHF cyclohydrolase and 5,10-methyleneTHF dehydrogenase activities

(see Section III.B.1) (58). C_1-THF synthase is encoded by the *Mthfd1* gene. 10-formylTHF synthetase catalyzes the ATP-dependent conversion of THF and formate to 10-formylTHF, ADP, and inorganic phosphate. The reaction is reversible (1). The enzyme requires monovalent cations (NH_4^+, K^+, or Rb^+) to achieve maximal activity; in *Clostridium cylindrosporum* and *Clostridium acidiurici*, these cations serve to maintain the quaternary structure of the enzyme (59) and decrease the K_m of formate by stabilizing its negative charge (60). The enzyme also requires a divalent metal ion, usually Mg^{2+}, which is coordinated between the β- and γ-phosphates of the ATP substrate (61).

Mechanism – The 10-formylTHF synthetase reaction proceeds by a random sequential mechanism, based on results from steady-state kinetic measurements (62) and partial exchange reactions (63). The reaction initiates with the formation of a formylphosphate intermediate generated through a nucleophilic attack by formate on the γ-phosphate of MgATP. The activated formyl group is then transferred directly to N-10 of THF with the loss of phosphate to form 10-formylTHF (64,65). Involvement of the formylphosphate intermediate is supported by the transfer of ^{18}O from formate to inorganic phosphate (66) and the synthesis of ATP from ADP and carbamoyl phosphate, a structural analogue of formylphosphate (67). However, the most conclusive proof comes from experiments that successfully used synthetic formyl phosphate as a substrate for the enzyme (64).

Regulation – To date, there have been few reports regarding the regulation of 10-formylTHF synthetase expression and activity. The enzyme is inhibited by THF and purine nucleotides (68,69). Perry *et al* demonstrated that nitrous oxide-induced vitamin B12 deficiency stimulates 10-formylTHF synthetase activity in rats (70). However, these results were not confirmed by an independent group who showed that nitrous oxide exposure decreased hepatic C1-THF synthase expression (71).

Mammalian *Mthfd1,* which encodes all three activities of cytoplasmic C_1-THF synthase, is expressed ubiquitously and is transcriptionally upregulated in response to conditions that require increased DNA synthesis (30). The promoter region of the rat C_1-THF synthase gene contains several transcription factor binding sites through which this regulation could occur, including NF-κB, HNF-4α1, RARα1, C/EBP, and PPAR. However, the rat promoter region does not share significant homology with the human *Mthfd1* promoter region (58). In mice, the upregulation of C_1-THF synthase expression is thought to occur through insulin-like growth factor-1 (IGF1), which increases the stability of the mRNA transcript (72). In yeast, C_1-THF synthase mRNA levels are decreased in the presence of adenine, histidine, methionine, and pantothenic acid (73).

Physiological Function/Gene Variants –Cytoplasmic 10-formylTHF synthetase activity is believed to be the primary entry point of one-carbons for cytoplasmic folate-dependent biosynthetic reactions. Once formed, 10-formylTHF can be used as cofactor for purine biosynthesis (74), or the one-carbon can be sequentially dehydrated and reduced for use in the biosynthesis of thymidylate and methionine (Figure 1.1). However, studies using *Saccharomyces cervisiae* have raised the possibility that 10-formylTHF synthetase may play other roles in purine biosynthesis in addition to its catalytic activity. Barlowe *et al* (75) observed that yeast lacking the *ADE3* gene that encodes C1-THF synthase are auxotrophic for purines; yeast carrying point mutations in *ADE3* that inactivated all three of its enzymatic activities did not require purines for growth, suggesting that adequate cytoplasmic 10-formylTHF was produced in the absence of 10-formylTHF synthetase activity. In addition, the heterologous expression of *Clostridium acidiurici* 10-formylTHF synthetase in an a*de3* deletion strain did not restore the wildtype phenotype (75). Collectively, these studies indicate that C1-THF synthase possesses other potentially

noncatalytic activities required for pure biosynthesis. However, Song *et al* reported that a monofunctional 10-formylTHF synthetase activity can restore the wildtype phenotype in the *ade3* deletion strain (76), a result consistent with the hypothesis that the catalytic activity of cytoplasmic 10-formylTHF synthetase is involved in purine biosynthesis.

A common SNP in human *Mthfd1*, G1958A, results in the substitution of glutamine for arginine at position 653 which encodes the 10-formyl-THF synthetase domain of C1-THF synthase. The effect of this substitution on the physical or catalytic properties is not known. Although R653Q does not affect homocysteine levels, plasma folate levels or red blood cell folate levels (77), it was found to increase a mother's risk of having a child with a neural tube defect (NTD) in several different populations (77-79). This polymorphism has also been identified as a maternal risk factor for severe placenta abruption and unexplained second trimester loss (80,81).

3. Glutamate Formiminotransferase & Glycine Formiminotransferase

Reaction **–** The catabolism of histidine and purines generates one-carbon units that enter the cytoplasmic folate-activated one-carbon pool as 5,10-methenylTHF (Figure 1.1). During their catabolism, the imidazole ring of histidine, adenine, and guanine is converted to a formimino group, which can be transferred to THF to form 5-formiminoTHF.

Mechanism – In mammalian liver cells, formiminoglutamic acid, an intermediate in histidine catabolism, reacts with THF to form 5-formiminoTHF in a reaction catalyzed by glutamate formiminotransferase (82). Formiminotransferase activity exists as part of a bifunctional enzyme complex with formimidoyltetrahydrofolate cyclodeaminase activity on the C-terminal domain of the protein, which allows for the rapid conversion of 5-formiminoTHF to 5,10-

methenylTHF (83,84). The bifunctional enzyme is assembled as a circular tetramer of dimers and channels folate polyglutamates between catalytic sites (85). Similarly, formiminoglycine, which is a product of purine ring degradation, is also a source of 5-formiminoTHF through the activity of glycine formiminotransferase. As in histidine catabolism, 5-formiminoTHF is converted to 5,10-methenylTHF and is available for one-carbon transfer reactions in the cytoplasm (86).

Regulation – Histidine and purine catabolism occurs in the liver in mammalian cells and can be influenced by vitamin B12 levels, metals, and THF. Vitamin B12 deficiency has been shown to increase the urinary excretion of formiminoglutamate, presumably because unsubstituted THF is not available during severe vitamin B12 deficiency for the formiminotransferase reaction (see Methionine Synthase below). Both glutamate formiminotransferase (87) and glycine formiminotransferase (88) are inhibited by various cations, including Mn^{2+} and Zn^{2+}, and the cyclodeaminase activity of the bifunctional enzyme is inhibited by THF.

Physiological Function/Gene Variants – The quantitative contribution of purine and histidine catabolism to the cytoplasmic folate-activated one-carbon pool is not known. However, severe inborn errors of metabolism are associated with impairments in histidine and purine catabolism. Histidinemia and glutamate formiminotransferase deficiency are autosomal recessive disorders resulting from mutations in the histidase (HAL) and formiminotransferase/cyclodeaminase (FTCD) genes, respectively. Both have been characterized by mental retardation, speech impairment, and developmental delay; severe glutamate formiminotransferase deficiency is also associated with elevated serum folate (89). Three disease-causing mutations that significantly reduce glutamate formiminotransferase activity have also been found (89). The R135C mutation is located within an extended loop of the formiminotransferase domain that is involved in folate-binding; R229P is thought to

disrupt the formiminotransferase dimerization interface. The 1033insG mutation results in the production of a monofunctional enzyme that allows the transfer of the forminimo group to THF, but cannot catalyze the second reaction, the production of 5,10-methenylTHF.

B. Folate Interconverting Enzymes

1. 5,10-MethenylTHF Cyclohydrolase and 5,10-methyleneTHF Dehydrogenase (MTHFC/MTHFD)

Reaction – As mentioned above, mammalian C_1-THF synthase is a homodimer and trifunctional enzyme consisting of two functionally independent domains encoded by *Mthfd1*. The C-terminal domain contains 10-formylTHF synthetase activity whereas the N-terminal domain contains 5,10-methenylTHF cyclohydrolase (MTHFC) and 5,10-methyleneTHF dehydrogenase (MTHFD) activities (90,91). MTHFC catalyzes the reversible interconversion of 10-formylTHF and 5,10-methenylTHF, whereas MTHFD catalyzes the $NADP^+$-dependent and reversible interconversion of 5,10-methenylTHF and 5,10-methyleneTHF.

Mechanism –MTHFC and $NADP^+$-dependent MTHFD share an overlapping active site on C_1-THF synthase, which allows for the interconversion of folate-activated one-carbon units between the formate and formaldehyde levels of oxidation (92,93). There is evidence that the folate substrates are channeled between the MTHFD and MTHFC active sites without dissociating from the complex and equilibrating with the cytoplasmic milieu. Exogenous methenylTHF does not compete as a substrate for the cyclohydrolase reaction with the methenylTHF produced in the dehydrogenase reaction (68,94). Substrate channeling permits increased metabolic rates in the presence of low substrate concentrations, and protects

reaction intermediates from competing reactions or degradation (Reviewed in (95)). Within the bifunctional complex, the reaction catalyzed by 10-methenylTHF cyclohydrolase is rate-limiting in the overall conversion of 10-formylTHF to 5,10-methyleneTHF (96).

Regulation – The regulation of C1-THF synthase is described above for 10-formylTHF synthetase; no specific regulation of the cyclohydrolase or dehydrogenase activities apart from regulation of *Mthfd1* is known.

Physiological Function/Gene Variants – The reversible reactions catalyzed by MTHFC and MTHFD are essential for the provision of folate-activated one-carbons for thymidylate biosynthesis and homocysteine remethylation when the dehydrogenase reaction proceeds in the reductive direction (Figure 1.1). A SNP in *Mthfd1* has been identified that affects the MTHFD/MTHFC domain and has an association with disease. Although its functional significance is currently unknown, R134K was shown to be associated with a significant increase in risk for postmenopausal breast cancer (97).

2. 10-FormyTHF Dehydrogenase (FDH)

Reaction – 10-formylTHF dehydrogenase (FDH) catalyzes the irreversible and $NADP^+$-dependent oxidation of 10-formylTHF to THF and CO_2. FDH consists of two functionally distinct domains connected by an intermediate linker. The C-terminal domain catalyzes an $NADP^+$-dependent aldehyde-dehydrogenase reaction, and the N-terminal domain catalyzes the hydrolysis of 10-formylTHF to THF and formate (hydrolase reaction) (98,99). Although the two domains can function independently, the two active sites work in concert through a 4'-phosphopantetheine swinging arm that is bound through a phosphoester bond to Ser354; the swinging arm transfers formate between the two active sites (98).

Mechanism – The 10-formylTHF dehydrogenase reaction initiates with a hydrolase reaction where a water molecule, activated by aspartate 142, acts as a nucleophile by attacking the formyl carbon atom of 10-formylTHF to produce a hydrated aldehyde intermediate (98,100). In the absence of $NADP^+$, this intermediate can be further cleaved to release formate. In the presence of $NADP^+$, the reaction continues through an aldehyde-dehydrogenase-like mechanism where the formyl group of the intermediate is cleaved with oxidation to CO_2.

Regulation – FDH is one of the most abundant folate enzymes, but is expressed primarily in the liver, kidney and the central nervous system (84). FDH displays product inhibition by THF and also contains a second THF-tight-binding site that is separate from its active site (101). The product inhibition by THF can be suppressed by both cSHMT and C_1-THF synthase (102), presumably by channeling the THF polyglutamate cofactor to these acceptor proteins.

Physiological Function/Gene Variants – It is not known if the individual reactions catalyzed by the N-terminal and C-terminal domains of FDH have any physiological significance. The dehydrogenase reaction, on the other hand, has been proposed to have several important metabolic roles. These include: 1) recycling THF cofactors by removing excess 10-formylTHF, 2) protecting the cell from formate toxicity through its conversion to CO_2, 3) regulation of *de novo* purine biosynthesis, 4) removal of excess one-carbon units from folate metabolism in the form of CO_2 and 5) sequestering and storing cellular folate in the form of THF. These proposed physiological functions were investigated in human neuroblastoma (103) and no evidence was found that FDH sequestered THF, nor that it regulated *de novo* purine biosynthesis. FDH was shown, however, to regulate cellular concentrations of 10-formylTHF and the homocysteine remethylation cycle, presumably by regulating the supply folate-activated one-carbon units.

Two SNPS within the FDH gene have been shown to alter the risk of developing postmenopausal breast cancer. One gene variant [rs2276731 (T/C)] is associated with an increased risk, while the other [rs2002287 (T/C)] is associated with a decreased risk. Both SNPs are located within introns, and therefore they may exist in linkage-disequilibrium with a coding SNP such as V812I, G481S, or F330V (97).

3. 5,10-MethenylTHF Synthetase (MTHFS)

Reaction - 5,10-methenylTHF synthetase (MTHFS, also referred to as 5-formylTHF cyclo-ligase) catalyzes the ATP-dependent and irreversible conversion of 5-formylTHF to 5,10-methenylTHF. It is the only enzyme identified to date that utilizes 5-formylTHF as a substrate. Like 10-formylTHF synthetase, MTHFS activity requires Mg^{2+}, which is involved in the binding of the ATP substrate to the enzyme (104). The MTHFS reaction and the cSHMT-catalyzed synthesis of 5-formylTHF from 5,10-methenylTHF constitute a futile cycle that serves to buffer intracellular 5-formylTHF concentrations (105).

Mechanism - The MTHFS catalyzed reaction occurs via a sequential mechanism with a nucleophilic attack by the 5-formyl oxygen on the γ-phosphate of ATP to form an N5-imminium phosphate intermediate. This intermediate undergoes cyclization via nucleophilic attack by N10 to form a phosphoimidazolidine tetrahedral intermediate, which is the rate-limiting step in catalysis (106,107). The N10 attack on the N5-imminium phosphate is made possible through the hydrophobic and aromatic properties of a conserved active site Tyr. This residue defines the architecture of the MTHFS active site, forming a pocket that restricts the motion of N10 (108). The above steps in the MTHFS mechanism are all reversible. The final step is the irreversible step, in which the phosphoimidazolidine tetrahedral intermediate is broken down through phosphate elimination to generate the 5,10-methenylTHF product (106).

Regulation –In humans, MTHFS is expressed in all tissues, with the highest mRNA levels found in the liver, heart, and kidney, and the lowest levels found in the brain (109). MTHFS enzymatic activity is regulated primarily by folate coenzymes. 5-methylTHF and 10-formylTHF, the latter of which is in chemical equilibrium with the product of the MTHFS reaction, act as tight binding inhibitors of MTHFS (110).

Physiological Function/Gene Variants – To date, two metabolic roles have been ascribed to MTHFS. Anguera *et al* (2003) found that the expression of human MTHFS cDNA in cell culture models led to an increase in the catabolism of monoglutamate forms of folate, indicating that MTHFS may regulate cellular folate concentrations by affecting rates of folate turnover. MTHFS is also thought to regulate *de novo* purine biosynthesis through two distinct mechanisms. First, MTHFS activity reduces levels of 5-formylTHF, an inhibitor of the purine-synthesizing enzyme phosphoribosylaminoimidazolecarboxamide formyltransferase (AICARFT) (111). Second, MTHFS expression enhances purine biosynthesis either by enriching cellular 10-formylTHF pools or by channeling 10-formylTHF to AICARFT and/or phosphoribosylglycinamide formyltransferase (GARFT) (110).

One MTHFS variant allele has been associated with a clinical outcome (112). The MTHFS T202A variant allele was associated with poorer prognosis in individuals with same-stage lung cancer. The functional significance of this polymorphism, as well as its effect on folate levels and purine biosynthesis, has yet to be determined.

4. 5,10-MethyleneTHF Reductase (MTHFR)

Reaction - MethyleneTHF reductase (MTHFR) is a flavoprotein consisting of two identical subunits. The C-terminal domain of each subunit contains the binding site for AdoMet, an allosteric inhibitor; the N-terminal domain catalyzes the NADPH-dependent reduction of 5,10-methyleneTHF to 5-methylTHF for use in the

remethylation of homocysteine to methionine. The MTHFR reaction is virtually irreversible *in vivo* and therefore commits one-carbon units to methionine biosynthesis (1,4).

Mechanism – The reaction catalyzed by MTHFR proceeds by two half reactions. In the reductive half-reaction, the 4S-hydrogen of NADPH is transferred as a hydride to N5 of the FAD cofactor. After $NADP^+$ dissociates from the enzyme, 5,10-methyleneTHF binds. In the oxidative half-reaction, 5,10-methyleneTHF is protonated at the N10 position by a general acid catalyst (113) leading to the opening of the imidazolidine ring and generating the N5-iminium cation intermediate. Transfer of a hydride from N5 of the reduced FAD to C11 of the methylene group results in the production of 5-methylTHF (114).

Regulation – Regulation of MTHFR is critical for AdoMet-dependent methylation reactions and to prevent elevated homocysteine levels in the cell. The complexity of the MTHFR transcript allows for the regulation of its expression at several levels. Exon 1 of MTHFR undergoes extensive alternative splicing, generating transcripts that vary in the length of their 5'UTR (115). The length of the 5'UTR has been shown to influence translational efficiency, as longer, more GC-rich UTRs slow the scanning of the translation initiation machinery (116). Multiple polyadenylation signals result in MTHFR transcripts that vary in the length of their 3'UTR. Additionally, two distinct promoters and translation start sites generate two isoforms of the MTHFR protein. Transcription initiation from the upstream promoter followed by translation from the downstream AUG results in the production of a 70 kDa protein; transcription initiation from the downstream promoter followed by translation from the upstream AUG generates a 77 kDa protein (115). MTHFR expression from the downstream promoter has been shown to be regulated by NF-κB in a tissue-specific manner (117). At the protein level, MTHFR activity is regulated by the

AdoMet/AdoHcy ratio in the cell (118). AdoMet preferentially binds to MTHFR in the inactive T state and thus increases the T/R ratio in the cell (119). Although AdoHcy does not itself alter MTHFR enzymatic activity, it can reverse the inhibitory effect of AdoMet by competing for its binding site (118). Recently, phosphorylation of the MTHFR N-terminal domain at Thr34 was shown to reduce the inhibition of enzymatic activity by AdoMet by altering the equilibrium between the T and R states of the protein so that it favors the active R state (120). NADPH, the reducing equivalent in the MTHFR reaction, binds to R subunits, and thus acts as an AdoMet antagonist (119).

Physiological Function/Gene Variants – MTHFR serves as the link between nucleotide biosynthesis and AdoMet-dependent methylation reactions. Its activity depletes one-carbon units that can be used for DNA synthesis and increases the concentration of one-carbon units available for the remethylation of homocysteine to methionine and for the subsequent production of AdoMet. Thus, although MTFHR is expressed ubiquitously, its mRNA levels are the highest in the testis, where DNA methylation is critical for germ cell maturation and genomic imprinting (121). Mild MTHFR deficiency, as characterized by an enzyme with 35-45% residual activity, is the most common inborn error of folate metabolism, affecting 5-20% of North Americans and Europeans (122). The primary cause is a common C to T substitution at nucleotide 677, which results in the amino acid change A222V in the catalytic domain of the protein (123). The C677T SNP does not affect the kinetic properties of MTHFR, but rather enhances the loss of the FAD cofactor by displacing helix α5 (122,124,125). This creates a thermolabile protein (126). Mild MTHFR deficiency is associated with mild hyperhomocysteinemia, especially in those with low folate concentrations (127), and decreased plasma and red cell folate levels (128,129). Clinically, C677T has been shown, in some cases, to be associated with an increased

risk for cardiovascular disease (130-132), neural tube defects (133-135), cleft lip and palate (136,137), thrombosis (138-140) and schizophrenia (141-144). It has also been shown to be protective against several types of cancers, including ALL (145), childhood acute leukemia (146), and colorectal cancer (147,148).

Another common MTHFR SNP, A1298C (E429A), exists in strong linkage disequilibrium with C677T (149). Unlike C677T which is located in the N-terminal domain of the protein, A1298C affects the regulatory (C-terminal) domain of the protein and is therefore catalytically indistinguishable from the wild-type enzyme (125). Individuals with the A1298C polymorphism exhibit increased red cell folate levels, but have no significant change in vitamin B12, plasma folate, or homocysteine levels (129). Clinically, the polymorphism was shown to be associated with a decreased risk for ALL (145) and childhood acute leukemia (146).

C. Biosynthetic Enzymes

1. Phosphoribosylglycinamide Formyltransferase (GARFT) and Phosphoribosylaminoimidazolecarboxamide Formyltransferase (AICARFT)

Reaction – De novo purine biosynthesis is a ten-step reaction whereby 5-phosphoribosylpyrophosphate (PRPP) is converted to inosine monophosphate (IMP), the precursor of adenine and guanine nucleotides. Of the ten steps involved in *de novo* purine biosynthesis, two are catalyzed by folate-dependent enzymes. In the third reaction, phosphoribosylglycinamide formyltransferase (GARFT) transfers the formyl group of 10-formylTHF to glycinamide ribotide (GAR) to form formylglycinamide ribonucleotide (FGAR) and THF. In the ninth reaction, phosphoribosylaminoimidazolecarboxamide formyltransferase (AICARFT) transfers the formyl group of 10-formylTHF to aminoimidazolecarboxomide ribotide (AICAR)

to form formylaminoimidazolecarboxomide ribonucleotide (FAICAR) and THF. In eukaryotic cells, GARFT and AICARFT activities are part of multi-functional enzymes. GARFT activity comprises the C-terminal domain of a protein that also contains the active sites of GAR synthetase (GARS) and aminoimidazole ribotide synthetase (AIRS) (150,151), and AICARFT resides on the same polypeptide as IMP cyclohydrolase. Substrate channeling among GARFT, GARS, and AIRS drives the AICARFT reaction forward by coupling the energetically unfavorable production of FAICAR to the highly favorable cyclohydrolase reaction (152).

Mechanism – Despite performing similar reactions, GARFT and AICARFT act through distinct mechanisms. The reaction catalyzed by GARFT occurs by an ordered sequential mechanism (153), with 10-formylTHF binding to the active site first through interactions with His108 and Asn106. His108, which has a high the pK_a due to the formation of a salt bridge with Asp144, aids in the nucleophilic attack of GAR on 10-formylTHF by withdrawing electrons from the formyl group of the cofactor. A water molecule hydrogen bonded to Asp144 then catalyzes the transfer of a proton from the amino group of GAR to the N10 of THF (154,155).

Unlike GAR, AICAR contains a relatively non-nucleophilic C5 amine that must first be activated in order for the formylation reaction to occur (152,156,157). In one proposed mechanism, activation of the C5 amine results from Phe542 orienting the AICAR carboxamide upward and out of the imidazole ring plane, allowing the carboxamide to hydrogen bond to the C5 amino group and thus increases the nucleophilicity of the amine. Proton abstraction from the amino group via His268 then occurs concomitant with the nucleophilic attack of this group on 10-formylTHF. The transition state of this reaction is thought to be stabilized by Lys267, a residue that may also play a role in the subsequent protonation of THF (158). These findings are in partial disagreement with earlier proposed mechanisms (159).

Regulation – To date, little is known about the tissue specific or genetic regulation of GARFT and AICARFT expression. The putative promoter region of the gene encoding GARFT was found to have four SP1 sites, but the importance of these sites in transcriptional control has yet to be determined. GARFT is developmentally regulated in the human cerebellum, with high expression found during prenatal development, and no expression detected in that tissue shortly after birth (160).

Physiological Function – GARFT and AICARFT play a key role in *de novo* nucleotide biosynthesis by catalyzing the incorporation of formate into the C8 and C2 positions of the purine ring, respectively. Once formed, purine nucleotides function as precursors for DNA, RNA, coenzymes, energy transfer molecules, and regulatory factors. Although the salvage pathway is thought to be the major source of purines in differentiated mammalian cells (161), the *de novo* pathway was found to supply most of the adenine and guanine nucleotides during human embryonic development (160).

Compared to normal cells, cancer cells have an increased dependence on *de novo* purine biosynthesis for adenine and guanine nucleotides. Thus, both GARFT and AICARFT are chemotherapeutic targets. 6-*R*-dideazatetrahydrofolate (DDATHF, Lometrexol) is an antifolate that specifically targets GARFT. In contrast to the natural substrate of the enzyme, DDATHF contains carbon atoms at positions 5 and 10 which render it unable to serve as a substrate (162,163). The antimetabolate methotrexate (4-amino-10-methylpteroyglutamic acid) inactivates several folate-dependent enzymes, including both GARFT and AICARFT, by depleting 10-formylTHF (164). Inhibition of AICARFT by methotrexate and dihydrofolate polyglutamates results in an anti-inflammatory response (165-167). A common SNP in the AICARFT gene, C347G (Thr116Ser), is associated with a better therapeutic response to methotrexate in patients with rheumatoid arthritis, although the mechanism by which the polymorphism influences drug efficacy remains unknown (168).

Another AICARFT gene variant, A1277G (K426R), completely abolishes AICARFT enzymatic activity, presumably by disrupting the binding of a potassium ion that plays a key role in tertiary structure stabilization. To date, this mutation has only been identified in one allele of a 4-year old girl who presented with profound mental retardation, epilepsy, dysmorphic features, and congenital blindness. Her other allele showed a frameshift in exon 2 due a duplication/deletion event (125-129dup GGGAT; 130-132 delGCT) that resulted in mRNA instability (169).

2. Thymidylate Synthase

Reaction – Thymidylate synthase (TS) catalyzes the 5,10-methyleneTHF-dependent conversion of deoxyuridine monophosphate (dUMP) to the DNA precursor deoxythymidine monophosphate (dTMP). This is the only folate-dependent reaction whereby the folate cofactor serves both as a one-carbon donor and source of reducing equivalents. When 5,10-methyleneTHF is limiting in the cell, TS must compete with MTHFR for this cofactor. Thus, in addition to its role in DNA synthesis, TS expression may also indirectly influence homocysteine levels (170).

Mechanism –The TS reaction initiates with the opening of the imidazole ring and activation of the methyleneTHF cofactor to the reactive 5-iminium cation. Ring opening is facilitated through either the TS-assisted protonation of N10, a protonated water molecule that acts as a general acid catalyst, or the formation of a hydrogen bond between N10 and an active site residue such as Glu60. dUMP must also be activated by the thiol group of Cys198, which either directly attacks C6 of the substrate to produce a nucleophilic enolate, or transfers a hydrogen to a water molecule that acts as a base. The enolate then attacks C6 of the iminium cation to form a ternary covalent intermediate complex. Tyr146-assisted deprotonation of C5 (171) followed by the elimination of THF from this complex results in an exocyclic

methylene intermediate. Hydride transfer from THF to this intermediate yields the products dTMP and dihydrofolate (172).

Regulation – TS is a housekeeping gene but its expression is increased markedly in dividing cells. (173,174). Although protein and mRNA levels increase as cells progress from the G_1 to the S phase of the cell cycle, TS gene transcription remains constant, suggesting that regulation occurs primarily at the post-transcriptional level (175-177). The cell cycle-directed regulation of TS is thought to be controlled by a spliceable intron located downstream of the transcription start site (178,179) and several transcriptional control elements in the promoter region (180). The transcription factor GABP, acting synergistically with Sp1, stimulates TS promoter activity by binding to the Ets site (181). The mouse LSF element has been shown to be necessary for the S phase-specific expression of the gene in growth-stimulated cells (182). In the G_0 and G_1 stages, E2F interacts with the retinoblastoma tumor suppressor, histone deacetylase, and SWI/SF chromatin remodeling proteins, forming a repressor complex that inhibits the enzyme's transcription (183). This inhibition can be overcome by the ectopic expression of E2F (184).

In addition to regulation by various promoter elements, TS expression can also be controlled through polyadenylation, site-specific cleavage, and translational repression. TS contains two polyadenylation signals which affect the length of the 3'UTR and thus have an impact on mRNA stability (185). A naturally occurring antisense RNA (rTSα) produced from a gene (rTS) that overlaps with the 3'end of the TS gene down-regulates TS expression by inducing the site-specific cleavage of TS RNA (186). In the absence of bound folate cofactors, TS can also bind to its own mRNA and repress its translation (187).

Physiological Function/Gene Variants - The reaction catalyzed by TS is the only source of *de novo* dTMP synthesis, making TS indispensable for DNA

replication and repair. Impairments in TS enzymatic activity, whether due to polymorphisms or pharmacological agents, are associated with decreased DNA synthesis, increased uracil misincorporation into DNA, chromosome damage, fragile site induction, and apoptotic cell death (188).

Because of its importance in DNA synthesis, TS is the target of several anti-neoplastic agents including the fluoropyrimidines 5-fluorouracil (5-FU) and 5-fluoro-2-deoxyuridine (FdUrd), and the anti-folates ralitrexed, premetrexed, and methotrexate. These chemotherapeutic drugs generate metabolites that inhibit TS enzymatic activity and have been effective in the treatment of head, neck, breast, stomach, and colon cancers (189). Although these agents decrease TS catalytic function, they also increase its intracellular concentration (190,191) either by inhibiting the binding of TS to its mRNA or by decreasing the rate of ubiquitin-independent enzyme degradation (192,193). This phenomenon is thought to lead to cellular resistance and decreased drug efficacy.

Within the 5'UTR of TS, there is a common 28-nucleotide G/C-rich tandem repeat polymorphism that is thought to influence a patient's response to TS-based chemotherapy. The number of these repeats can vary, with the most common number being two (2R) or three (3R). These repeat regions contain USF-1 transcription factor-binding sites (194) and act as TS promoter enhancers; they also serve to increase its translation. Thus, individuals with the 2R/2R genotype produce significantly less TS protein than those with the 3R/3R genotype (195,196) and show a better response to fluoropyrimidine and mexotrexate therapy. However, they also suffer increased toxicity due to cytotoxic damage to normal tissues (197,198). Within the second repeat of the 3R allele and the first repeat of the 2R allele, there is a G→C polymorphism that results in a reduction in TS expression, presumably due to the disruption of a USF-1 binding site (194,199,200).

Another TS gene variant results from a 6 base pair insertion/deletion in the 3'UTR of the transcript (201). This deletion affects mRNA stability and translation (186), and results in the reduction of TS expression (202). It also leads to an increase in red blood cell folate concentrations and a decrease in homocysteine levels (203). The homozygous insertion genotype has been found to be associated with an increased risk for spina bifida, especially when present in combination with the 2R/2R genotype (204).

3. Methionine Synthase (MS)

Reaction – Methionine Synthase (MS) is a cobalamin (vitamin B12)-dependent enzyme that, in mammalian tissue, functions within the transmethylation cycle by catalyzing the 5-methylTHF-dependent remethylation of homocysteine to methionine. The MS catalyzed reaction occurs via three separate methyl transfer reactions that take place in different binding domains of the four functional modules that comprise MS. The N-terminal module utilizes a $(Cys)_3Zn^{+2}$ cluster to bind homocysteine. A second module binds and activates 5-methylTHF for methyl transfer. A third module binds cobalamin. The C-terminal module binds *S*-adenosylmethionine (AdoMet) and is required for reductive reactivation of the cobalamin cofactor (205-208). Each methyl transfer requires a different arrangement of modules which is made possible by the interdomain connectors of the enzyme (209).

Mechanism – The catalytic mechanism initiates with the methylation of cob(I)alamin by 5-methylTHF to form an enzyme-bound methylcob(III)alamin intermediate and THF. Methyl transfer from methylcob(III)alamin to homocysteine produces methionine and regenerates cob(I)alamin for use in subsequent methylation cycles (210). Cob(I)alamin and methylcob(III)alamin are susceptible to oxidation and photolysis, respectively, resulting in the occasional formation of a cob(II)alamin

species that inactivates the enzyme. Mammalian MS is reactivated through reducing equivalents that are generated by methionine synthase reductase, a P_{450}-reductase like protein that binds NADPH, FAD, and FMN (211).

Regulation – MS expression is regulated by several factors, including vitamin B12, *cis*-acting elements located within its mRNA and nitrous oxide. Vitamin B12 was found to stimulate MS translation by interacting (via an auxiliary protein) with an Internal Ribosome Entry Site (IRES) located within the 5'UTR of the transcript (212). The 5' leader sequence of human MS mRNA also contains two upstream open reading frames that recruit the 40S ribosomal subunit and cause it to stall on the UTR, thus inhibiting the translation of MS (213).

Loss of vitamin B12, due to nutritional deficiency or nitrous oxide exposure, inhibits nucleotide biosynthesis because of the accumulation of cytoplasmic folate cofactors as 5-methylTHF. The effect of vitamin B12 deficiency on 5-methylTHF accumulation is referred to as "methyl trap" (214,215). 5-methylTHF accumulates because the MTHFR reaction is irreversible *in vivo*, and MS is the only 5-methylTHF utilizing enzyme. When cellular vitamin B12 levels are adequate, the regulation of MTHFR by AdoMet protects against a methyl trap by inhibiting the 5-methylTHF synthesis and preventing the depletion of 5,10-methyleneTHF pools required for thymidylate biosynthesis. The feedback inhibition of AdoMet also ensures that, during times when methionine is abundant, one carbon units are spared for the synthesis of DNA precursors (118).

Physiological Function/Gene Variants – MS serves three important physiological functions: 1) the regeneration the THF cofactor, 2) the synthesis of the essential amino acid methionine and 3) the removal of cellular homocysteine, which is a risk factor for cardiovascular disease (216), neural tube defects (136), and Alzheimer's disease (217). MS is an essential enzyme as evidenced by the embryonic

lethality of the MS knockout mouse (218). Although betaine homocysteine methyltransferase (BHMT) can also remethylate homocysteine to form methionine, its expression is limited primarily to the liver and kidney, whereas MS displays ubiquitous expression (219).

Rare mutations in the MS gene, such as P1173L, result in an autosomal recessive disease that is associated with homocysteinemia, homocysteinuria, hypomethioninemia, megaloblastic anemia, neural dysfunction, and mental retardation (220). More subtle clinical outcomes are associated with the common polymorphic variant, A2756G, which affects the domain involved in methylation and reactivation of the B12 cofactor (221) and results in decreased plasma homocysteine levels (222). A2756G was found to be positively associated with aberrant methylation in patients with colorectal, breast, or lung tumors (223) and has been implicated as a risk factor for systemic lupus erythematosus (224), bipolar disorder, schizophrenia (225), and for having a child with spina bifida (226), oralfacial clefts (227), and Down Syndrome (228).

D. Folate Binding Proteins

1. Glycine N-Methyltransferase (GNMT) - GNMT is a relatively abundant methytransferase that catalyzes the AdoMet-dependent methylation of glycine to sarcosine. Its metabolic role is to govern transmethylation reactions by regulating and buffering the AdoMet/AdoHyc ratio. GNMT activity is allosterically regulated by 5-methylTHF, which is a tight-binding inhibitor of GNMT. Under conditions of adequate AdoMet concentrations, AdoMet inhibits MTHFR and limits 5-methylTHF synthesis to decrease rates of methionine synthesis. GNMT remains active under these conditions and metabolizes excess AdoMet. In contrast, when AdoMet levels

are low, the production of 5-methylTHF by MTHFR inhibits GNMT activity and conserves the limited amount of methionine for essential methylation reactions (8).

Part IV: Introduction to Mitochondrial One-Carbon Metabolism

Relatively little is known about one-carbon metabolism in the mitochondria compared to one-carbon metabolism in the cytoplasm, and virtually nothing is known about its regulation. Interestingly, many of the enzyme activities associated with the interconversion of THF-activated one-carbons in the cytoplasm are also found in the mitochondrial compartment. However, unlike the cytoplasm, the interconversion of one-carbon substituted folates in mitochondria is driven in the oxidative direction towards formate production and/or differs with respect to the source of reducing equivalents (1,30). Approximately 40% of total cellular folate polyglutamates are present in mitochondria as a stable pool that does not exchange with the cytoplasmic compartment (229,230). The primary functions of mitochondrial one-carbon metabolism are: 1) to generate one-carbon units in the form of formate for cytoplasmic one-carbon metabolism, 2) to generate the amino acid glycine, and 3) to synthesize formylmethionyl-tRNA for protein synthesis. Communication between mitochondrial and cytoplasmic folate metabolism is facilitated through the exchange of one-carbon donor substrates including serine, glycine and formate (1).

The essentiality of mitochondrial folate metabolism for glycine synthesis was revealed when complementation groups of glycine auxotrophs were isolated from mutagenic screens of Chinese Hamster Ovary Cells (CHO). Cell lines were identified with mutations in the genes that encode the mitochondrial folate-dependent proteins SHMT2 (*glyA*) (231) and the mitochondrial folate transporter (*glyB*) (232). Other studies have demonstrated that mitochondria effectively convert serine to glycine and formate; isolated mitochondria from rats are capable of synthesizing formate from

serine (71,233). However, the definitive pathway for mitochondrial synthesis of formate from serine has yet to be established (30), and not all of the enzymes required for this pathway have been identified.

A. Enzymes that Generate One-Carbon Units

1. Mitochondrial Serine Hydroxymethyltransferase (SHMT2)

Serine is a primary source of one-carbon units carried by THF for folate-dependent biosynthetic reactions in humans (234). The metabolism of serine to formate and glycine in mitochondria is initiated by the pyridoxal-phosphate-dependent mitochondrial isozyme of serine hydroxymethyltransferase (SHMT2). Although the cytoplasmic and mitochondrial isozymes share similar physical and catalytic properties, their physiological functions appear to be distinct. As mentioned previously, CHO cells lacking SHMT2 are autotrophic for glycine; the C3 of serine is also a primary source of one-carbon units for cytoplasmic one-carbon metabolism in human MCF-7 cells (31,231). SHMT2 may also function in the conversion of glycine to serine during gluconeogenesis (30,33).

Little is known about the regulation of SHMT2 expression and activity. Unlike the cytoplasmic cSHMT isozyme, SHMT2 is ubiquitously expressed in human tissues (2). Its activity is sensitive to pyridoxal-phosphate levels (44,103). SHMT2 transcription is *myc* responsive consistent with its role in generating one-carbons for cytoplasmic metabolism; expression of the SHMT2 cDNA in c-myc-null cells partially complements growth inhibition associated with loss of myc expression (235).

2. Glycine Cleavage System, Aminomethyltransferase (GCS, AMT)

The glycine cleavage system is a multienzyme complex that catalyzes the reversible oxidation of glycine to CO_2, ammonia and 5,10-methyleneTHF (236). The complex consists of 4 proteins: 1) the P-protein, which catalyzes the pyridoxal-phosphate-dependent decarboxylation of glycine, 2) the H-protein, a lipoic acid-requiring hydrogen carrier, 3) the T-protein which is a THF-dependent aminomethyltransferase (AMT) and 4) the L-protein, a lipoamide dehydrogenase. The complex is located in the inner mitochondrial membrane and expressed in the liver, kidney, the glia-astrocyte lineage of the brain and the neuroepithelium during development (237). Recent stable isotope tracer studies in human subjects demonstrate that GCS accounts for nearly 40% of overall glycine flux and that the 5,10-methyleneTHF produced from glycine catabolism makes major contributions to cytoplasmic THF-dependent purine and thymidylate biosynthesis (238)

Little is known regarding the regulation of GCS, but it has been shown to be essential for normal embryonic development. Nonketotic hyperglycinemia (NKH) is an autosomal recessive inborn error of metabolism whose clinical manifestations include severe mental retardation, seizures, apnea, and hypotonia and result from the accumulation of glycine in all tissues including the central nervous system. NKH is usually associated with mutations in the P-protein or T-protein (239).

3. Dimethylglycine Dehydrogenase (DMGDH) and Sarcosine Dehydrogenase (SDH)

The oxidative catabolism of choline occurs through the sequential conversion of choline → betaine → dimethylglycine → sarcosine → glycine; dimethylglycine and sarcosine catabolism occurs in liver mitochondria matrix through the activity of dimethylglycine dehydrogenase (DMGDH) and sarcosine dehydrogenase (SDH)

respectively. Both enzymes contain a covalently bound flavin adenine dinucleotide (FAD) and are major folate-binding proteins in liver (240). The reaction mechanisms are not established (8) but the electrons generated are transferred ultimately to the electron-transport chain. The quantitative contribution of choline degradation to the cytoplasmic folate-activated one-carbon pool is not known.

Inborn errors of metabolism are associated with both DMGDH and SDH deficiency. DMGDH deficiency results in muscle fatigue and body odor; sarcosinemia is a rare autosomal disorder with a broad and variable spectrum of symptoms including mental retardation and growth failure (241).

4. 10-FormylTHF Synthetase (FTHFS)

The final step in the putative conversion of the hydroxymethyl group of serine to formate in mitochondria requires the generation of formate from 10-formylTHF (1). This reaction can occur in mitochondria through the reverse reaction of 10-formylTHF synthetase, driven by a favorable ADP/ATP ratio in mitochondria (1). Mitochondria contain a monofunctional FTHFS enzyme that is encoded by *MthfdL1,* which is expressed ubiquitously in mammalian cells (242-244). Further studies of this recently-identified FTHFS enzyme will determine if its primary function is to generate formate from 10-formylTHF.

B. Folate Interconverting Enzymes

1. 5,10-MethenylTHF Cyclohydrolase and 5,10-methyleneTHF Dehydrogenase (MTHFC, MTHFD)

Human mitochondria contain isozymes of MTHFD and MTHFC activities encoded by a single gene, *Mthfd2,* which is believed to have evolved through gene

duplication and mutation of *Mthfd1* (245,246). *Mthfd2* does not encode FTHFS activity, and the mitochondrial MTHFD activity is distinguished from its cytoplasmic counterpart by its NAD-dependence which serves to drive the reaction in the oxidative direction to generate 10-formylTHF (30). *Mthfd2* is an essential gene during mouse development, but is not found in adult tissues. Its expression appears to be limited to embryonic and transformed cells (247). Deletion in murine embryonic fibroblasts creates a glycine auxotrophy, indicating a role for this enzyme in generating unsubstituted THF for SHMT2 and potentially generating fomate from serine. Therefore, while a complete folate-dependent pathway for generating formate from serine exists in embryonic cells, the lack of identified MTHFD and MTHFC activities in adult tissues represents a gap in our understanding of mitochondrial folate metabolism and/or the interaction between cytoplasmic and mitochondrial one-carbon metabolism in adult tissues.

C. Biosynthetic Enzymes

1. Methionyl-tRNA$_f^{Met}$ Formyltransferase (MFT).

Protein synthesis in mitochondria and prokaryotes is initiated with formyl-methionyl-tRNA (fMet-tRNA), which is formed by the 10-formylTHF-dependent formylation of Met-tRNA catalyzed Methionyl-tRNA$_f^{Met}$ Formyltransferase (MFT) (248,249). This is the only known biosynthetic reaction that occurs in mitochondria, other than amino-acid interconversion reactions (Figure 1.1). Although MFT-deficient *Saccharomyces cerevisiae* display normal mitochondrial function and mitochondrial protein synthesis (250), MFT does offer selective advantage under severe growth conditions (251). Formylation of Met-tRNA confers specificity to its interaction with initiation factor 2 (IF-2); bovine IF-2 binds fMet-tRNA with 25-fold greater affinity

than Met-tRNA and mitochondrial ribosomes bind fMet-tRNA 50-fold tighter than Met-tRNA in the presence of IF-2 (252).

Part V: Nuclear Folate-Mediated One-Carbon Metabolism

There is increasing evidence that folate-mediated thymidylate synthesis occurs in both the nucleus and cytoplasm (Figure 1.1). Approximately ten percent of cellular folate is present in the nucleus, and TS and cSHMT have been localized to the nucleus in several mammalian cell types in S-phase (51,253-257). The three enzymes that constitute the thymidylate synthase cycle (cSHMT, TS, and dihydrofolate reductase (DHFR)) are all substrates for UBC9-mediated modification with the small ubiquitin-like modifier (SUMO), which targets proteins for nuclear localization during S-phase (9,51). Nuclear TS was shown to form part of a putative "replitase complex" along with DNA polymerase α, ribonucleotide reductase, thymidylate kinase, NDP kinase, the folate-dependent enzyme DHFR (254,258,259), and possibly cSHMT (9). Because cSHMT exhibits a narrow range of tissue-specific expression compared to TS and DHFR, it is unlikely that all cells synthesize thymidylate in the nucleus. Although the biological significance of nuclear dTMP synthesis at the cellular level remains unclear, it has been hypothesized that its association with the replitase complex allows for *de novo* thymidylate synthesis directly at the replication fork during S-phase and may lower uracil misincorporation into DNA.

REFERENCES

1. Appling, D. R. (1991) *Faseb J* **5**, 2645-2651
2. Girgis, S., Suh, J. R., Jolivet, J., and Stover, P. J. (1997) *J Biol Chem* **272**, 4729-4734
3. Schirch, V., and Strong, W. B. (1989) *Arch Biochem Biophys* **269**, 371-380
4. Wagner, C. (1995) in *Folate in Health and Disease* (L.B., B., ed), pp. 23-42, CRC Press
5. Shane, B. (1995) in *Folate in Health and Disease* (Bailey, L. B., ed), pp. 1-22, Marcel Dekker, Inc., New York
6. Moran, R. G. (1999) *Semin Oncol* **26**, 24-32
7. Shane, B. (1989) *Vitam Horm* **45**, 263-335
8. Porter, D. H., Cook, R. J., and Wagner, C. (1985) *Arch Biochem Biophys* **243**, 396-407
9. Woeller, C. F., Anderson, D. D., Szebenyi, D. M., and Stover, P. J. (2007) *J Biol Chem* **282**, 17623-17631
10. Strong, W. B., Tendler, S. J., Seither, R. L., Goldman, I. D., and Schirch, V. (1990) *J Biol Chem* **265**, 12149-12155
11. Suh, J. R., Herbig, A. K., and Stover, P. J. (2001) *Annu Rev Nutr* **21**, 255-282
12. Scott, J. M., Dinn, J. J., Wilson, P., and Weir, D. G. (1981) *Lancet* **2**, 334-337
13. van der Put, N. M., and Blom, H. J. (2000) *Eur J Obstet Gynecol Reprod Biol* **92**, 57-61
14. Scott, J. M. (2001) *Bibl Nutr Dieta* **55**, 192-195
15. Ueland, P. M., Refsum, H., Beresford, S. A., and Vollset, S. E. (2000) *Am J Clin Nutr* **72**, 324-332
16. Gerhard, G. T., and Duell, P. B. (1999) *Curr Opin Lipidol* **10**, 417-428

17. Lindenbaum, J. a. A., R.H. (1995) in *Folate in Health and Disease* (Bailey, L. B., ed), Marcel Dekker, Inc., New York
18. Blount, B. C., Mack, M. M., Wehr, C. M., MacGregor, J. T., Hiatt, R. A., Wang, G., Wickramasinghe, S. N., Everson, R. B., and Ames, B. N. (1997) *Proc Natl Acad Sci U S A* **94**, 3290-3295
19. Ames, B. N. (2001) *Mutat Res* **475**, 7-20
20. Choi, S. W., and Mason, J. B. (2000) *J Nutr* **130**, 129-132
21. Pogribny, I. P., Basnakian, A. G., Miller, B. J., Lopatina, N. G., Poirier, L. A., and James, S. J. (1995) *Cancer Res* **55**, 1894-1901
22. Kim, Y. I. (1999) *Nutr Rev* **57**, 314-321
23. Bailey, L. B. (1995) in *Folate in Health and Disease* (Bailey, L. B., ed), Marcel Dekker, Inc., New York
24. McNulty, H. (1995) *Br J Biomed Sci* **52**, 110-119
25. Scott, J. M. (1998) *Nat Med* **4**, 895-896
26. Miranda, T. B., and Jones, P. A. (2007) *J Cell Physiol* **213**, 384-390
27. Winter-Vann, A. M., Kamen, B. A., Bergo, M. O., Young, S. G., Melnyk, S., James, S. J., and Casey, P. J. (2003) *Proc Natl Acad Sci U S A* **100**, 6529-6534
28. Stead, L. M., Jacobs, R. L., Brosnan, M. E., and Brosnan, J. T. (2004) *Adv Enzyme Regul* **44**, 321-333
29. Garrow, T. A., Brenner, A. A., Whitehead, V. M., Chen, X. N., Duncan, R. G., Korenberg, J. R., and Shane, B. (1993) *J Biol Chem* **268**, 11910-11916
30. Christensen, K. E., and MacKenzie, R. E. (2006) *Bioessays* **28**, 595-605
31. Herbig, K., Chiang, E. P., Lee, L. R., Hills, J., Shane, B., and Stover, P. J. (2002) *J Biol Chem* **277**, 38381-38389
32. Strong, W. B., and Schirch, V. (1989) *Biochemistry* **28**, 9430-9439

33. Nijhout, H. F., Reed, M. C., Lam, S. L., Shane, B., Gregory, J. F., 3rd, and Ulrich, C. M. (2006) *Theor Biol Med Model* **3**, 40

34. Renwick, S. B., Snell, K., and Baumann, U. (1998) *Structure* **6**, 1105-1116

35. Schirch, V., and Szebenyi, D. M. (2005) *Curr Opin Chem Biol* **9**, 482-487

36. Szebenyi, D. M., Liu, X., Kriksunov, I. A., Stover, P. J., and Thiel, D. J. (2000) *Biochemistry* **39**, 13313-13323

37. Trivedi, V., Gupta, A., Jala, V. R., Saravanan, P., Rao, G. S., Rao, N. A., Savithri, H. S., and Subramanya, H. S. (2002) *J Biol Chem* **277**, 17161-17169

38. Tatum, C. M., Jr., Benkovic, P. A., Benkovic, S. J., Potts, R., Schleicher, E., and Floss, H. G. (1977) *Biochemistry* **16**, 1093-1102

39. Szebenyi, D. M., Musayev, F. N., di Salvo, M. L., Safo, M. K., and Schirch, V. (2004) *Biochemistry* **43**, 6865-6876

40. Stover, P., and Schirch, V. (1990) *J Biol Chem* **265**, 14227-14233

41. Stover, P., and Schirch, V. (1993) *Trends Biochem Sci* **18**, 102-106

42. Stover, P., and Schirch, V. (1991) *J Biol Chem* **266**, 1543-1550

43. Girgis, S., Nasrallah, I. M., Suh, J. R., Oppenheim, E., Zanetti, K. A., Mastri, M. G., and Stover, P. J. (1998) *Gene* **210**, 315-324

44. Scheer, J. B., Mackey, A. D., and Gregory, J. F., 3rd. (2005) *J Nutr* **135**, 233-238

45. Perry, C., Yu, S., Chen, J., Matharu, K. S., and Stover, P. J. (2007) *Arch Biochem Biophys* **462**, 21-27

46. Nakshatri, H., Bouillet, P., Bhat-Nakshatri, P., and Chambon, P. (1996) *Gene* **174**, 79-84

47. Perry, C., Sastry, R., Nasrallah, I. M., and Stover, P. J. (2005) *J Biol Chem* **280**, 396-400

48. Oppenheim, E. W., Adelman, C., Liu, X., and Stover, P. J. (2001) *J Biol Chem* **276**, 19855-19861

49. Woeller, C. F., Fox, J. T., Perry, C., and Stover, P. J. (2007) *J Biol Chem*

50. Chasin, L. A., Feldman, A., Konstam, M., and Urlaub, G. (1974) *Proc Natl Acad Sci U S A* **71**, 718-722

51. Anderson, D. D., Woeller, C. F., and Stover, P. J. (2007) *Clin Chem Lab Med* **45**, 1760-1763

52. Skibola, C. F., Smith, M. T., Hubbard, A., Shane, B., Roberts, A. C., Law, G. R., Rollinson, S., Roman, E., Cartwright, R. A., and Morgan, G. J. (2002) *Blood* **99**, 3786-3791

53. Hishida, A., Matsuo, K., Hamajima, N., Ito, H., Ogura, M., Kagami, Y., Taji, H., Morishima, Y., Emi, N., and Tajima, K. (2003) *Haematologica* **88**, 159-166

54. Heil, S. G., Van der Put, N. M., Waas, E. T., den Heijer, M., Trijbels, F. J., and Blom, H. J. (2001) *Mol Genet Metab* **73**, 164-172

55. Relton, C. L., Wilding, C. S., Laffling, A. J., Jonas, P. A., Burgess, T., Binks, K., Tawn, E. J., and Burn, J. (2004) *Mol Genet Metab* **81**, 273-281

56. Relton, C. L., Wilding, C. S., Pearce, M. S., Laffling, A. J., Jonas, P. A., Lynch, S. A., Tawn, E. J., and Burn, J. (2004) *J Med Genet* **41**, 256-260

57. Lim, U., Peng, K., Shane, B., Stover, P. J., Litonjua, A. A., Weiss, S. T., Gaziano, J. M., Strawderman, R. L., Raiszadeh, F., Selhub, J., Tucker, K. L., and Cassano, P. A. (2005) *J Nutr* **135**, 1989-1994

58. Howard, K. M., Muga, S. J., Zhang, L., Thigpen, A. E., and Appling, D. R. (2003) *Gene* **319**, 85-97

59. Welch, W. H., Irwin, C. L., and Himes, R. H. (1968) *Biochem Biophys Res Commun* **30**, 255-261

60. Scott, J. M., and Rabinowitz, J. C. (1967) *Biochem Biophys Res Commun* **29**, 418-423
61. Himes, R. H., and Cohn, M. (1967) *J Biol Chem* **242**, 3628-3635
62. Joyce, B. K., and Himes, R. H. (1966) *J Biol Chem* **241**, 5725-5731
63. McGuire, J. J., and Rabinowitz, J. C. (1978) *J Biol Chem* **253**, 1079-1085
64. Mejillano, M. R., Jahansouz, H., Matsunaga, T. O., Kenyon, G. L., and Himes, R. H. (1989) *Biochemistry* **28**, 5136-5145
65. Song, S., Jahansouz, H., and Himes, R. H. (1993) *FEBS Lett* **332**, 150-152
66. Himes, R. H., and Rabinowitz, J. C. (1962) *J Biol Chem* **237**, 2915-2925
67. Buttlaire, D. H., Himes, R. H., and Reed, G. H. (1976) *J Biol Chem* **251**, 4159-4161
68. Mackenzie, R. E., and Baugh, C. M. (1980) *Biochim Biophys Acta* **611**, 187-195
69. Leaphart, A. B., Trent Spencer, H., and Lovell, C. R. (2002) *Arch Biochem Biophys* **408**, 137-143
70. Perry, J., Deacon, R., Lumb, M., and Chanarin, I. (1980) *Biochem Biophys Res Commun* **97**, 1329-1333
71. Barlowe, C. K., and Appling, D. R. (1988) *Biochem Biophys Res Commun* **157**, 245-249
72. Peri, K. G., and MacKenzie, R. E. (1991) *FEBS Lett* **294**, 113-115
73. Appling, D. R., and Rabinowitz, J. C. (1985) *J Biol Chem* **260**, 1248-1256
74. Smith, G. K., Mueller, W. T., Benkovic, P. A., and Benkovic, S. J. (1981) *Biochemistry* **20**, 1241-1245
75. Barlowe, C. K., and Appling, D. R. (1990) *Mol Cell Biol* **10**, 5679-5687
76. Song, J. M., and Rabinowitz, J. C. (1993) *Proc Natl Acad Sci U S A* **90**, 2636-2640

77. Brody, L. C., Conley, M., Cox, C., Kirke, P. N., McKeever, M. P., Mills, J. L., Molloy, A. M., O'Leary, V. B., Parle-McDermott, A., Scott, J. M., and Swanson, D. A. (2002) *Am J Hum Genet* **71**, 1207-1215

78. De Marco, P., Merello, E., Calevo, M. G., Mascelli, S., Raso, A., Cama, A., and Capra, V. (2006) *J Hum Genet* **51**, 98-103

79. Parle-McDermott, A., Kirke, P. N., Mills, J. L., Molloy, A. M., Cox, C., O'Leary, V. B., Pangilinan, F., Conley, M., Cleary, L., Brody, L. C., and Scott, J. M. (2006) *Eur J Hum Genet* **14**, 768-772

80. Parle-McDermott, A., Mills, J. L., Kirke, P. N., Cox, C., Signore, C. C., Kirke, S., Molloy, A. M., O'Leary, V. B., Pangilinan, F. J., O'Herlihy, C., Brody, L. C., and Scott, J. M. (2005) *Am J Med Genet A* **132**, 365-368

81. Parle-McDermott, A., Pangilinan, F., Mills, J. L., Signore, C. C., Molloy, A. M., Cotter, A., Conley, M., Cox, C., Kirke, P. N., Scott, J. M., and Brody, L. C. (2005) *Mol Hum Reprod* **11**, 477-480

82. Revel, H. R., and Magasanik, B. (1958) *J Biol Chem* **233**, 930-935

83. Tabor, H., Mehler, A. H., Hayaishi, O., and White, J. (1952) *J Biol Chem* **196**, 121-128

84. Mackenzie, R. E. (1984) in *Folates and Pterins* (Benkovic, R. L. B. a. S., ed) Vol. 1, pp. 255-306, Wiley-Interscience, New York

85. Murley, L. L., and MacKenzie, R. E. (1995) *Biochemistry* **34**, 10358-10364

86. Pricer, W. E., Jr., and Rabinowitz, J. C. (1956) *J Biol Chem* **222**, 537-554

87. Miller, A., and Waelsch, H. (1957) *J Biol Chem* **228**, 365-381

88. Uyeda, K., and Rabinowitz, J. C. (1965) *J Biol Chem* **240**, 1701-1710

89. Hilton, J. F., Christensen, K. E., Watkins, D., Raby, B. A., Renaud, Y., de la Luna, S., Estivill, X., MacKenzie, R. E., Hudson, T. J., and Rosenblatt, D. S. (2003) *Hum Mutat* **22**, 67-73

90. Paukert, J. L., Straus, L. D., and Rabinowitz, J. C. (1976) *J Biol Chem* **251**, 5104-5111

91. Tan, L. U., Drury, E. J., and MacKenzie, R. E. (1977) *J Biol Chem* **252**, 1117-1122

92. Cohen, L., and Mackenzie, R. E. (1978) *Biochim Biophys Acta* **522**, 311-317

93. Schirch, L. (1978) *Arch Biochem Biophys* **189**, 283-290

94. Wasserman, G. F., Benkovic, P. A., Young, M., and Benkovic, S. J. (1983) *Biochemistry* **22**, 1005-1013

95. Spivey, H. O., and Merz, J. M. (1989) *Bioessays* **10**, 127-130

96. Pawelek, P. D., and MacKenzie, R. E. (1998) *Biochemistry* **37**, 1109-1115

97. Stevens, V. L., McCullough, M. L., Pavluck, A. L., Talbot, J. T., Feigelson, H. S., Thun, M. J., and Calle, E. E. (2007) *Cancer Epidemiol Biomarkers Prev* **16**, 1140-1147

98. Donato, H., Krupenko, N. I., Tsybovsky, Y., and Krupenko, S. A. (2007) *J Biol Chem* **282**, 34159-34166

99. Cook, R. J., Lloyd, R. S., and Wagner, C. (1991) *J Biol Chem* **266**, 4965-4973

100. Tsybovsky, Y., Donato, H., Krupenko, N. I., Davies, C., and Krupenko, S. A. (2007) *Biochemistry* **46**, 2917-2929

101. Fu, T. F., Maras, B., Barra, D., and Schirch, V. (1999) *Arch Biochem Biophys* **367**, 161-166

102. Kim, D. W., Huang, T., Schirch, D., and Schirch, V. (1996) *Biochemistry* **35**, 15772-15783

103. Anguera, M. C., Field, M. S., Perry, C., Ghandour, H., Chiang, E. P., Selhub, J., Shane, B., and Stover, P. J. (2006) *J Biol Chem* **281**, 18335-18342

104. Chen, S., Yakunin, A. F., Proudfoot, M., Kim, R., and Kim, S. H. (2005) *Proteins* **61**, 433-443

105. Stover, P., Kruschwitz, H., and Schirch, V. (1993) *Adv Exp Med Biol* **338**, 679-685

106. Huang, T., and Schirch, V. (1995) *J Biol Chem* **270**, 22296-22300

107. Kounga, K., Vander Velde, D. G., and Himes, R. H. (1995) *FEBS Lett* **364**, 215-217

108. Field, M. S., Szebenyi, D. M., Perry, C. A., and Stover, P. J. (2007) *Arch Biochem Biophys* **458**, 194-201

109. Anguera, M. C., Suh, J. R., Ghandour, H., Nasrallah, I. M., Selhub, J., and Stover, P. J. (2003) *J Biol Chem* **278**, 29856-29862

110. Field, M. S., Szebenyi, D. M., and Stover, P. J. (2006) *J Biol Chem* **281**, 4215-4221

111. Bertrand, R., and Jolivet, J. (1989) *J Biol Chem* **264**, 8843-8846

112. Matakidou, A., El Galta, R., Rudd, M. F., Webb, E. L., Bridle, H., Eisen, T., and Houlston, R. S. (2007) *Br J Cancer* **97**, 247-252

113. Trimmer, E. E., Ballou, D. P., Ludwig, M. L., and Matthews, R. G. (2001) *Biochemistry* **40**, 6216-6226

114. Sumner, J. a. M., RG. (1992) *J Am Chem Soc* **114**, 6949-6956

115. Tran, P., Leclerc, D., Chan, M., Pai, A., Hiou-Tim, F., Wu, Q., Goyette, P., Artigas, C., Milos, R., and Rozen, R. (2002) *Mamm Genome* **13**, 483-492

116. van der Velden, A. W., and Thomas, A. A. (1999) *Int J Biochem Cell Biol* **31**, 87-106

117. Pickell, L., Tran, P., Leclerc, D., Hiscott, J., and Rozen, R. (2005) *Biochim Biophys Acta* **1731**, 104-114

118. Kutzbach, C., and Stokstad, E. L. (1971) *Biochim Biophys Acta* **250**, 459-477

119. Jencks, D. A., and Mathews, R. G. (1987) *J Biol Chem* **262**, 2485-2493

120. Yamada, K., Strahler, J. R., Andrews, P. C., and Matthews, R. G. (2005) *Proc Natl Acad Sci U S A* **102**, 10454-10459

121. Gaughan, D. J., Barbaux, S., Kluijtmans, L. A., and Whitehead, A. S. (2000) *Gene* **257**, 279-289

122. Pejchal, R., Campbell, E., Guenther, B. D., Lennon, B. W., Matthews, R. G., and Ludwig, M. L. (2006) *Biochemistry* **45**, 4808-4818

123. Shivapurkar, N., Tang, Z., Frost, A., and Alabaster, O. (1995) *Cancer Lett* **91**, 125-132

124. Guenther, B. D., Sheppard, C. A., Tran, P., Rozen, R., Matthews, R. G., and Ludwig, M. L. (1999) *Nat Struct Biol* **6**, 359-365

125. Yamada, K., Chen, Z., Rozen, R., and Matthews, R. G. (2001) *Proc Natl Acad Sci U S A* **98**, 14853-14858

126. Kang, S. S., Wong, P. W., Zhou, J. M., Sora, J., Lessick, M., Ruggie, N., and Grcevich, G. (1988) *Metabolism* **37**, 611-613

127. Jacques, P. F., Bostom, A. G., Williams, R. R., Ellison, R. C., Eckfeldt, J. H., Rosenberg, I. H., Selhub, J., and Rozen, R. (1996) *Circulation* **93**, 7-9

128. Molloy, A. M., Daly, S., Mills, J. L., Kirke, P. N., Whitehead, A. S., Ramsbottom, D., Conley, M. R., Weir, D. G., and Scott, J. M. (1997) *Lancet* **349**, 1591-1593

129. Parle-McDermott, A., Mills, J. L., Molloy, A. M., Carroll, N., Kirke, P. N., Cox, C., Conley, M. R., Pangilinan, F. J., Brody, L. C., and Scott, J. M. (2006) *Mol Genet Metab* **88**, 290-294

130. Klerk, M., Verhoef, P., Clarke, R., Blom, H. J., Kok, F. J., and Schouten, E. G. (2002) *Jama* **288**, 2023-2031

131. Kluijtmans, L. A., van den Heuvel, L. P., Boers, G. H., Frosst, P., Stevens, E. M., van Oost, B. A., den Heijer, M., Trijbels, F. J., Rozen, R., and Blom, H. J. (1996) *Am J Hum Genet* **58**, 35-41

132. Morita, H., Taguchi, J., Kurihara, H., Kitaoka, M., Kaneda, H., Kurihara, Y., Maemura, K., Shindo, T., Minamino, T., Ohno, M., Yamaoki, K., Ogasawara, K., Aizawa, T., Suzuki, S., and Yazaki, Y. (1997) *Circulation* **95**, 2032-2036

133. Christensen, B., Arbour, L., Tran, P., Leclerc, D., Sabbaghian, N., Platt, R., Gilfix, B. M., Rosenblatt, D. S., Gravel, R. A., Forbes, P., and Rozen, R. (1999) *Am J Med Genet* **84**, 151-157

134. Ou, C. Y., Stevenson, R. E., Brown, V. K., Schwartz, C. E., Allen, W. P., Khoury, M. J., Rozen, R., Oakley, G. P., Jr., and Adams, M. J., Jr. (1996) *Am J Med Genet* **63**, 610-614

135. van der Put, N. M., Steegers-Theunissen, R. P., Frosst, P., Trijbels, F. J., Eskes, T. K., van den Heuvel, L. P., Mariman, E. C., den Heyer, M., Rozen, R., and Blom, H. J. (1995) *Lancet* **346**, 1070-1071

136. Mills, J. L., McPartlin, J. M., Kirke, P. N., Lee, Y. J., Conley, M. R., Weir, D. G., and Scott, J. M. (1995) *Lancet* **345**, 149-151

137. Zhu, J., Ren, A., Hao, L., Pei, L., Liu, J., Zhu, H., Li, S., Finnell, R. H., and Li, Z. (2006) *Am J Med Genet A* **140**, 551-557

138. Keijzer, M. B., den Heijer, M., Blom, H. J., Bos, G. M., Willems, H. P., Gerrits, W. B., and Rosendaal, F. R. (2002) *Thromb Haemost* **88**, 723-728

139. Quere, I., Perneger, T. V., Zittoun, J., Bellet, H., Gris, J. C., Daures, J. P., Schved, J. F., Mercier, E., Laroche, J. P., Dauzat, M., Bounameaux, H., Janbon, C., and de Moerloose, P. (2002) *Lancet* **359**, 747-752

140. Zalavras Ch, G., Giotopoulou, S., Dokou, E., Mitsis, M., Ioannou, H. V., Tzolou, A., Kolaitis, N., and Vartholomatos, G. (2002) *Int Angiol* **21**, 268-271

141. Lewis, S. J., Zammit, S., Gunnell, D., and Smith, G. D. (2005) *Am J Med Genet B Neuropsychiatr Genet* **135**, 2-4

142. Muntjewerff, J. W., Hoogendoorn, M. L., Kahn, R. S., Sinke, R. J., Den Heijer, M., Kluijtmans, L. A., and Blom, H. J. (2005) *Am J Med Genet B Neuropsychiatr Genet* **135**, 69-72

143. Muntjewerff, J. W., Kahn, R. S., Blom, H. J., and den Heijer, M. (2006) *Mol Psychiatry* **11**, 143-149

144. Scher, A. I., Terwindt, G. M., Verschuren, W. M., Kruit, M. C., Blom, H. J., Kowa, H., Frants, R. R., van den Maagdenberg, A. M., van Buchem, M., Ferrari, M. D., and Launer, L. J. (2006) *Ann Neurol* **59**, 372-375

145. Skibola, C. F., Smith, M. T., Kane, E., Roman, E., Rollinson, S., Cartwright, R. A., and Morgan, G. (1999) *Proc Natl Acad Sci U S A* **96**, 12810-12815

146. Wiemels, J. L., Smith, R. N., Taylor, G. M., Eden, O. B., Alexander, F. E., and Greaves, M. F. (2001) *Proc Natl Acad Sci U S A* **98**, 4004-4009

147. Chen, J., Giovannucci, E., Kelsey, K., Rimm, E. B., Stampfer, M. J., Colditz, G. A., Spiegelman, D., Willett, W. C., and Hunter, D. J. (1996) *Cancer Res* **56**, 4862-4864

148. Ma, J., Stampfer, M. J., Giovannucci, E., Artigas, C., Hunter, D. J., Fuchs, C., Willett, W. C., Selhub, J., Hennekens, C. H., and Rozen, R. (1997) *Cancer Res* **57**, 1098-1102

149. Stegmann, K., Ziegler, A., Ngo, E. T., Kohlschmidt, N., Schroter, B., Ermert, A., and Koch, M. C. (1999) *Am J Med Genet* **87**, 23-29

150. Aimi, J., Qiu, H., Williams, J., Zalkin, H., and Dixon, J. E. (1990) *Nucleic Acids Res* **18**, 6665-6672

151. Schild, D., Brake, A. J., Kiefer, M. C., Young, D., and Barr, P. J. (1990) *Proc Natl Acad Sci U S A* **87**, 2916-2920

152. Wall, M., Shim, J. H., and Benkovic, S. J. (2000) *Biochemistry* **39**, 11303-11311

153. Caperelli, C. A. (1989) *J Biol Chem* **264**, 5053-5057

154. Klein, C., Chen, P., Arevalo, J. H., Stura, E. A., Marolewski, A., Warren, M. S., Benkovic, S. J., and Wilson, I. A. (1995) *J Mol Biol* **249**, 153-175

155. Qiao, Q. A., Cai, Z. T., Feng, D. C., and Jiang, Y. S. (2004) *Biophys Chem* **110**, 259-266

156. Bulock, K. G., Beardsley, G. P., and Anderson, K. S. (2002) *J Biol Chem* **277**, 22168-22174

157. Yamazaki, A. a. O., M. (1978) *J. Heterocyclic Chem* **15**, 353

158. Wolan, D. W., Greasley, S. E., Beardsley, G. P., and Wilson, I. A. (2002) *Biochemistry* **41**, 15505-15513

159. Shim, J. H., Wall, M., Benkovic, S. J., Diaz, N., Suarez, D., and Merz, K. M., Jr. (2001) *J Am Chem Soc* **123**, 4687-4696

160. Brodsky, G., Barnes, T., Bleskan, J., Becker, L., Cox, M., and Patterson, D. (1997) *Hum Mol Genet* **6**, 2043-2050

161. Meredith, M., Rabaglia, M., and Metz, S. (1995) *Biochim Biophys Acta* **1266**, 16-22

162. Beardsley, G. P., Moroson, B. A., Taylor, E. C., and Moran, R. G. (1989) *J Biol Chem* **264**, 328-333

163. Erba, E., Sen, S., Sessa, C., Vikhanskaya, F. L., and D'Incalci, M. (1994) *Br J Cancer* **69**, 205-211

164. Allegra, C. J., Fine, R. L., Drake, J. C., and Chabner, B. A. (1986) *J Biol Chem* **261**, 6478-6485

165. Cronstein, B. N., Naime, D., and Ostad, E. (1993) *J Clin Invest* **92**, 2675-2682

166. Gadangi, P., Longaker, M., Naime, D., Levin, R. I., Recht, P. A., Montesinos, M. C., Buckley, M. T., Carlin, G., and Cronstein, B. N. (1996) *J Immunol* **156**, 1937-1941

167. Szabados, E., Hindmarsh, E. J., Phillips, L., Duggleby, R. G., and Christopherson, R. I. (1994) *Biochemistry* **33**, 14237-14245

168. Dervieux, T., Furst, D., Lein, D. O., Capps, R., Smith, K., Walsh, M., and Kremer, J. (2004) *Arthritis Rheum* **50**, 2766-2774

169. Marie, S., Heron, B., Bitoun, P., Timmerman, T., Van Den Berghe, G., and Vincent, M. F. (2004) *Am J Hum Genet* **74**, 1276-1281

170. Trinh, B. N., Ong, C. N., Coetzee, G. A., Yu, M. C., and Laird, P. W. (2002) *Hum Genet* **111**, 299-302

171. Liu, Y., Barrett, J. E., Schultz, P. G., and Santi, D. V. (1999) *Biochemistry* **38**, 848-852

172. Carreras, C. W., and Santi, D. V. (1995) *Annu Rev Biochem* **64**, 721-762

173. Ayusawa, D., Shimizu, K., Koyama, H., Kaneda, S., Takeishi, K., and Seno, T. (1986) *J Mol Biol* **190**, 559-567

174. Conrad, A. H. (1971) *J Biol Chem* **246**, 1318-1323

175. Ash, J., Liao, W. C., Ke, Y., and Johnson, L. F. (1995) *Nucleic Acids Res* **23**, 4649-4656

176. Jenh, C. H., Geyer, P. K., and Johnson, L. F. (1985) *Mol Cell Biol* **5**, 2527-2532

177. Navalgund, L. G., Rossana, C., Muench, A. J., and Johnson, L. F. (1980) *J Biol Chem* **255**, 7386-7390

178. Ash, J., Ke, Y., Korb, M., and Johnson, L. F. (1993) *Mol Cell Biol* **13**, 1565-1571

179. Ke, Y., Ash, J., and Johnson, L. F. (1996) *Mol Cell Biol* **16**, 376-383

180. Dong, S., Lester, L., and Johnson, L. F. (2000) *J Cell Biochem* **77**, 50-64

181. Rudge, T. L., and Johnson, L. F. (2002) *Exp Cell Res* **274**, 45-55

182. Powell, C. M., Rudge, T. L., Zhu, Q., Johnson, L. F., and Hansen, U. (2000) *Embo J* **19**, 4665-4675

183. Angus, S. P., Wheeler, L. J., Ranmal, S. A., Zhang, X., Markey, M. P., Mathews, C. K., and Knudsen, E. S. (2002) *J Biol Chem* **277**, 44376-44384

184. DeGregori, J., Leone, G., Ohtani, K., Miron, A., and Nevins, J. R. (1995) *Genes Dev* **9**, 2873-2887

185. Takeishi, K., Kaneda, S., Ayusawa, D., Shimizu, K., Gotoh, O., and Seno, T. (1985) *Nucleic Acids Res* **13**, 2035-2043

186. Chu, J., and Dolnick, B. J. (2002) *Biochim Biophys Acta* **1587**, 183-193

187. Chu, E., Koeller, D. M., Casey, J. L., Drake, J. C., Chabner, B. A., Elwood, P. C., Zinn, S., and Allegra, C. J. (1991) *Proc Natl Acad Sci U S A* **88**, 8977-8981

188. Hori, T., Ayusawa, D., Shimizu, K., Koyama, H., and Seno, T. (1984) *Cancer Res* **44**, 703-709

189. Takemura, Y., and Jackman, A. L. (1997) *Anticancer Drugs* **8**, 3-16

190. Gorlick, R., Metzger, R., Danenberg, K. D., Salonga, D., Miles, J. S., Longo, G. S., Fu, J., Banerjee, D., Klimstra, D., Jhanwar, S., Danenberg, P. V., Kemeny, N., and Bertino, J. R. (1998) *J Clin Oncol* **16**, 1465-1469

191. Van der Wilt, C. L., Pinedo, H. M., Smid, K., and Peters, G. J. (1992) *Cancer Res* **52**, 4922-4928

192. Forsthoefel, A. M., Pena, M. M., Xing, Y. Y., Rafique, Z., and Berger, F. G. (2004) *Biochemistry* **43**, 1972-1979

193. Kitchens, M. E., Forsthoefel, A. M., Rafique, Z., Spencer, H. T., and Berger, F. G. (1999) *J Biol Chem* **274**, 12544-12547

194. Mandola, M. V., Stoehlmacher, J., Muller-Weeks, S., Cesarone, G., Yu, M. C., Lenz, H. J., and Ladner, R. D. (2003) *Cancer Res* **63**, 2898-2904

195. Horie, N., Aiba, H., Oguro, K., Hojo, H., and Takeishi, K. (1995) *Cell Struct Funct* **20**, 191-197

196. Kawakami, K., and Watanabe, G. (2003) *Cancer Res* **63**, 6004-6007

197. Krajinovic, M., Costea, I., and Chiasson, S. (2002) *Lancet* **359**, 1033-1034

198. Pullarkat, S. T., Stoehlmacher, J., Ghaderi, V., Xiong, Y. P., Ingles, S. A., Sherrod, A., Warren, R., Tsao-Wei, D., Groshen, S., and Lenz, H. J. (2001) *Pharmacogenomics J* **1**, 65-70

199. Kawakami, K., Omura, K., Kanehira, E., and Watanabe, Y. (1999) *Anticancer Res* **19**, 3249-3252

200. Lincz, L. F., Scorgie, F. E., Garg, M. B., and Ackland, S. P. (2007) *Int J Cancer* **120**, 1930-1934

201. Ulrich, C. M., Bigler, J., Velicer, C. M., Greene, E. A., Farin, F. M., and Potter, J. D. (2000) *Cancer Epidemiol Biomarkers Prev* **9**, 1381-1385

202. Mandola, M. V., Stoehlmacher, J., Zhang, W., Groshen, S., Yu, M. C., Iqbal, S., Lenz, H. J., and Ladner, R. D. (2004) *Pharmacogenetics* **14**, 319-327

203. Kealey, C., Brown, K. S., Woodside, J. V., Young, I., Murray, L., Boreham, C. A., McNulty, H., Strain, J. J., McPartlin, J., Scott, J. M., and Whitehead, A. S. (2005) *Hum Genet* **116**, 347-353

204. Volcik, K. A., Shaw, G. M., Zhu, H., Lammer, E. J., Laurent, C., and Finnell, R. H. (2003) *Birth Defects Res A Clin Mol Teratol* **67**, 924-928

205. Drennan, C. L., Huang, S., Drummond, J. T., Matthews, R. G., and Lidwig, M. L. (1994) *Science* **266**, 1669-1674

206. Goulding, C. W., Postigo, D., and Matthews, R. G. (1997) *Biochemistry* **36**, 8082-8091

207. Katrina Peariso, C. W. G., Sha Huang, Rowena G. Matthews, and James E. Penner-Hahn. (1998) *J Am Chem Soc* **120**, 8410-8416

208. Ludwig, M. L., and Matthews, R. G. (1997) *Annu Rev Biochem* **66**, 269-313

209. Gokhale, R. S., and Khosla, C. (2000) *Curr Opin Chem Biol* **4**, 22-27

210. Banerjee, R. V., Harder, S. R., Ragsdale, S. W., and Matthews, R. G. (1990) *Biochemistry* **29**, 1129-1135

211. Leclerc, D., Wilson, A., Dumas, R., Gafuik, C., Song, D., Watkins, D., Heng, H. H., Rommens, J. M., Scherer, S. W., Rosenblatt, D. S., and Gravel, R. A. (1998) *Proc Natl Acad Sci U S A* **95**, 3059-3064

212. Oltean, S., and Banerjee, R. (2005) *J Biol Chem* **280**, 32662-32668

213. Col, B., Oltean, S., and Banerjee, R. (2007) *Biochim Biophys Acta* **1769**, 532-540

214. Lassen, H. C., Henriksen, E., Neukirch, F., and Kristensen, H. S. (1956) *Lancet* **270**, 527-530

215. Shane, B., and Stokstad, E. L. (1985) *Annu Rev Nutr* **5**, 115-141

216. Refsum, H., Ueland, P. M., Nygard, O., and Vollset, S. E. (1998) *Annu Rev Med* **49**, 31-62

217. Clarke, R., Smith, A. D., Jobst, K. A., Refsum, H., Sutton, L., and Ueland, P. M. (1998) *Arch Neurol* **55**, 1449-1455

218. Swanson, D. A., Liu, M. L., Baker, P. J., Garrett, L., Stitzel, M., Wu, J., Harris, M., Banerjee, R., Shane, B., and Brody, L. C. (2001) *Mol Cell Biol* **21**, 1058-1065

219. Chen, L. H., Liu, M. L., Hwang, H. Y., Chen, L. S., Korenberg, J., and Shane, B. (1997) *J Biol Chem* **272**, 3628-3634

220. Gulati, S., Brody, L. C., and Banerjee, R. (1999) *Biochem Biophys Res Commun* **259**, 436-442

221. Leclerc, D., Campeau, E., Goyette, P., Adjalla, C. E., Christensen, B., Ross, M., Eydoux, P., Rosenblatt, D. S., Rozen, R., and Gravel, R. A. (1996) *Hum Mol Genet* **5**, 1867-1874

222. Harmon, D. L., Shields, D. C., Woodside, J. V., McMaster, D., Yarnell, J. W., Young, I. S., Peng, K., Shane, B., Evans, A. E., and Whitehead, A. S. (1999) *Genet Epidemiol* **17**, 298-309

223. Paz, M. F., Avila, S., Fraga, M. F., Pollan, M., Capella, G., Peinado, M. A., Sanchez-Cespedes, M., Herman, J. G., and Esteller, M. (2002) *Cancer Res* **62**, 4519-4524

224. Burzynski, M., Duriagin, S., Mostowska, M., Wudarski, M., Chwalinska-Sadowska, H., and Jagodzinski, P. P. (2007) *Lupus* **16**, 450-454

225. Kempisty, B., Sikora, J., Lianeri, M., Szczepankiewicz, A., Czerski, P., Hauser, J., and Jagodzinski, P. P. (2007) *Psychiatr Genet* **17**, 177-181

226. Doolin, M. T., Barbaux, S., McDonnell, M., Hoess, K., Whitehead, A. S., and Mitchell, L. E. (2002) *Am J Hum Genet* **71**, 1222-1226

227. Mostowska, A., Hozyasz, K. K., and Jagodzinski, P. P. (2006) *Clin Genet* **69**, 512-517

228. Bosco, P., Gueant-Rodriguez, R. M., Anello, G., Barone, C., Namour, F., Caraci, F., Romano, A., Romano, C., and Gueant, J. L. (2003) *Am J Med Genet A* **121**, 219-224

229. Horne, D. W., Patterson, D., and Cook, R. J. (1989) *Arch Biochem Biophys* **270**, 729-733

230. Lin, B. F., Huang, R. F., and Shane, B. (1993) *J Biol Chem* **268**, 21674-21679

231. Pfendner, W., and Pizer, L. I. (1980) *Arch Biochem Biophys* **200**, 503-512

232. Titus, S. A., and Moran, R. G. (2000) *J Biol Chem* **275**, 36811-36817

233. Garcia-Martinez, L. F., and Appling, D. R. (1993) *Biochemistry* **32**, 4671-4676

234. Davis, S. R., Stacpoole, P. W., Williamson, J., Kick, L. S., Quinlivan, E. P., Coats, B. S., Shane, B., Bailey, L. B., and Gregory, J. F., 3rd. (2004) *Am J Physiol Endocrinol Metab* **286**, E272-279

235. Nikiforov, M. A., Chandriani, S., O'Connell, B., Petrenko, O., Kotenko, I., Beavis, A., Sedivy, J. M., and Cole, M. D. (2002) *Mol Cell Biol* **22**, 5793-5800

236. Okamura-Ikeda, K., Hosaka, H., Yoshimura, M., Yamashita, E., Toma, S., Nakagawa, A., Fujiwara, K., Motokawa, Y., and Taniguchi, H. (2005) *J Mol Biol* **351**, 1146-1159

237. Ichinohe, A., Kure, S., Mikawa, S., Ueki, T., Kojima, K., Fujiwara, K., Iinuma, K., Matsubara, Y., and Sato, K. (2004) *Eur J Neurosci* **19**, 2365-2370

238. Lamers, Y., Williamson, J., Gilbert, L. R., Stacpoole, P. W., and Gregory, J. F., 3rd. (2007) *J Nutr* **137**, 2647-2652

239. Dinopoulos, A., Matsubara, Y., and Kure, S. (2005) *Mol Genet Metab* **86**, 61-69

240. Wittwer, A. J., and Wagner, C. (1980) *Proc Natl Acad Sci U S A* **77**, 4484-4488

241. Binzak, B. A., Wevers, R. A., Moolenaar, S. H., Lee, Y. M., Hwu, W. L., Poggi-Bach, J., Engelke, U. F., Hoard, H. M., Vockley, J. G., and Vockley, J. (2001) *Am J Hum Genet* **68**, 839-847

242. Christensen, K. E., Patel, H., Kuzmanov, U., Mejia, N. R., and MacKenzie, R. E. (2005) *J Biol Chem* **280**, 7597-7602

243. Walkup, A. S., and Appling, D. R. (2005) *Arch Biochem Biophys* **442**, 196-205

244. Prasannan, P., Pike, S., Peng, K., Shane, B., and Appling, D. R. (2003) *J Biol Chem* **278**, 43178-43187

245. Di Pietro, E., Wang, X. L., and MacKenzie, R. E. (2004) *Biochim Biophys Acta* **1674**, 78-84

246. Di Pietro, E., Sirois, J., Tremblay, M. L., and MacKenzie, R. E. (2002) *Mol Cell Biol* **22**, 4158-4166

247. Peri, K. G., and MacKenzie, R. E. (1993) *Biochim Biophys Acta* **1171**, 281-287

248. Bianchetti, R., Lucchini, G., Crosti, P., and Tortora, P. (1977) *J Biol Chem* **252**, 2519-2523

249. Takeuchi, N., Kawakami, M., Omori, A., Ueda, T., Spremulli, L. L., and Watanabe, K. (1998) *J Biol Chem* **273**, 15085-15090

250. Tibbetts, A. S., Oesterlin, L., Chan, S. Y., Kramer, G., Hardesty, B., and Appling, D. R. (2003) *J Biol Chem* **278**, 31774-31780

251. Vial, L., Gomez, P., Panvert, M., Schmitt, E., Blanquet, S., and Mechulam, Y. (2003) *Biochemistry* **42**, 932-939

252. Spencer, A. C., and Spremulli, L. L. (2004) *Nucleic Acids Res* **32**, 5464-5470

253. Brown, S. S., Neal, G. E., and Williams, D. C. (1965) *Biochem J* **97**, 34C-36C

254. Prem veer Reddy, G., and Pardee, A. B. (1980) *Proc Natl Acad Sci U S A* **77**, 3312-3316

255. Samsonoff, W. A., Reston, J., McKee, M., O'Connor, B., Galivan, J., Maley, G., and Maley, F. (1997) *J Biol Chem* **272**, 13281-13285

256. Wong, N. A., Brett, L., Stewart, M., Leitch, A., Longley, D. B., Dunlop, M. G., Johnston, P. G., Lessells, A. M., and Jodrell, D. I. (2001) *Br J Cancer* **85**, 1937-1943

257. Bissoon-Haqqani, S., Moyana, T., Jonker, D., Maroun, J. A., and Birnboim, H. C. (2006) *J Histochem Cytochem* **54**, 19-29

258. Boorstein, R. J., and Pardee, A. B. (1983) *Biochem Biophys Res Commun* **117**, 30-36

259. Noguchi, H., Prem veer Reddy, G., and Pardee, A. B. (1983) *Cell* **32**, 443-451

CHAPTER 2

INTRODUCTION TO INTERNAL RIBOSOME ENTRY SITE-MEDIATED TRANSLATION INITIATION

Part I: Abstract

Translation initiation can occur by two distinct mechanisms: cap-dependent ribosome scanning and internal ribosome entry. In cap-dependent translation initiation, the 40S ribosomal subunit binds to the 5' cap structure of the mRNA and scans through the 5' untranslated region (UTR) to reach the start codon of the open reading frame. During internal ribosome entry, the 40S ribosomal subunit binds to the 5'UTR of the transcript at a position close to or directly at the initiation codon. This position is termed the internal ribosome entry site (IRES). This chapter discusses the identification of IRES elements, the mechanisms whereby they may function, and the cellular situations where they are required. Special emphasis is placed on IRESes that regulate folate-mediated one-carbon metabolism.

Part II: Mechanisms of Translation Initiation

Cap-Dependent Translation

For the majority of eukaryotic mRNAs, translation initiation proceeds by a cap-dependent mechanism (Figure 2.1). The 43S initiation complex (which contains the 40S ribosomal subunit, the initiator methionine-tRNA bound to eukaryotic initiation factor 2 (eIF2) and GTP, eIF1A, and eIF3) is recruited to the 7-methyl-guanosine (m^7G) cap structure located at the 5' terminus of the transcript through interactions with eIF4F (1,2). eIF4F is a three-subunit complex composed of the cap-

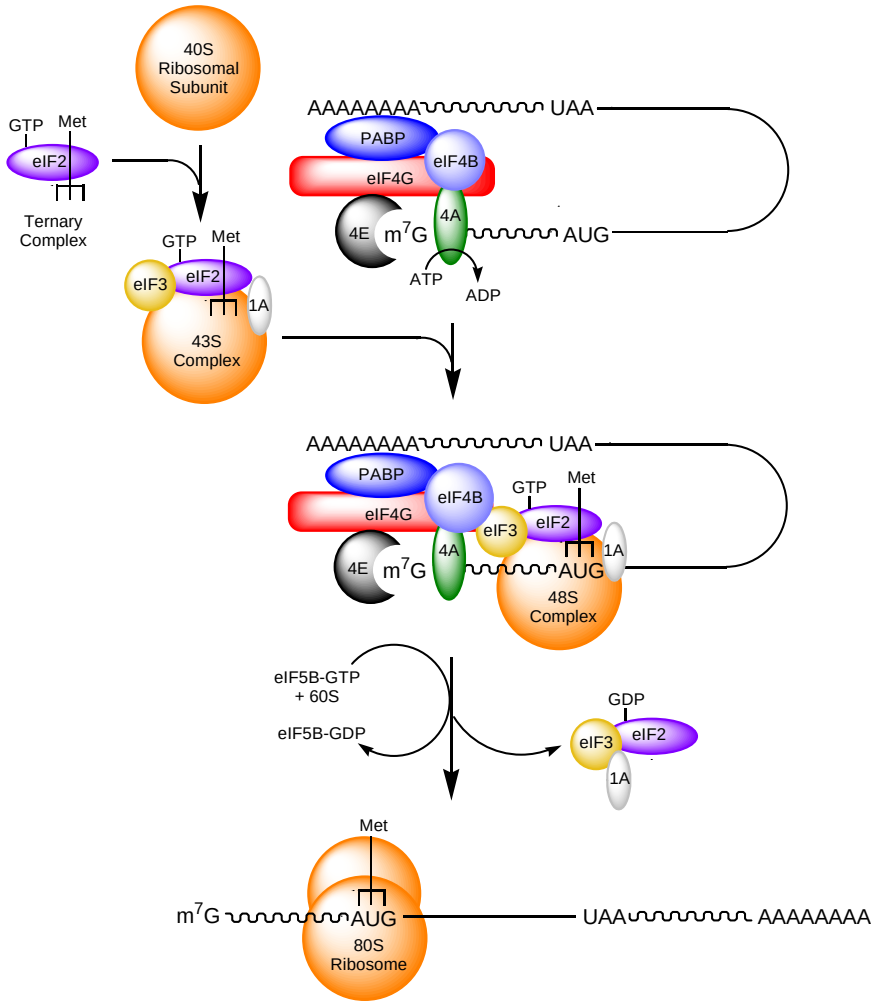

Figure 2.1. Cap-dependent translation initiation. Cap-dependent translation initiation begins with the recruitment of the 43S complex, which consists of the small 40S ribosomal subunit, GTP-bound eIF2, methionine-bound initiator tRNA, eIF1A, and eIF3, to the m^7G cap at the 5' end of an mRNA transcript. eIF3 acts as a bridge between the 43S complex and eIF4G, which is bound to the cap via interaction with eIF4E and to the poly(A) tail of the transcript via interaction with the poly(A)-binding protein (PABP). Through the coordinated activities of eIF1A, eIF4B, and the ATP-dependent helicase eIF4A, the 43S complex then scans along the 5'UTR of the mRNA until the AUG start codon of the open reading frame is paired with the anticodon of the initiator tRNA (48S complex). Upon 48S complex formation, GTP is hydrolyzed by eIF2. This triggers the release of eIF2, eIF3, and eIF1A, and enables the eIF5B-mediated joining of the large 60S ribosomal subunit. The resulting 80S ribosome is poised to begin translation elongation.

binding protein eIF4E, the DEA(D/H)-box RNA helicase eIF4A, and eIF4G, which serves as a scaffold for the coordinated assembly of the translation initiation machinery. Upon binding to the cap structure, eIF1A, eIF4A, and eIF4B act synergistically to enable the ATP-dependent scanning of the 43S complex along the 5' untranslated region (UTR) of the mRNA in the 5' to 3' direction (3,4). Ribosome scanning culminates in the formation of the 48S complex in which the initiator AUG is base paired to the anticodon of the initiator tRNA. Once positioned on the initiation codon, the eIFs bound to the 40S ribosomal subunit are displaced (2,5), and eIF5B mediates the joining of the 60S ribosomal subunit to the 40S subunit (6,7). This results in the formation of the protein synthesis-competent 80S ribosome in which the initiator tRNA is positioned in the ribosomal P site.

Internal Ribosome Entry Site-Mediated Translation

Because cannonical cap-dependent translation requires ribosome scanning, it is generally not efficient when any of the eIFs is limiting (8) and when the 5'UTR of the mRNA transcript is greater than 150 nucleotides in length (9), has a secondary structure with a change in Gibb's free energy (ΔG) of less than -50 kcal/mol (10), and contains multiple non-conserved AUG triplets upstream of the initiation codon (8). Yet picornaviruses, which possess all of these barriers to ribosome scanning and lack a 7-methyl-guanosine cap structure, are efficiently translated following infection, suggesting that picornaviral mRNAs are translated by a cap-independent initiation mechanism. In 1988 it was discovered that the 40S ribosomal subunit can be recruited to a *cis*-element located within the 5' UTR of the picornaviral transcript. These elements, now called internal ribosome entry sites (IRESes), allow for the assembly of the translational machinery at a position close to or directly at the initiation codon, and thereby circumvent ribosome scanning through a long and structured 5'UTR. IRES

elements also allow for 40S recruitment in a manner that is independent of eIF4F integrity (11,12).

Shortly after the identification of IRESes within the viral genome, it became evident that many cellular mRNAs from yeast, *Drosophila*, birds, and mammals can also be translated via internal initiation. As with the picornaviral transcripts, a number of these cellular mRNAs possess structural features in their 5'UTRs that would impede a cap-dependent ribosome scanning mechanism. It is now estimated that 3-5% of cellular mRNAs contain IRESes (13).

Part III: Identifying IRES Elements

IRESes cannot be recognized by a specific RNA sequence or structural motif; however, the majority of the IRESs identified to date are GC-rich and exhibit complex stem loop structures (14). The current protocol for the identification of IRES elements involves inserting the 5'UTR of a transcript into the intercistronic spacer region of a bicistronic construct. Expression of the downstream cistron indicates the ability of the 5'UTR to promote internal ribosome binding. When performing such experiments, extreme care must be taken to 1) rule out the existence of cryptic promoter activity and cryptic splice sites within the 5'UTR that would result in the synthesis of a functionally monocistronic mRNA, 2) ensure the integrity of the translated bicistronic mRNA, and 3) control for other mechanisms such as termination-reinitiation that could result in the translation of the downstream cistron (15,16).

As an alternative to bicistronic constructs, a suspected IRES element can also be inserted into a circularized mRNA engineered to contain a single continuous open reading frame (17,18). The spatial constraints imposed by circularization of the mRNA molecule do not interfere with IRES function, but cannot support a cap-dependent mechanism of translation initiation.

Part IV: Mechanism of IRES-Mediated Translation

Just as there are few similarities that exist among IRESes in terms of sequence and structure, there is no universal mechanism for internal ribosome entry. For example, whereas the IRES-mediated translation of the encephalomyocarditis virus requires all of the canonical initiation factors except eIF4E (19,20), the IRES-mediated translation of the hepatitis C and cricket paralysis viruses is eIF-independent (21-23); and whereas some IRESes are stimulated by the 3'UTR of the transcript (24-26), others are not. Despite their differences, a couple of commonalities do exist among the known mechanisms of IRES-mediated translation: many IRES activities are stimulated by the poly(A) tail of the transcript, and almost all cellular IRESes require one or more IRES *trans*-acting factors (ITAFs).

The Poly(A)Tail

Almost all eukaryotic mRNAs possess a 3' poly(A) that is 50-300 nucleotides in length. The poly(A) tail of most transcripts is bound with multiple copies of the poly(A)-binding protein (PABP), a 70 kDa protein with four highly conserved RNA recognition motifs (27,28). During translation initiation, PABPs interact with eIF4G, bringing together the 5' and 3' ends of the transcript to form a "closed loop" (Figure 2.1) (29-32). PABP-mediated circularization of the mRNA is known to stimulate both cap-dependent and IRES-mediated translation (29-35), although the exact mechanism by which it does so is still a matter of debate. It has been suggested that the "closed loop" improves translation efficiency by facilitating the utilization or recycling of 40S ribosomal subunits (30,36), promoting 60S ribosomal subunit joining at the start codon (37), and/or causing a conformational change that stimulates eIF4F activity (38).

ITAFs

ITAFs are non-canonical initiation factors that bind directly to the mRNA and are thought to facilitate the recruitment of the 40S ribosomal subunit to the IRES either by interacting with the translation initiation machinery or by modulating the conformation of the transcript (8,39,40). The list of known ITAFs is continually growing. Whereas some ITAFs such as La autoantigen and the polypyrimidine tract binding protein have been shown to be involved in the IRES-mediated translation of numerous transcripts (41-50), others seem to function more specifically. Surprisingly, most of the ITAFs identified to date belong to the group of heterogeneous nuclear ribonucleoproteins (hnRNPs). These include hnRNP A1, C1/C2, I, E1/E2, K, and L (43,51-53). hnRNPs are known to play a role in nuclear RNA processing and thus reside primarily in the nucleus of the cell. However, following the appropriate cellular signal, they relocalize to the cytoplasm where they participate in IRES-mediated translation (54). Such compartmentalization of ITAFs allows for the precise regulation of IRES-mediated translation.

Part V: The Function of Cellular IRESes

Cap-dependent translation initiation is a highly regulated process that is controlled by the availability of eIF4F and the delivery of the ternary complex (eIF2-GTP- initiator methionine-tRNA) to the 43S ribosomal subunit (55). The availability of eIF4E is governed by the concentration of eIF4E-binding proteins. In their hypophosphorylated state, eIF4E-binding proteins interact with eIF4E and prevent its association with eIF4G (56-60). eIF4G itself is controlled by proteolysis. Cleavage of eIF4G disrupts its function by separating the cap and poly(A)-binding domains of the protein from the eIF3 and eIF4A-binding sites (61). Finally, the α subunit of eIF2 can be phosphorylated at Ser51 by the protein kinase HCR, PKR, or GCN2.

Phosphorylation of eIF2α increases the affinity of eIF2 for the guanine-nucleotide-exchange factor eIF2B, and thereby decreases the amount of available ternary complexes (55,62,63).

The sequestration of eIF4E, cleavage of eIF4G, and phosphorylation of eIF2α all inhibit cap-dependent protein synthesis and occur during mitosis, quiescence, differentiation, and apoptosis, and in response to stress conditions such as amino acid starvation, hypoxia, heat/cold shock, viral infection, and exposure to UV radiation (reviewed in (64)). These mechanisms that regulate cap-dependent translation do not affect IRES-mediated translation (58,59). Thus, many of the mRNAs whose expression is required for programmed cell death, cell cycle progression, development, and stress response have been found to harbor IRES elements in their 5'UTRs (Table 2.1). Since internal initiation escapes eIF-mediated translational control, it is believed that IRES-mediated translation has evolved as a regulatory mechanism that enables cells to respond to diverse physiological states against the background of a general reduction in protein synthesis.

Part VI: IRESes that Regulate Folate-Mediated One-Carbon Metabolism

As discussed in Chapter 1, folate-mediated one-carbon metabolism is essential for the *de novo* biosynthesis of purines and thymidylate and for the remethylation of homocysteine to methionine. Purine nucleotides function as precursors for DNA, RNA, coenzymes, energy transfer molecules, and regulatory factors, and their *de novo* biosynthesis is required during human embryonic development (65). Thymidylate is necessary for faithful DNA replication and repair. Decreased levels of thymidylate result in increased uracil misincorporation into DNA, which in turn leads to chromosome damage, fragile site induction, and apoptotic cell death (66). The remethylation of homocysteine to methionine serves to remove cellular homocysteine,

Table 2.1. Mammalian mRNAs that contain IRES

Gene Product	Cellular Function	Reference
cat-1	mediates uptake of arginine and lysine	(67)
p58 PITSLRE	regulates cell cycle progression	(68)
p27	regulates cell cycle progression	(69)
c-, N-, L-myc	Control cell growth, differentiation, and apoptosis	(70-72)
p53	regulates cell cycle arrest and apoptosis	(73)
Apaf-1	initiates apoptosis	(74)
Bag-1	inhibits apoptosis	(75)
XIAP	inhibits apoptosis	(76)
DAP-5	mediates apoptosis induced by INFγ	(77)
VEGFA	increases vascular permeability and angiogenesis	(78)
HIF-1α	plays key role in homeostatic responses to hypoxia	(79)
BiP	aids in folding of nascent proteins upon heat shock	(80)
Rbm3	regulates protein synthesis in response to cold shock	(81)
PDGF2/*c-sis*	autocrine and paracrine growth factor	(82)
FGF2	controls cell proliferation and differentiation	(83)
SNM1	repairs DNA interstrand crosslinks	(84)
elg1	regulates genome stability	(85)

which is a risk factor for cardiovascular disease (86), neural tube defects (87), and Alzheimer's disease (88), and to generate the methyl groups required for transcriptional control. Given the important roles of the folate-dependent enzymes in development, the maintenance of genome stability, and gene expression, it is imperative that they continue to be produced under a variety of physiological and environmental conditions. As some of these conditions may result in the suspension of global cap-dependent protein synthesis, it is no surprise that several of the enzymes involved in folate-mediated one-carbon metabolism have been found to contain IRES elements within their 5UTRs.

The Thymidylate Synthase IRES

Thymidylate synthase (TS) catalyzes the 5,10-methyleneTHF-dependent conversion of deoxyuridine monophosphate (dUMP) to the DNA precursor deoxythymidine monophosphate (dTMP). The 5'UTR of TS varies in length from 140-200 nucleotides depending on the number of tandem repeats, and has a GC content of 76% resulting in extensive secondary structure (Figure 2.2A). Insertion of the TS 5'UTR into a bicistronic mRNA results in expression of the downstream cistron. This expression occurs at a level significantly higher than that of a control β-globulin 5'UTR and is not affected by the presence of an ApppG cap, a structure that is not recognized by eIF4E. The 5'UTR of TS is able to initiate IRES-mediated translation irrespective of the number of tandem repeats present (89).

The Methionine Synthase IRES

Methionine synthase (MS) is a cobalamin (vitamin B12)-dependent enzyme that catalyzes the 5-methyltetrahydrofolate (5-methylTHF)-dependent remethylation of homocysteine to methionine. It is an essential protein as evidenced by the

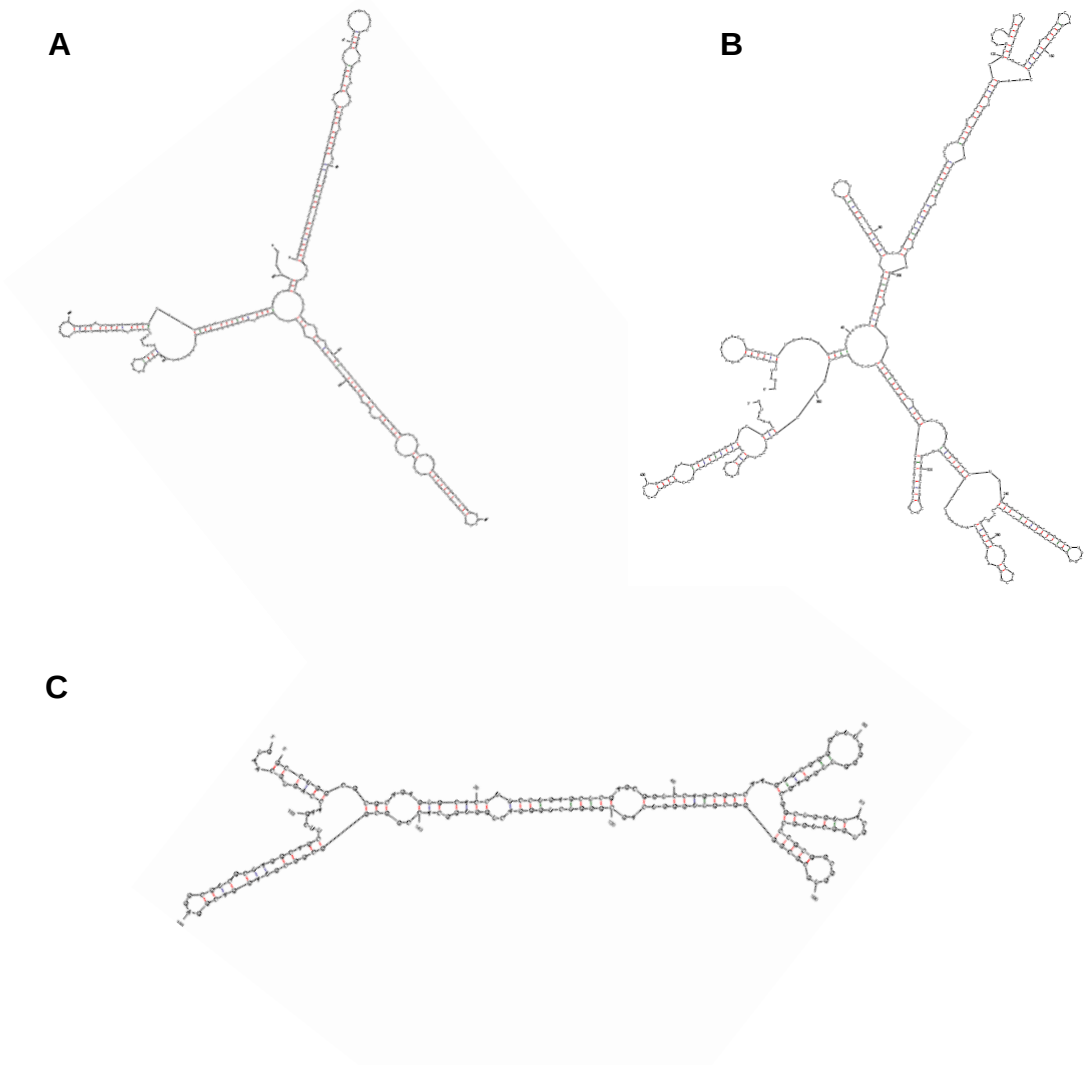

Figure 2.2. The 5'UTRs of transcripts encoding folate-dependent enzymes. (A) The TS 5'UTR is 140 nucleotides in length and has a ΔG of -147 kcal/mol. (B) The MS 5'UTR is 423 nucleotides in length and has a ΔG of -175 kcal/mol. (C) The cSHMT 5'UTR is 190 nucleotides in length and has a ΔG of -90 kcal/mol. Note that although all three 5'UTRs have been shown to contain IRES elements, they do not share common structural motifs. The secondary structures of the UTRs were predicted using the Mfold program (version 3.2) developed by Zuker and Turner.

embryonic lethality of the MS knockout mouse (90). The human MS 5'UTR is 423 nucleotides in length. It contains two upstream open reading frames and has a complex secondary structure with an estimated ΔG of -175 kcal/mol (Figure 2.2B). Insertion of the MS 5'UTR into a bicistronic construct results in expression of the downstream cistron at a level comparable to that of the well-characterized immunoglobulin heavy-chain binding protein (BiP) IRES. Translation of the downstream cistron is not affected by the introduction of a hairpin that inhibits cap-dependent translation or by the rapamycin-induced activation of the eIF4E-binding protein. Northern blot analysis of the mRNA following transfection did not reveal any smaller products arising from a cryptic splice site, and the MS 5'UTR did not exhibit any promoter activity. Treatment of cells with vitamin B12 increased the IRES activity of MS by 60%, presumably by activating a B12-responsive ITAF. Although the physiological significance of the MS IRES is currently unknown, it has been hypothesized that it has evolved as an adaptation to the presence of the rare, but essential, vitamin B12 (91).

The Cytoplasmic Serine Hydroxymethyltransferase IRES

Cytoplasmic serine hydroxymetyltransferase (cSHMT) catalyzes the production of glycine and 5,10-methyleneTHF from serine and THF. The 5,10-methyleneTHF derived from the cSHMT reaction is ultimately used by TS to produce thymidylate at the expense of S-adenosylmethionine (AdoMet) synthesis (92,93). Although cSHMT knockout mice are viable and fertile, they do exhibit elevated levels of uracil in their DNA and decreased levels of AdoMet in their livers (94).

The human cSHMT mRNA has two alternatively spliced forms of its 5'UTR that are encoded by exons 1-3 (95). Exon 2, which encodes an Alu J SINE insertion in reverse orientation (96), is alternatively spliced in a cell-specific manner (97). The

5'UTR that lacks exon 2 is 190 nucleotides in length and contains 71% GC content. It exhibits complex secondary structure with a predicted ΔG of - 90 kcal/mol (Figure 2.2C). When this cSHMT 5'UTR is inserted into a bicistronic construct, the downstream cistron is expressed 15% and 3% relative to expression of the upstream cistron *in vitro* and in unstressed cells, respectively (26). When the 3'UTR of cSHMT is added to the bicistronic construct at the 3' end of the downstream cistron, the downstream cistron is expressed 40% and 6% relative to expression of the upstream cistron *in vitro* and in unstressed cells, respectively (26). Translation of the downstream cistron is not the result of termination-reinitiation, as it is abolished by the replacement of the 5'UTR with the reverse complement of the 5'UTR. It is also not affected by the rapamycin-induced activation of the eIF4E-binding protein, and cannot be explained by cryptic splicing or promoter activity, as *in vitro* transcribed RNA was used instead of DNA in all experiments. The IRES activity of cSHMT is comparable to that of BiP (26), but like all cellular IRES activities, is much less than the IRES activity of viruses (98).

Like the MS IRES, the cSHMT IRES is nutrient-responsive. Overexpression of the iron-storage protein heavy chain ferritin (H ferritin) markedly elevates cSHMT IRES activity and protein levels (26). Furthermore, when bicistronic mRNAs containing the human cSHMT 5'UTR are transfected into mouse embryonic fibroblasts isolated from *H ferritin*$^{+/-}$ embryos, the human cSHMT 5'UTR exhibits 30% less IRES activity than when it is transfected into mouse embryonic fibroblasts isolated from *H ferritin*$^{+/+}$ embryos (26).

The IRES-mediated translation of cSHMT is also stimulated by CUG-binding protein 1 (CUGBP1), an isoform of the hnRNP hNab50 (99). CUGBP1-depleted HeLa cells have reduced cSHMT IRES activity compared to control cells. However, the decrease in IRES activity is only significant when the 3'UTR of cSHMT is

included in the bicistronic mRNA, suggesting that CUGBP1 acts through the 3' end of the transcript (26).

Part VII: Summary

Until 1988, one of the cardinal rules of translation initiation was that eukaryotic ribosomes could only bind to the 5' end of an mRNA transcript. The discovery of an IRES element within the 5'UTR of picornaviral mRNA drastically altered this dogma and paved the way for the identification of numerous IRESes in cellular transcripts. Over the past 20 years, great strides have been made in understanding the cap-independent mechanism of ribosome recruitment. It is now known that IRES activity requires one or more ITAFs and can be stimulated by the poly(A) tail of the transcript. In terms of functionality, it has become clear that IRES-mediated translation allows protein synthesis to escape the controls that regulate cap-dependent initiation and enables translation to occur when ribosome scanning would otherwise be inhibited by a long and structured 5'UTR.

Of the various transcripts shown to contain IRESes, many produce proteins that are involved in the control of cell proliferation, cell growth, gene expression, and cell death. Among them are TS, MS, and cSHMT, which, through their involvement in folate-mediated one-carbon metabolism, play key roles in *de novo* nucleotide biosynthesis, DNA repair, and cellular methylation reactions. Although the TS, MS, and cSHMT IRESes have been extensively characterized and some of the factors that influence their activity have been identified, many questions still remain. For example, what are the physiological conditions that stimulate the cap-independent translation of these transcripts? And what is the mechanism by which the mRNA, potential ITAFs, and translation initiation factors interact and recruit ribosomes? The studies presented herein aim to answer these questions for the cSHMT IRES by 1)

elucidating the interactions among the 5'UTR, 3'UTR, poly(A) tail, 40S ribosomal subunit, and CUGBP1 that contribute to the IRES-activity (Chapter 3),

2) investigating the role of H ferritin in IRES-mediated translation (Chapter 4), and

3) determining physiological function of the cSHMT IRES (Chapter 5).

REFERENCES

1. Gingras, A. C., Raught, B., and Sonenberg, N. (1999) *Annu Rev Biochem* **68**, 913-963
2. Hershey, J. B. W. a. M., W.C. (2000) (N. Sonenberg, J. W. B. H., and M.B. Matthews, ed), pp. 33-88, Cold Spring Harbour Press, Cold Spring Harbour, NY
3. Pestova, T. V., Borukhov, S. I., and Hellen, C. U. (1998) *Nature* **394**, 854-859
4. Rogers, G. W., Jr., Komar, A. A., and Merrick, W. C. (2002) *Prog Nucleic Acid Res Mol Biol* **72**, 307-331
5. Pestova, T. V., Kolupaeva, V. G., Lomakin, I. B., Pilipenko, E. V., Shatsky, I. N., Agol, V. I., and Hellen, C. U. (2001) *Proc Natl Acad Sci U S A* **98**, 7029-7036
6. Lee, J. H., Pestova, T. V., Shin, B. S., Cao, C., Choi, S. K., and Dever, T. E. (2002) *Proc Natl Acad Sci U S A* **99**, 16689-16694
7. Pestova, T. V., Lomakin, I. B., Lee, J. H., Choi, S. K., Dever, T. E., and Hellen, C. U. (2000) *Nature* **403**, 332-335
8. Hellen, C. U., and Sarnow, P. (2001) *Genes Dev* **15**, 1593-1612
9. De Pietri Tonelli, D., Mihailovich, M., Schnurbus, R., Pesole, G., Grohovaz, F., and Zacchetti, D. (2003) *Nucleic Acids Res* **31**, 2508-2513
10. van der Velden, A. W., and Thomas, A. A. (1999) *Int J Biochem Cell Biol* **31**, 87-106
11. Jang, S. K., Krausslich, H. G., Nicklin, M. J., Duke, G. M., Palmenberg, A. C., and Wimmer, E. (1988) *J Virol* **62**, 2636-2643
12. Pelletier, J., and Sonenberg, N. (1988) *Nature* **334**, 320-325

13. Johannes, G., Carter, M. S., Eisen, M. B., Brown, P. O., and Sarnow, P. (1999) *Proc Natl Acad Sci U S A* **96**, 13118-13123

14. Martinez-Salas, E., Lopez de Quinto, S., Ramos, R., and Fernandez-Miragall, O. (2002) *Biochimie* **84**, 755-763

15. Kozak, M. (2003) *Gene* **318**, 1-23

16. Kozak, M. (2005) *Nucleic Acids Res* **33**, 6593-6602

17. Chen, C. Y., and Sarnow, P. (1995) *Science* **268**, 415-417

18. Chen, C. Y., and Sarnow, P. (1998) *Methods Mol Biol* **77**, 355-363

19. Pestova, T. V., Hellen, C. U., and Shatsky, I. N. (1996) *Mol Cell Biol* **16**, 6859-6869

20. Pestova, T. V., Shatsky, I. N., and Hellen, C. U. (1996) *Mol Cell Biol* **16**, 6870-6878

21. Ji, H., Fraser, C. S., Yu, Y., Leary, J., and Doudna, J. A. (2004) *Proc Natl Acad Sci U S A* **101**, 16990-16995

22. Otto, G. A., and Puglisi, J. D. (2004) *Cell* **119**, 369-380

23. Pestova, T. V., Shatsky, I. N., Fletcher, S. P., Jackson, R. J., and Hellen, C. U. (1998) *Genes Dev* **12**, 67-83

24. Dobrikova, E., Florez, P., Bradrick, S., and Gromeier, M. (2003) *Proc Natl Acad Sci U S A* **100**, 15125-15130

25. Song, Y., Friebe, P., Tzima, E., Junemann, C., Bartenschlager, R., and Niepmann, M. (2006) *J Virol* **80**, 11579-11588

26. Woeller, C. F., Fox, J. T., Perry, C., and Stover, P. J. (2007) *J Biol Chem* **282**, 29927-29935

27. Deo, R. C., Bonanno, J. B., Sonenberg, N., and Burley, S. K. (1999) *Cell* **98**, 835-845

28. Gorlach, M., Burd, C. G., and Dreyfuss, G. (1994) *Exp Cell Res* **211**, 400-407

29. Imataka, H., Gradi, A., and Sonenberg, N. (1998) *Embo J* **17**, 7480-7489

30. Kahvejian, A., Roy, G., and Sonenberg, N. (2001) *Cold Spring Harb Symp Quant Biol* **66**, 293-300

31. Tarun, S. Z., Jr., Wells, S. E., Deardorff, J. A., and Sachs, A. B. (1997) *Proc Natl Acad Sci U S A* **94**, 9046-9051

32. Wells, S. E., Hillner, P. E., Vale, R. D., and Sachs, A. B. (1998) *Mol Cell* **2**, 135-140

33. Gallie, D. R. (1991) *Genes Dev* **5**, 2108-2116

34. Munroe, D., and Jacobson, A. (1990) *Mol Cell Biol* **10**, 3441-3455

35. Thoma, C., Bergamini, G., Galy, B., Hundsdoerfer, P., and Hentze, M. W. (2004) *Mol Cell* **15**, 925-935

36. Jacobson, A. (1996) in *Translational Control* (J.W.B. Hershey, M. B. M., and N. Sonenberg, ed), pp. 451-480, Cold Spring Harbor Laboratory Press, Cold Spring Harbor, NY

37. Searfoss, A., Dever, T. E., and Wickner, R. (2001) *Mol Cell Biol* **21**, 4900-4908

38. Lopez-Lastra, M., Rivas, A., and Barria, M. I. (2005) *Biol Res* **38**, 121-146

39. Komar, A. A., and Hatzoglou, M. (2005) *J Biol Chem* **280**, 23425-23428

40. Stoneley, M., and Willis, A. E. (2004) *Oncogene* **23**, 3200-3207

41. Borovjagin, A., Pestova, T., and Shatsky, I. (1994) *FEBS Lett* **351**, 299-302

42. Costa-Mattioli, M., Svitkin, Y., and Sonenberg, N. (2004) *Mol Cell Biol* **24**, 6861-6870

43. Giraud, S., Greco, A., Brink, M., Diaz, J. J., and Delafontaine, P. (2001) *J Biol Chem* **276**, 5668-5675

44. Gosert, R., Chang, K. H., Rijnbrand, R., Yi, M., Sangar, D. V., and Lemon, S. M. (2000) *Mol Cell Biol* **20**, 1583-1595

45. Holcik, M., and Korneluk, R. G. (2000) *Mol Cell Biol* **20**, 4648-4657

46. Hunt, S. L., and Jackson, R. J. (1999) *Rna* **5**, 344-359

47. Kim, Y. K., Back, S. H., Rho, J., Lee, S. H., and Jang, S. K. (2001) *Nucleic Acids Res* **29**, 5009-5016

48. Kim, Y. K., and Jang, S. K. (1999) *J Gen Virol* **80 (Pt 12)**, 3159-3166

49. Mitchell, S. A., Brown, E. C., Coldwell, M. J., Jackson, R. J., and Willis, A. E. (2001) *Mol Cell Biol* **21**, 3364-3374

50. Ray, P. S., and Das, S. (2002) *Nucleic Acids Res* **30**, 4500-4508

51. Bonnal, S., Pileur, F., Orsini, C., Parker, F., Pujol, F., Prats, A. C., and Vagner, S. (2005) *J Biol Chem* **280**, 4144-4153

52. Hahm, B., Kim, Y. K., Kim, J. H., Kim, T. Y., and Jang, S. K. (1998) *J Virol* **72**, 8782-8788

53. Holcik, M., Gordon, B. W., and Korneluk, R. G. (2003) *Mol Cell Biol* **23**, 280-288

54. Lewis, S. M., and Holcik, M. (2008) *Oncogene* **27**, 1033-1035

55. Gebauer, F., and Hentze, M. W. (2004) *Nat Rev Mol Cell Biol* **5**, 827-835

56. Lawrence, J. C., Jr., and Abraham, R. T. (1997) *Trends Biochem Sci* **22**, 345-349

57. Lin, T. A., Kong, X., Haystead, T. A., Pause, A., Belsham, G., Sonenberg, N., and Lawrence, J. C., Jr. (1994) *Science* **266**, 653-656

58. Pause, A., Belsham, G. J., Gingras, A. C., Donze, O., Lin, T. A., Lawrence, J. C., Jr., and Sonenberg, N. (1994) *Nature* **371**, 762-767

59. Poulin, F., Gingras, A. C., Olsen, H., Chevalier, S., and Sonenberg, N. (1998) *J Biol Chem* **273**, 14002-14007

60. Richter, J. D., and Sonenberg, N. (2005) *Nature* **433**, 477-480

61. Lamphear, B. J., Kirchweger, R., Skern, T., and Rhoads, R. E. (1995) *J Biol Chem* **270**, 21975-21983

62. Clemens, M. J. (1994) *Mol Biol Rep* **19**, 201-210

63. Price, N. T., and Proud, C. G. (1990) *Biochim Biophys Acta* **1054**, 83-88

64. Spriggs, K. A., Stoneley, M., Bushell, M., and Willis, A. E. (2008) *Biol Cell* **100**, 27-38

65. Brodsky, G., Barnes, T., Bleskan, J., Becker, L., Cox, M., and Patterson, D. (1997) *Hum Mol Genet* **6**, 2043-2050

66. Takemura, Y., and Jackman, A. L. (1997) *Anticancer Drugs* **8**, 3-16

67. Fernandez, J., Yaman, I., Mishra, R., Merrick, W. C., Snider, M. D., Lamers, W. H., and Hatzoglou, M. (2001) *J Biol Chem* **276**, 12285-12291

68. Cornelis, S., Bruynooghe, Y., Denecker, G., Van Huffel, S., Tinton, S., and Beyaert, R. (2000) *Mol Cell* **5**, 597-605

69. Kullmann, M., Gopfert, U., Siewe, B., and Hengst, L. (2002) *Genes Dev* **16**, 3087-3099

70. Jopling, C. L., Spriggs, K. A., Mitchell, S. A., Stoneley, M., and Willis, A. E. (2004) *Rna* **10**, 287-298

71. Jopling, C. L., and Willis, A. E. (2001) *Oncogene* **20**, 2664-2670

72. Nanbru, C., Lafon, I., Audigier, S., Gensac, M. C., Vagner, S., Huez, G., and Prats, A. C. (1997) *J Biol Chem* **272**, 32061-32066

73. Ray, P. S., Grover, R., and Das, S. (2006) *EMBO Rep* **7**, 404-410

74. Coldwell, M. J., Mitchell, S. A., Stoneley, M., MacFarlane, M., and Willis, A. E. (2000) *Oncogene* **19**, 899-905

75. Coldwell, M. J., deSchoolmeester, M. L., Fraser, G. A., Pickering, B. M., Packham, G., and Willis, A. E. (2001) *Oncogene* **20**, 4095-4100

76. Holcik, M., Lefebvre, C., Yeh, C., Chow, T., and Korneluk, R. G. (1999) *Nat Cell Biol* **1**, 190-192

77. Henis-Korenblit, S., Strumpf, N. L., Goldstaub, D., and Kimchi, A. (2000) *Mol Cell Biol* **20**, 496-506

78. Huez, I., Creancier, L., Audigier, S., Gensac, M. C., Prats, A. C., and Prats, H. (1998) *Mol Cell Biol* **18**, 6178-6190

79. Lang, K. J., Kappel, A., and Goodall, G. J. (2002) *Mol Biol Cell* **13**, 1792-1801

80. Macejak, D. G., and Sarnow, P. (1991) *Nature* **353**, 90-94

81. Chappell, S. A., Owens, G. C., and Mauro, V. P. (2001) *J Biol Chem* **276**, 36917-36922

82. Bernstein, J., Sella, O., Le, S. Y., and Elroy-Stein, O. (1997) *J Biol Chem* **272**, 9356-9362

83. Vagner, S., Gensac, M. C., Maret, A., Bayard, F., Amalric, F., Prats, H., and Prats, A. C. (1995) *Mol Cell Biol* **15**, 35-44

84. Zhang, X., Richie, C., and Legerski, R. J. (2002) *DNA Repair (Amst)* **1**, 379-390

85. Baird, S. D., Lewis, S. M., Turcotte, M., and Holcik, M. (2007) *Nucleic Acids Res* **35**, 4664-4677

86. Refsum, H., Ueland, P. M., Nygard, O., and Vollset, S. E. (1998) *Annu Rev Med* **49**, 31-62

87. Mills, J. L., McPartlin, J. M., Kirke, P. N., Lee, Y. J., Conley, M. R., Weir, D. G., and Scott, J. M. (1995) *Lancet* **345**, 149-151

88. Clarke, R., Smith, A. D., Jobst, K. A., Refsum, H., Sutton, L., and Ueland, P. M. (1998) *Arch Neurol* **55**, 1449-1455

89. Wie, S. a. K., L. (2008) in *Translational Control*, Cold Spring Harbor Laboratory, Cold Spring Harbor, NY

90. Swanson, D. A., Liu, M. L., Baker, P. J., Garrett, L., Stitzel, M., Wu, J., Harris, M., Banerjee, R., Shane, B., and Brody, L. C. (2001) *Mol Cell Biol* **21**, 1058-1065

91. Oltean, S., and Banerjee, R. (2005) *J Biol Chem* **280**, 32662-32668

92. Herbig, K., Chiang, E. P., Lee, L. R., Hills, J., Shane, B., and Stover, P. J. (2002) *J Biol Chem* **277**, 38381-38389

93. Oppenheim, E. W., Adelman, C., Liu, X., and Stover, P. J. (2001) *J Biol Chem* **276**, 19855-19861

94. MacFarlane, A. J., Liu, X., Perry, C. A., Flodby, P., Allen, R. H., Stabler, S. P., and Stover, P. J. (2008) *J Biol Chem* **283**, 25846-25853

95. Liu, X., Reig, B., Nasrallah, I. M., and Stover, P. J. (2000) *Biochemistry* **39**, 11523-11531

96. Xing, J., Hedges, D. J., Han, K., Wang, H., Cordaux, R., and Batzer, M. A. (2004) *J Mol Biol* **344**, 675-682

97. Girgis, S., Nasrallah, I. M., Suh, J. R., Oppenheim, E., Zanetti, K. A., Mastri, M. G., and Stover, P. J. (1998) *Gene* **210**, 315-324

98. Fox, J. T., and Stover, P. J. (Unpublished Results)

99. Timchenko, L. T., Miller, J. W., Timchenko, N. A., DeVore, D. R., Datar, K. V., Lin, L., Roberts, R., Caskey, C. T., and Swanson, M. S. (1996) *Nucleic Acids Res* **24**, 4407-4414

CHAPTER 3

MECHANISM OF THE INTERNAL RIBOSOME ENTRY SITE-MEDIATED TRANSLATION OF CYTOPLASMIC SERINE HYDROXYMETHYLTRANSFERASE

Abstract

The 5' untranslated region (UTR) of cytoplasmic serine hydroxymethyltransferase (cSHMT) contains an internal ribosome entry site (IRES) that regulates thymidylate biosynthesis. IRESes permit efficient 5'-cap-independent translation by interacting with IRES *trans*-acting factors (ITAFs) and recruiting the 40S ribosomal subunit, although the mechanism of IRES-mediated translation has yet to be established. In this study, we show that the cSHMT IRES is the first example of a cellular IRES that is poly(A) tail-independent. Interactions between the 5'UTR and 3'UTR functionally replace interactions between the poly(A) tail and the poly(A) binding protein (PABP) to achieve maximal IRES-mediated translational efficiency. Depletion of the cSHMT ITAF CUG-Binding Protein 1 (CUGBP1) from *in vitro* translation extracts or deletion of the CUGBP1-binding site on the 3'UTR of the cSHMT transcript decreases the IRES activity of non-polyadenylated biscistronic mRNAs relative to polyadenylated biscistronic mRNAs and results in a requirement for PABP. We also identify a novel ITAF, heterogeneous nuclear ribonucleoprotein H2 (hnRNP H2), that stimulates cSHMT IRES activity by binding to the 5'UTR of the transcript and interacting with CUGBP1. Collectively, these data support a model for the IRES-mediated translation of cSHMT whereby the circularization of the mRNA typically provided by the eukaryotic initiation factor (eIF)4G/PABP/poly(A) tail interaction is instead achieved through the hnRNP H2/CUGBP1-mediated interaction

of the 5' and 3'UTRs of the cSHMT transcript. This circularization enhances the IRES activity of cSHMT by facilitating the recruitment and/or recycling of 40S ribosomal subunits, which bind to the transcript in the middle of the 5'UTR and migrate to the initiation codon via eIF4A-mediated scanning.

Introduction

Internal ribosome entry sites (IRESes) are *cis*-acting elements that enable the cap-independent recruitment of 40S ribosomal subunits to the 5' untranslated region (UTR) of an mRNA transcript. Although originally identified in viruses (1,2), IRESes have recently been discovered in many cellular mRNAs, particularly in those encoding proteins involved in development, differentiation, cell cycle progression, cell growth, apoptosis, and stress response (reviewed in (3,4)). It is now estimated that as many as 3-5% of cellular mRNAs can be translated by a cap-independent mechanism (5). Although the list of cellular IRESes continues to grow, little is known about their mechanism of action. However, there is increasing evidence that in addition to the 40S ribosomal subunit and canonical initiation factors, the poly(A) tail of the transcript and IRES-specific *trans*-acting factors (ITAFs) play major roles during cap-independent translation.

Almost all eukaryotic mRNAs possess a 3' poly(A) tail that can enhance both cap-dependent and IRES-mediated translation initiation (6,7). The interaction of Poly(A) Binding Protein (PABP) with eukaryotic initiation factor (eIF) 4G results in the formation of a "closed loop" by linking the poly(A) tail and either the 5'-cap (in cap-dependent translation) or the 5'UTR (in IRES-mediated translation). Looping through the 5' and 3' ends of the transcript is thought to increase translation rates by facilitating the recycling of 40S ribosomal subunits, promoting 40S recruitment, and/or stimulating the formation of the 80S ribosome (8-16). It has also recently been

reported that the poly(A) tail can enhance 48S complex assembly through a process that is independent of PABP (17).

ITAFs are RNA-binding proteins that functionally interact with IRES elements to positively or negatively regulate internal initiation. Many of the ITAFs identified to date belong to the group of heterogeneous nuclear ribonucleoproteins (hnRNPs). These include hnRNP A1, C1/C2, I, E1/E2, K, and L (18-21). hnRNPs are located primarily in the nucleus, but are known to translocate to the cytoplasm in specific cell or tissue types and as part of certain stress responses. It is hypothesized that hnRNPs and other ITAFs exert their effect on IRES activity by aiding in the recruitment of the 40S ribosomal subunit through their interactions with the canonical initiation factors or ribosomal components, or by acting as RNA chaperones to control the configuration of the IRES (Reviewed in (4,22)). Studies of viral IRESes have suggested that ITAFs can also establish an RNA/protein bridge between the IRES and the 3' end of the transcript (23).

In this study, we investigate the role of the poly(A) tail, ITAFs, and the 40S ribosomal subunit in the IRES-mediated translation of cytoplasmic serine hydroxymethyltransferase (cSHMT), an enzyme that regulates folate-dependent *de novo* thymidylate biosynthesis during S-phase (24,25) and in response to UV exposure (Chapter 5). The data presented here lead to the development of a model for the IRES-mediated translation of cSHMT and provide a mechanism that accounts for the previously reported finding that cSHMT IRES activity is stimulated by the cSHMT 3'UTR (25).

Materials and Methods

Cell culture and preparation of extracts- Mammary adenocarcinoma (MCF-7) cells were obtained from ATCC (HTB22) and were cultured in α-MEM (Hyclone

Laboratories) containing 11% fetal bovine serum (Hyclone Laboratories) at 37^{o}C and 5% CO_2. When the cells reached approximately 95% confluence, they were harvested by trypsinization and washed in phosphate-buffered saline. To obtain whole cell extract, cells were resuspended in lysis buffer (50 mM Tris pH 7.5, 150 mM NaCl, 1% NP-40, 5 mM EDTA, 1 mM PMSF, 1:100 dilution of Sigma Protease Inhibitor Cocktail) and lysed on ice for 30 min. When necessary, the cell extract was treated with λ phosphatase (Sigma) in the presence of 2 mM $MnCl_2$ for 30 min at 30^{o}C. λ phosphatase activity was then inhibited by the addition of EDTA to a final concentration of 50 mM followed by heating at 65^{o}C for 1h. The protein concentration of the extract was determined using the Lowry Assay as modified by Bensadoun (26).

Vectors- The generation of bicistronic DNA templates containing the BiP IRES, the cSHMT 5'UTR, the full length cSHMT 3'UTR, and the reverse complement of the cSHMT 5'UTR is described elsewhere (25). The paip2 coding sequence (27) was subcloned into the pGEX4T-2 vector (GE Healthcare) using the primers 5'-TA**GGATCC**ATGAAAGATCCAAGTCGCAG-3' and 5'-TA**GTCGAC**TCAAATATTTCCGTACTTCAC-3'
where the BamHI and SalI restriction sites are shown in bold. The CUGBP1-pMAL vector was a gift from Lubov Timchenko. The hnRNP H2 cDNA (a gift from Jeffrey Wilusz) was subcloned into the pMAL-c2E vector (New England BioLabs) using the primers 5'-TC**GGATCC**ATGATGCTGAGCACGGAAG-3' and 5'-TA**GTCGAC**CTAAGCAAGGTTTGACTG-3' where the BamHI and SalI restriction sites are shown in bold. The cSHMT 3'UTR truncations were cloned using the following primers: 3'UTR Fwd = 5'-AGGAGCGGGCCCACTCTGGAC-3', 3'UTR (157) Rev = 5'-GTGAAGAAAACATGAAAAAAG-3', 3'UTR (200) Rev = 5'-GTCCCAGAATTACTAACAATGAG-3', 3'UTR (236) Rev = 5'-

GAAAGCCAGGTTCAAATTTAAATCC-3', 3'UTR (317) Rev = 5'-TTGCCCTACACCACCATCTA-3'
3'UTR (477) Rev = 5'-AGCCTCAGAAGCTAATTCAG-3', 3'UTR (637) Rev = 5'-CTGGTTGCTTCTCACACCAG-3'. The cSHMT 5'UTR truncations were cloned using the following primers: 5'UTR Fwd= 5'-GCCTGGCGCGCAGAGTGCACCTTCC-3', 5'UTR Rev = 5'-TGCACTGGTTCGAAGCTGCCTAGCGAC-3', 5'UTR (104) Rev = 5'-GCGCACCGCCGCGGGCCAGCCACG-3', 5'UTR (105) Fwd= 5'-GGGGCGTTGGGTCAGCGGGTCTGGG-3', 5'UTR (50) Fwd = 5'-TTCGGGGTTTGGGGTTGGAGCGGCTG-3', 5'UTR (150) Rev = 5'-GCCGCCGCCGGTGCCACCAGTCCC-3', 5'UTR (114) Rev = 5'-CCAACGCCCCGCGCACCGCCGCGG-3', 5'UTR (131) Rev = 5'-GTCCCAGACCCGCTGACCCAACGCC-3'. The pcDNA 3 template containing the HCV IRES 3' of the Renilla luciferace reporter gene and 5' of the Firefly luciferase reporter gene was a gift from the laboratory of Partho Ray.

In vitro transcription- DNA templates were linearized and purified using the Roche PCR clean-up column. The templates were transcribed using Ambion's MEGAscript kit (for uncapped mRNA) or mMESSAGE mMACHINE kit (for capped mRNA) according to the manufacturer's protocol. For preparation of radiolabeled mRNA for electrophoretic gel mobility shift assays, 50μCi of [α–^{32}P]-labeled rUTP (800Ci/mM, Perkin Elmer) was included in *in vitro* transcription reactions. The crude mRNA was treated with DNase I (Ambion) for 15 min at 40°C and precipitated in 2 M LiCl at -80°C. All RNA procedures were conducted under RNase-free conditions and all mRNA was stored with Recombinant RNasin® Ribonuclease Inhibitor (Promega). The mRNA was quantified by spectrophotometry and its quality verified by electrophoresis.

RNA affinity chromatography- 1.0 nmol of the indicated *in vitro* transcribed mRNA (uncapped and polyadenylated) was incubated with 1.0 nmol biotinylated oligo (dT) probe (Promega) and 200 µl packed streptavidin agarose (Novagen) in TMK buffer (50 mM Tris pH 7.5, 10 mM $MgCl_2$, 150 mM KCl) for 1 h at 4°C. After extensive washing with TMK buffer, the agarose was resuspended in TMK buffer containing 1.0 nmol of *in vitro* transcribed RevUTR mRNA (competitor mRNA, uncapped and non-polyadenylated), 3.0 mg whole cell extract, 150 µg yeast tRNA (Ambion), and 600 units Recombinant RNasin® Ribonuclease Inhibitor (Promega). Following incubation for 1 h at 4°C, the agarose was washed extensively with TMK buffer, and bound proteins were eluted in 2X SDS-PAGE sample buffer (160 mM Tris pH 6.8, 20 mM DTT, 4% SDS, 20% glycerol) at 95°C for 5 min. The eluted proteins were separated by SDS-PAGE and either stained with coomassie blue or subjected to western blot analysis. Sequencing was performed at the Harvard Microchemistry Facility by microcapillary reverse-phase HPLC nano-electrospray tandem mass spectrometry (µLC/MS/MS).

RNA immunoprecipitation- MCF-7 cells were grown to approximately 95% confluence and then treated with 10,000 µJ/cm^2 UVC (254 nm) using the Stratagene UV Stratalinker 2400. 22h following UV treatment, the cells were treated with formaldehyde at a final concentration of 1%. After a 20 min incubation at room temperature, the crosslinking reaction was quenched by the addition of glycine to a final concentration of 125 mM. Following a 10 min incubation at room temperature, the cells were washed in cold phosphate-buffered saline and resuspended in lysis buffer (50 mM Tris pH 7.5, 150 mM NaCl, 1% NP-40, 5 mM EDTA, 1 mM PMSF, 1:100 dilution of Sigma Protease Inhibitor Cocktail, 1 unit/mL Recombinant RNasin® Ribonuclease Inhibitor (Promega)). Following a 30 min incubation on ice and centrifugation at 13,000 rpm for 10 min at 4°C, the supernatant was removed and

diluted 1:10 in IP buffer (0.01% SDS, 1.1% Triton X-100, 1.2 mM EDTA, 16.7 mM Tris pH 8, 167 mM NaCl, 1 mM PMSF, 1:100 dilution of Sigma Protease Inhibitor Cocktail, 1 unit/mL Recombinant RNasin® Ribonuclease Inhibitor (Promega)). 1 mL aliquots of the diluted lysate were incubated with 10 µg antibody overnight at 4°C. The antibodies used include ImmunoPure goat IgG (Pierce), ImmunoPure mouse IgG (Pierce), goat anti-hnRNP H (N-16, Santa Cruz Biotechnology), and mouse anti-CUGBP1 (3B1, Santa Cruz Biotechnology). 100 µl packed Immobilized Protein G (Pierce) was then added and the lysate incubated for 2 h at 4°C in the presence of 0.1 mg/mL BSA. After washing the beads once in low-salt wash buffer (0.1% SDS, 1% Triton X-100, 2 mM EDTA, 20 mM Tris pH 8, 150 mM NaCl), once in high-salt wash buffer (0.1% SDS, 1% Triton X-100, 2 mM EDTA, 20 mM Tris pH 8, 500 mM NaCl), once in LiCl wash buffer (0.25 M LiCl, 1% NP-40, 1% deoxycholate, 1 mM EDTA, 10 mM Tris pH 8) and twice in TE (10 mM Tris pH 8, 1 mM EDTA), bound proteins were eluted in elution buffer (1% SDS, 0.1 M $NaHCO_3$, 1 unit/mL Recombinant RNasin® Ribonuclease Inhibitor (Promega)) at room temperature for 15 min. To reverse the crosslinking, NaCl was added to a final concentration of 200 mM, and the samples were heated at 65°C for 3h. Following treatment with Proteinase K for 45 min at 42°C, the nucleic acids were purified by phenol/chloroform extraction followed by ethanol precipitation. DNA was then removed by treatment with DNase I (Promega) according to the manufacturer's protocol. Reverse transcription was carried out on the remaining RNA using the SuperScript III First-Strand Synthesis System for RT-PCR (Invitrogen) according to the manufacturer's protocol. The resulting cDNA was amplified using the 5'UTR (50) Fwd, 5'UTR (150) Rev, 3'UTR Fwd, and 3'UTR (236) Rev primers described above.

Western blotting- Proteins were separated by SDS-PAGE and transferred to a PVDF membrane. The membrane was blocked with 5% non-fat dry milk in

phosphate-buffered saline containing 1% NP-40 for 1 hour at room temperature, incubated with primary antibody overnight at 4^{o}C, and incubated with horseradish peroxidase-conjugated anti-IgG for 1-3 h at room temperature. After each incubation, the membrane was washed with phosphate-buffered saline/0.1% Tween20. Proteins were visualized using Super Signal® substrate (Pierce) followed by autoradiography. When necessary, membranes were stripped with 0.2 M NaOH. Mouse anti-CUGBP1 (3B1, Santa Cruz Biotechnology) was used at a 1:10,000 dilution, sheep anti-human cSHMT was used at a 1:40,000 dilution, goat anti-hnRNP H (N-16, Santa Cruz Biotechnology) was used at a 1:500 dilution, mouse anti-PABP (10E10, Santa Cruz Biotechnology) was used at a 1:1000 dilution, mouse anti-phospho-serine/threonine (BD Transduction Laboratories) was used at a 1:1000 dilution, and mouse anti-GAPDH (Novus Biologicals) was used at a 1:40,000 dilution. Goat anti-mouse IgG, rabbit anti-sheep IgG, and rabbit anti-goat IgG were all purchased from Pierce and used at a 1:5,000 dilution.

Purification of recombinant proteins- BL21* cells were transformed with the pMAL, CUGBP1-pMAL, hnRNP H2-pMAL, paip2-pGEX, or pGEX vector and grown to mid-log phase. Protein synthesis was induced with isopropyl β-D-thiogalactopyranoside (final concentration 0.1 mM) for 16 h at 18^{o}C. The cells were lysed in B-PER (Pierce) followed by sonication with a Branson Digital Sonifier at 50% amplitude with intermittent icing. After removal of the insoluble material, the clarified supernatant was applied directly to an Amylose Resin (New England BioLabs) for purification of MBP-tagged proteins or GST-Bind Resin (Novagen) for purification of GST-tagged proteins, and the protein was purified according to the manufacturer's protocol. The purity of the protein was determined by SDS-PAGE, and its concentration was determined using the Lowry Assay as modified by Bensadoun (26).

RNA electrophoretic gel mobility shift assays- 20 nM [α–^{32}P]-labeled RNA and the indicated amount of recombinant protein were added to binding buffer (20 mM Tris pH 7.5, 5 mM $MgCl_2$, 1 mM EDTA, 8 mM DTT, 2 μg BSA, 1.25 μg yeast tRNA (Ambion), 10% glycerol, 40 units Recombinant RNasin® Ribonuclease Inhibitor (Promega)) for a total volume of 10 μL. The binding reaction was incubated at 37°C for 15 min and then run on a 4% native polyacrylamide gel at 32 mA. Electrophoresis buffer contained 25 mM Tris base, 0.2 M glycine, and 1 mM EDTA. For competition experiments, 200 nM, 1 μM, or 2 μM unlabeled RNA was pre-incubated with the protein for 5 min prior to its addition to the binding reaction.

Depletion of proteins from rabbit reticulocyte lysate and in vitro translation reactions- To deplete PABP, Flexi® Rabbit Reticulocyte Lysate (Promega) was incubated with GST-paip2-bound resin for 1 h at 4°C. The resin was then collected by centrifugation and the supernatant was subjected to a second incubation with GST-paip2-bound resin for 1 h at 4°C. The resin was then collected by centrifugation, and the supernatant used in *in vitro* translation reactions. To immunodeplete CUGBP1 or hnRNP H, Flexi® Rabbit Reticulocyte Lysate was incubated with mouse anti-CUGBP1 (3B1, Santa Cruz Biotechnology) or goat anti-hnRNP H (N-16, Santa Cruz Biotechnology) for 1 h at 4°C. Immobilized Protein A/G beads (Pierce) were then added. Following a 1 h incubation at 4°C, the beads were collected by centrifugation and the supernatant was used in *in vitro* translation reactions. *In vitro* translation reactions (25 μl) contained 12.5 μl Flexi® Rabbit Reticulocyte Lysate, 20 μM amino acids, 2 mM DTT, 100 ng yeast tRNA (Ambion), 80 mM KCl, 0.5 mM Mg acetate, 20 units Recombinant RNasin® Ribonuclease Inhibitor (Promega), and 125 ng *in vitro* transcribed mRNA. When necessary, the mRNA was pre-incubated with recombinant protein for 10 min at room temperature prior to its addition to the *in vitro* translation reaction. Reactions were carried out at 30ºC for 20 min. Renilla and Firefly

Luciferase expression was quantified on a Veritas Microplate Luminometer (Turner Biosystems) using the Dual-Glo Luciferase Assay System (Promega) according to the manufacturer's protocol.

siRNA and mRNA transfections- MCF-7 cells were grown to approximately 40% confluence in 6-well plates. The cells were transfected with 5 nM of either negative control siRNA (Ambion) or hnRNP H2 siRNA (Qiagen, sense: r(CAU GAG AGU ACA UAU UGA A)dTdT, antisense: r(UUC AAU AUG UAC UCU CAU G)dGdG) using the HiPerFect transfection reagent (Qiagen) according to the manufacturer's instructions. Following incubation with siRNA for approximately 50 h at 37^{o}C and 5% CO_2, the cells were treated with 10,000 μJ/cm^2 UVC (254 nm) using the Stratagene UV Stratalinker 2400. 12 h after UV treatment, the cells were incubated in Opti-MEM (Invitrogen) containing a 1:100 dilution of DMRIE-C transfection reagent (Invitrogen) and 5 μg/mL mRNA (capped and polyadenylated) for 4 h at 37^{o}C and 5% CO_2. The Opti-MEM was then replaced with α-MEM and the cells incubated for an additional 6 h at 37^{o}C and 5% CO_2. Renilla and Firefly Luciferase expression was quantified on a Veritas Microplate Luminometer (Turner Biosystems) using the Dual-Glo Luciferase Assay System (Promega) according to the manufacturer's protocol.

Yeast two-hybrid assay- CUGBP1 cDNA was amplified and cloned into the pGBK plasmid (Clontech) using the following primers: 5'-TC**GAATTC**ATGAACGGCACCCTGGA-3' and 5'-TC**GGATCC**TCAGTAGGGCTTGCTGT-3'. The EcoRI and BamHI sites are shown in bold. hnRNP H2 cDNA was amplified and cloned into the pGAD plasmid (Clontech) using the following primers: 5'-TC**CATATG**ATGATGCTGAGCACGGAAG -3' and 5'-TC**CTCGAG**CTAAGCAAGGTTTGACTG -3'. The NdeI and XhoI sites are shown

in bold. The pGBK-CUGBP1 vector was transformed into yeast strain AH109 and stable clones were maintained in Trp- dropout medium. The pGAD-hnRNP H2 vector was transformed into yeast strain Y187 and stable clones were maintained in Leu- dropout medium. The transformed yeast were then mated following the Clontech Matchmaker protocol. After a 24 h mating, cells were plated on His-, Leu-, Trp- dropout medium containing X-α-gal, and incubated at 30°C for 4 days. Clones were validated against negative controls according to the Matchmaker protocol.

Coimmunoprecipitation- MCF-7 cells were grown to approximately 95% confluence and formaldehyde was added at a final concentration of 1%. After a 20 min incubation at 37°C, the crosslinking reaction was quenched by the addition of glycine to a final concentration of 125 mM. After a 10 min incubation at 37°C, the cells were washed in cold Tris-buffered saline, harvested, and resuspended in lysis buffer (50 mM Tris pH 7.5, 150 mM NaCl, 1% NP-40, 5 mM EDTA, 1 mM PMSF, 1:100 dilution of Sigma Protease Inhibitor Cocktail). The cells were sonicated 5 X 30 sec with a Branson Digital Sonifier at 25% amplitude with intermittent icing. Following centrifugation at 13,000 rpm for 32 min at 4°C, the supernatant was removed and incubated with 10 μg antibody overnight at 4°C. The antibodies used include ImmunoPure Goat IgG (Pierce), mouse anti-HA (Santa Cruz Biotechnology), goat anti-hnRNP H (N-16, Santa Cruz Biotechnology), and mouse anti-CUGBP1 (3B1, Santa Cruz Biotechnology). 100 μl packed Immobilized Protein G (Pierce) was then added and the lysate incubated for 3 h at 4°C. After washing the beads extensively with lysis buffer, bound proteins were eluted in elution buffer (50 mM Tris pH 7.5, 10 mM EDTA, 1%SDS) at 95°C for 10 min. To reverse the crosslinking, 6X SDS-PAGE sample buffer (480 mM Tris pH 6.8, 60 mM DTT, 12% SDS, 60% glycerol) was added to a final concentration of 1X, and the samples were heated at 95°C for 20 min. For the recombinant protein immunoprecipitation, 1 μg MBP-

CUGBP1 was combined with 1 μg MBP-hnRNP H2 and 4 μg antibody in a final volume of 1 mL. Following an overnight incubation at 4°C, 100 μl packed Immobilized Protein G (Pierce) was added and the mixture incubated for 3 h at 4°C. After washing the beads extensively with lysis buffer, bound proteins were eluted in 2X SDS-PAGE sample buffer (160 mM Tris pH 6.8, 20 mM DTT, 4% SDS, 20% glycerol) at 95°C for 10 min.

Hippuristanol treatment- MCF-7 cells were transfected with *in vitro* transcribed mRNA according to the protocol above. 10 h after transfection, the indicated amount of hippuristanol (a gift from Junichi Tanaka) or an equal volume of vehicle (DMSO) was added to the culture medium and the cells were incubated at 37°C and 5% CO_2 for an additional 11 h. Luciferase activity was then quantified as stated above.

Introduction of ORFs into the cSHMT 5'UTR- A stop codon was introduced into the 5'UTR of the bicistronic construct lacking the 3'UTR according to the Quick Change II Site Directed Mutagenesis protocol (Stratagene) using the following primers: Stop Fwd= 5'-GTCGCTAGGCAGCTTCGAAC**TAG**TGCAATG-3' and Stop Rev= 5'-CATTGCA**CTA**GTTCGAAGCTGCCTAGCGAC-3'. Start codons were then introduced into the resulting construct via Quick Change II Site Directed Mutagenesis using the following primers: 52 AUG Fwd= 5'-GGTCCAGCGCCAAGT**ATG**GGGTTTGGGGTTGG-3', 52 AUG Rev= 5'-CCAACCCCAAACCC**CAT**ACTTGGCGCTGGACC-3', 70 AUG Fwd= 5'-GGGTTTGGGGTTGGA**ATG**GCTGGTCACGTGGC-3', 70 AUG Rev= 5'-GCCACGTGACCAGC**CAT**TCCAACCCCAAACCC-3', 82 AUG Fwd= 5'-GGAGCGGCTGGTAAC**ATG**GCTGGCCCGC-3', 82 AUG Rev= 5'-GCGGGCCAGC**CAT**GTTACCAGCCGCTCC-3', 103 AUG Fwd= 5'-GGCTGGCCCGCGGCGGAGC**ATG**GGGCGTTGGGTCAGC-3', 103 AUG Rev=

5’-GCTGACCCAACGCCC**CAT**GCTCCGCCGCGGGCCAGCC-3’, 118 AUG Fwd= 5’-GGGCGTTGGGTC**ATG**GGGTCTGGGACTGG-3’, 118 AUG Rev= 5’-CCAGTCCCAGACCC**CAT**GACCCAACGCCC-3’, 139 AUG Fwd= 5’-GGGACTGGTGGC**ATG**GGCGGCGGCGTAG-3’, 139 AUG Rev= 5’-CTACGCCGCCGCC**CAT**GCCACCAGTCCC-3’, 151 AUG Fwd= 5’-GCACCGGCGGCGGC**ATG**GGACGGAGGCGTCG-3’, 151 AUG Rev= 5’-CGACGCCTCCGTCC**CAT**GCCGCCGCCGGTGC-3’, 169 AUG Fwd= 5’-GGACGGAGGCGTGGC**ATG**GCAGCTTCGAAC-3’, and 169 AUG Rev= 5’-GTTCGAAGCTGC**CAT**GCCACGCCTCCGTCC-3’. The stop and start codons are shown in bold. To determine if the introduction of the start codon affected the secondary structure of the mRNA, each start codon was mutated via Quick Change II Site Directed Mutagenesis using the following primers: 52 GUG Fwd= 5’-GGTCCAGCGCCAAGT**GTG**GGGTTTGGGGTTGG-3’, 52 GUG Rev= 5’-CCAACCCCAAACCC**CAC**ACTTGGCGCTGGACC-3’, 70 UUG Fwd= 5’-GGGTTTGGGGTTGGA**TTG**GCTGGTCACGTGGC-3’, 70 UUG Rev= 5’-GCCACGTGACCAGC**CAA**TCCAACCCCAAACCC-3’, 82 UUG Fwd= 5’-GGAGCGGCTGGTAAC**TTG**GCTGGCCCGC-3’, 82 UUG Rev= 5’-GCGGGCCAGC**CAA**GTTACCAGCCGCTCC-3’, 103 UUG Fwd= 5’-GGCTGGCCCGCGGCGGAGC**TTG**GGGCGTTGGGTCAGC-3’, 103 UUG Rev= 5’-GCTGACCCAACGCCC**CAA**GCTCCGCCGCGGGCCAGCC-3’, 118 AUA Fwd= 5’-GGGCGTTGGGTC**ATA**GGGTCTGGGACTGG-3’, 118 AUA Rev= 5’-CCAGTCCCAGACCC**TAT**GACCCAACGCCC-3’, 139 AUA Fwd= 5’-GGGACTGGTGGC**ATA**GGCGGCGGCGTAGG-3’, 139 AUA Rev= 5’-CCTACGCCGCCGCC**TAT**GCCACCAGTCCC-3’, 151 UUG Fwd= 5’-GCACCGGCGGCGGC**TTG**GGACGGAGGCGTCG-3’, 151 UUG Rev= 5’-CGACGCCTCCGTCC**CAA**GCCGCCGCCGGTGC-3’, 169 UUG Fwd= 5’-

GGACGGAGGCGTGGC**TTG**GCAGCTTCGAAC-3', and 169 UUG Rev= 5'-GTTCGAAGCTGC**CAA**GCCACGCCTCCGTCC-3'. The mutated start codons are shown in bold. All mutations were verified by sequencing at the Cornell Biotechnology Resource Center.

Results

The poly(A) tail and PABP are not required for maximal cSHMT IRES activity. To investigate the influence of the poly(A) tail on the cap-independent translation of cSHMT, the IRES activity of bicistronic mRNAs with and without the stimulatory cSHMT 3'UTR (25) and with and without an A_{30} tail (Figure 3.1A) was determined *in vitro* using nuclease-treated rabbit reticulocyte lysate. This cell-free system was selected over a cell culture model as it eliminates the potential for artificially reduced translation efficiency of the non-polyadenylated bicistronic mRNA resulting from decreased competition with endogenous polyadenylated mRNAs. IRES-mediated translation, as measured by the ratio of Firefly Luciferase (Fluc) to Renilla Luciferase (Rluc) activity, was independent of the poly(A) tail when the cSHMT 3'UTR was present in the transcript (Figure 3.1B). However, removal of the 3'UTR resulted in a 40% decrease in the IRES-mediated translation of non-polyadenylated RNA relative to RNA containing a poly(A) tail (Figure 3.1B). Changes in the stability of the bicistronic mRNA lacking the 3'UTR were not responsible for the observed stimulatory effect of the poly(A) tail (Figure 3.1C).

The poly(A) tail affects IRES activity through its interaction with PABP (8-15). Depletion of PABP from rabbit reticulocyte lysate with immobilized poly(A)-interacting protein 2 (paip2) (27) significantly reduced PABP protein levels (Figure 3.1D). Depletion of PABP by this procedure has been shown not to affect the concentration of other initiation factors (7). PABP-depletion had no significant effect

Figure 3.1. The poly(A) tail and PABP are not required for maximal cSHMT IRES activity. (A) The bicistronic construct used to quantify cSHMT IRES activity. It consists of (in the 5' to 3' direction) a cap analog, the Renilla luciferase (Rluc) reporter gene, the human cSHMT 5'UTR, the Firefly luciferase (Fluc) reporter gene, and, where indicated, the human cSHMT 3'UTR and a 30 nucleotide poly(A) tail. (B) *In vitro* translation assays were carried out using rabbit reticulocyte lysate and *in vitro* transcribed bicistronic mRNAs with (5'UTR + 3'UTR) and without (5'UTR) the cSHMT 3'UTR. The white bars represent the ratio of IRES-mediated translation (Fluc) to cap-dependent translation (Rluc) of bicistronic mRNA containing a 30 nucleotide poly(A) tail, and the dark bars represent the Fluc/Rluc of bicistronic mRNA lacking a poly(A) tail. The relative ratio for each bicistronic mRNA containing a poly(A) tail was given a value of 1.0. The data represent the average of three independent experiments $\pm$ standard error. (C) The bicistronic mRNAs described in (A) were labeled with ^{32}P, and i*n vitro* translation assays were performed as described in Materials and Methods. The RNAs were resolved on an agarose gel and transferred to a positively charged nylon membrane. For each transcript, the left lane represents the mRNA before the *in vitro* translation reaction and the right lane represents the transcript after the *in vitro* translation reaction. (D) Rabbit reticulocyte lysate was incubated with either GST (control) or GST-paip2 (PABP-depleted). The depletion of PABP by GST-paip2 but not GST alone was confirmed by immunoblotting (right) using an antibody against PABP. GAPDH served as a control for equal protein loading. The graph on the left shows the relative IRES activity (as measured by Fluc/Rluc) of the bicistronic mRNAs in control (striped bars) and PABP-depleted (black bars) rabbit reticulocyte lysate. The relative luminosity for each bicistronic mRNA in the control reaction was given a value of 1.0. The data represent the average of three independent experiments $\pm$ standard error.

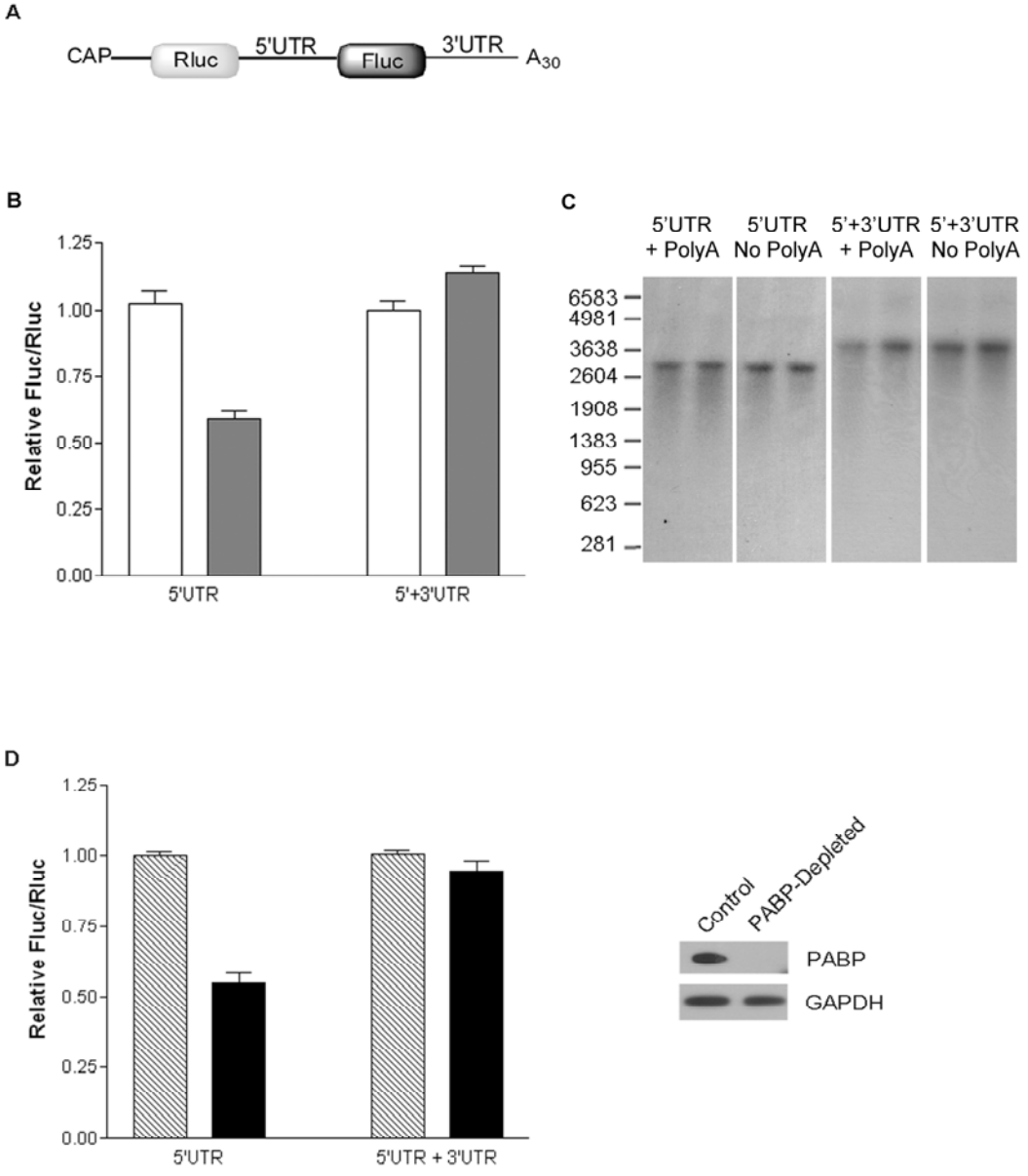
A
CAP
Rluc
5'UTR
Fluc
3'UTR
A30
B
Relative Fluc/Rluc
1.25
1.00
0.75
0.50
0.25
0.00
5'UTR
5'+3'UTR
C
5'UTR + PolyA
5'UTR No PolyA
5'+3'UTR + PolyA
5'+3'UTR No PolyA
6583
4981
3638
2604
1908
1383
955
623
281
D
Relative Fluc/Rluc
1.25
1.00
0.75
0.50
0.25
0.00
5'UTR
5'UTR + 3'UTR
Control
PABP-Depleted
PABP
GAPDH

on the IRES-mediated translation of the polyadenylated bicistronic mRNA containing the cSHMT 3'UTR, but reduced the IRES activity of the polyadenylated bicistronic mRNA lacking the 3'UTR by 45% (Figure 3.1D). These results led to the formulation of a model for the IRES-mediated translation of cSHMT in which interactions between ITAFs bound to the 5'UTR of the transcript and ITAFs bound to the 3'UTR serve to circularize the transcript, thereby eliminating the need for both the poly(A) tail and PABP (Figure 3.2).

CUGBP1 binds to the cSHMT 3'UTR. A promising candidate for the 3'UTR-binding protein in our model was CUG-Binding Protein 1 (CUGBP1), an isoform of the hnRNP hNab50 (28) that has been shown to stimulate the IRES-mediated translation of cSHMT (25). The effect of CUGBP1 on IRES activity is significant only when the 3'UTR of cSHMT is included in the transcript (25), indicating that the protein might act by binding to the 3'UTR of the mRNA. The binding of CUGBP1 to the cSHMT 3'UTR was confirmed in UV-treated mammary adenocarcinoma (MCF-7) cells by RNA immunoprecipitation using an antibody against CUGBP1, and amplification of the immunoprecipitated RNA with PCR primers specific to the cSHMT 3'UTR (Figure 3.3A).

The binding of CUGBP1 to the cSHMT 3'UTR was also confirmed *in vitro* by RNA electrophoretic mobility shift assays (EMSAs) using recombinant MBP-CUGBP1 and an excess of non-specific competitor tRNA (Figure 3.3B). The addition of MBP alone had no effect on the mobility of the cSHMT 3'UTR (data not shown), and MBP-CUGBP1 binding was abolished upon the addition of a molar excess of unlabeled 3'UTR (Figure 3.3B), indicating that the interaction is specific. As the EMSA was performed in the absence of other proteins, the results of the experiment indicate that CUGBP1 is capable of binding to the 3'UTR of cSHMT independent of

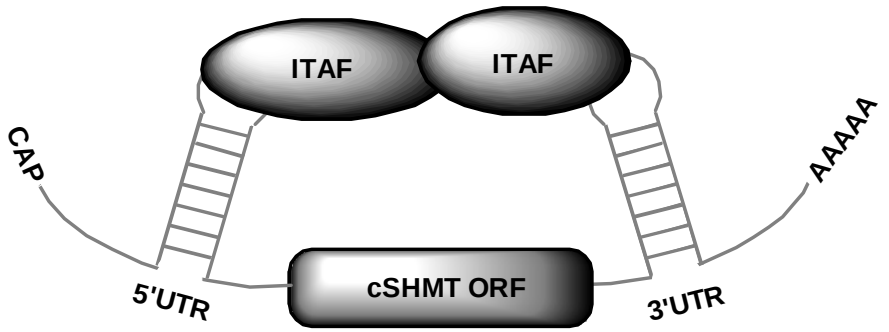

Figure 3.2. Proposed model for the IRES-mediated translation of cSHMT. In this model, an interaction between an ITAF bound to the 5'UTR of the cSHMT transcript and another ITAF bound to the 3'UTR of the cSHMT transcript serves to circularize the mRNA. This results in the formation of a "closed loop" similar to the one that is typically formed by the eIF4G/PABP/poly(A) tail interaction.

Figure 3.3. The interaction of CUGBP1 with the cSHMT UTRs. (A) RNA was immunoprecipitated from UV-treated MCF-7 whole cell extract using an antibody against IgG (control for non-specific binding) or CUGBP1. The RNA in lanes 1-3 (+RT) was reverse-transcribed into cDNA and then analyzed by PCR using primers specific to either the cSHMT 5'UTR or the cSHMT 3'UTR. The RNA in lanes 4-6 (-RT) did not undergo the reverse-transcription step. Rather, they were analyzed directly by PCR to control for DNA contamination in the immunoprecipitates. Lanes 1 and 4 (input) represent 1% of the RNA used in the immunoprecipitation. (B) Electrophoretic mobility shift assays were carried out in the presence of yeast tRNA using radiolabeled cSHMT 3'UTR and recombinant MBP-CUGBP1. A 10X, 50X, and 100X molar excess of unlabeled cSHMT 3'UTR was also added in lanes 3, 4, and 5, respectively, to determine binding specificity. (C) Electrophoretic mobility shift assays were carried out using radiolabeled cSHMT 3'UTR and increasing concentrations of MBP-CUGBP1. The fraction of the 3'UTR bound by the recombinant protein was quantified using ChemiImager 4400 from Alpha Innotech Corp. The dissociation constant (Kd) was determined using GraphPad Prism. (D) Electrophoretic mobility shift assays were carried out using radiolabeled cSHMT 3'UTR truncation mutants in the absence and presence of MBP-CUGBP1. The nucleotides of the 3'UTR that comprise the truncation mutant are listed above each gel. The nucleotide at the 5' end of the 3'UTR is labeled 1. The nucleotide at the 3' end of the 3'UTR is labeled 637. (E) MCF-7 whole cell extract was either not treated or treated with λ phosphatase (PPase) and analyzed by western blot using antibodies against CUGBP1 and phosphorylated serine and threonine residues. GAPDH serves as a control for equal protein loading. (F) The extracts from (E) were applied to RNA affinity columns to which either the cSHMT 5'UTR or the reverse complement of the cSHMT 5'UTR (RevUTR) had been attached. Proteins that bound to the UTRs were eluted and analyzed by western blotting using an antibody against CUGBP1.

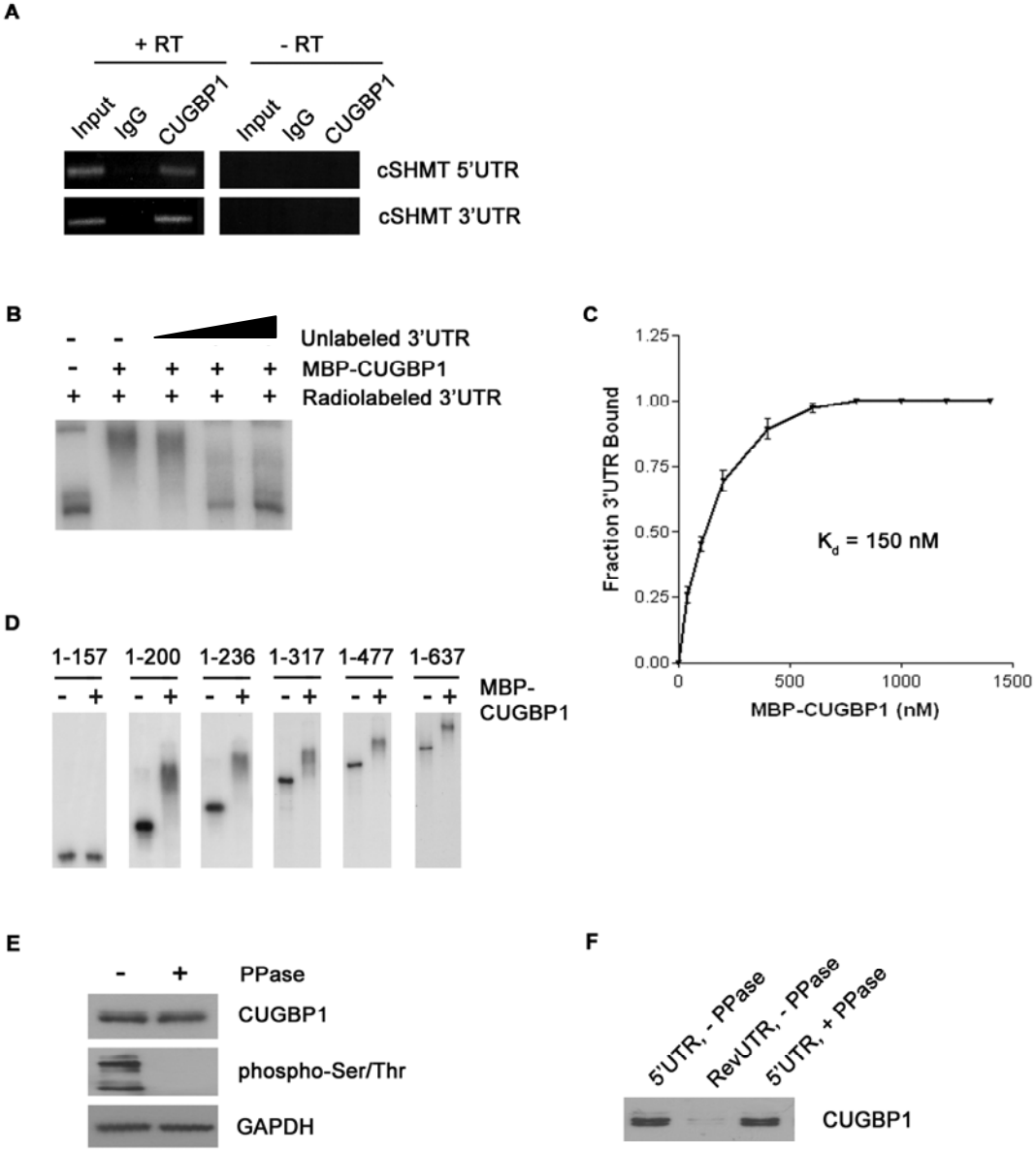
A
+ RT
- RT
Input
IgG
CUGBP1
Input
IgG
CUGBP1
cSHMT 5'UTR
cSHMT 3'UTR
B
Unlabeled 3'UTR
MBP-CUGBP1
Radiolabeled 3'UTR
C
Fraction 3'UTR Bound
1.25
1.00
0.75
0.50
0.25
0.00
0
500
1000
1500
MBP-CUGBP1 (nM)
K_d = 150 nM
D
1-157
1-200
1-236
1-317
1-477
1-637
MBP-CUGBP1
E
PPase
CUGBP1
phospho-Ser/Thr
GAPDH
F
5'UTR, - PPase
RevUTR, - PPase
5'UTR, + PPase
CUGBP1

any auxiliary factors. The dissociation constant (K_d) of CUGBP1 binding to the 5'UTR was determined to be 150 nM (Figure 3.3C).

CUGBP1 has been reported to bind several consensus sequences including $(CUG)_n$ triplet repeats (28), GU rich elements (GREs, UGUUUGUUUGU) (29), and Bruno response elements (BREs, AAUGUAUGUUAAUUGUAUGUAUUA) (30). The 3'UTR of cSHMT contains a partial BRE (UGUAUGUU) at nucleotide positions 496-503. However, mutation of this sequence did not affect the K_d of CUGBP1 binding in EMSAs (data not shown). To map the CUGBP1 binding site on the cSHMT 3'UTR, the ability of recombinant protein to bind a series of 3'UTR truncation mutants was determined by EMSA. Addition of MBP-CUGBP1 had no effect on the mobility of 3'UTR(1-157), but did decrease the mobility of 3'UTR(1-200), 3'UTR(1-236), 3'UTR(1-317), 3'UTR(1-477), and the full-length 3'UTR (3'UTR(1-637)) (Figure 3.3D). These results indicate that CUGBP1 binds to the 5' end of the cSHMT 3'UTR, between nucleotides 157 and 200. This region contains a partial GRE (UUUGUUU) located at nucleotide positions 167-173.

CUGBP1 binding to the cSHMT 5'UTR requires an auxiliary factor. MBP-CUGBP1 did not bind to the cSHMT 5'UTR in EMSAs (data not shown). However, the results from RNA immunoprecipitation experiments using an antibody against CUGBP1 revealed that the endogenous protein is associated with the cSHMT 5'UTR in UV-treated MCF-7 cells (Figure 3.3A). Taken together, these data suggest that CUGBP1 binding to the cSHMT 5'UTR requires either a post-translational modification that is absent from the bacterially-expressed protein or an auxiliary factor that binds to both the cSHMT 5'UTR and to CUGBP1.

CUGBP1 is known to be phosphorylated *in vivo* (31,32). To determine if the phosphorylation status of CUGBP1 affects its interaction with the cSHMT 5'UTR, RNA affinity chromatography was carried out using *in vitro* transcribed RNA and

either untreated or phosphatase-treated MCF-7 whole cell extract (Figure 3.3E). Phosphatase treatment did not interfere with the ability of the cSHMT 5'UTR to pull down CUGBP1 (Figure 3.3F), making it unlikely that a CUGBP1 post-translational modification is required for the RNA-protein interaction. We therefore hypothesized that CUGBP1 interacts with the 5'UTR through its association with a novel cSHMT ITAF that binds directly to the 5'UTR.

Identification of hnRNP H2 as a cSHMT 5'UTR-binding protein. To identify the cSHMT 5'UTR binding protein, RNA affinity chromatography was carried out using *in vitro* transcribed mRNA. The reverse complement of the cSHMT 5'UTR (RevUTR), which lacks IRES activity (25), was used as a control for non-specific binding. Analysis of the eluate revealed that a protein of approximately 50 kDa bound to the cSHMT 5'UTR but not the RevUTR (Figure 3.4A). Microcapillary reverse-phase HPLC nano-electrospray tandem mass spectrometry (μLC/MS/MS) identified this protein as heterogeneous nuclear ribonucleoprotein H2 (hnRNP H2). Immunoblotting using an antibody against hnRNP H confirmed these results (Figure 3.4B), although the antibody cannot distinguish between hnRNP H1 and hnRNP H2, which are 96% identical (33).

To further investigate the binding of hnRNP H2 to the cSHMT 5'UTR, EMSAs were carried out using recombinant MBP-hnRNP H2 and an excess of non-specific competitor tRNA. The results revealed that MBP-hnRNP H2 (but not MBP alone, data not shown) binds directly and specifically to the 5'UTR (Figure 3.4C) with a K_d of 260 nM (Figure 3.4D). To map the hnRNP H2 binding site, the ability of the recombinant protein to bind several different 5'UTR truncation mutants was determined by EMSA. MBP-hnRNP H2 bound to 5'UTR(105-190), 5'UTR(50-150), 5'UTR(1-114), 5'UTR(1-131) and the full-length 5'UTR (5'UTR(1-190)), but not to 5'UTR(1-104) (Figure 3.4E), indicating that nucleotides 105-114 comprise the hnRNP

Figure 3.4. The interaction of hnRNP H2 with the cSHMT UTRs. (A) MCF-7 whole cell extract was applied to RNA affinity columns to which either the cSHMT 5'UTR or the reverse complement of the cSHMT 5'UTR (RevUTR) had been attached. Proteins that bound to the UTRs were eluted, separated by SDS-PAGE, and visualized by coomassie blue staining. The protein marked with an (*) was excised from the gel and analyzed by reverse-phase HPLC nano-electrospray tandem mass spectrometry (μLC/MS/MS). (B) The SDS-PAGE gel from (A) was transferred to a PVDF membrane and analyzed by western blotting using an antibody against hnRNP H. (C) Electrophoretic mobility shift assays were carried out in the presence of yeast tRNA using radiolabeled cSHMT 5'UTR and recombinant MBP-hnRNP H2. A 10X, 50X, and 100X molar excess of unlabeled cSHMT 5'UTR was also added in lanes 3, 4, and 5, respectively, to determine binding specificity. (D) Electrophoretic mobility shift assays were carried out in using radiolabeled cSHMT 5'UTR and increasing concentrations of MBP-hnRNP H2. The fraction of the 5'UTR bound by the recombinant protein was quantified using ChemiImager 4400 from Alpha Innotech Corp. The dissociation constant (Kd) was determined using GraphPad Prism. (E) Electrophoretic mobility shift assays were carried out in using radiolabeled cSHMT 5'UTR truncation mutants in the absence and presence of MBP-hnRNP H2. The nucleotides of the 5'UTR that comprise the truncation mutant are listed above each gel. The nucleotide at the 5' end of the 5'UTR is labeled 1. The nucleotide at the 3' end of the 5'UTR is labeled 190. (F) RNA was immunoprecipitated from UV-treated MCF-7 whole cell extract using an antibody against IgG (control for non-specific binding) or hnRNP H. The RNA in lanes 1-3 (+RT) was reverse-transcribed into cDNA and then analyzed by PCR using primers specific to either the cSHMT 5'UTR or the cSHMT 3'UTR. The RNA in lanes 4-6 (-RT) did not undergo the reverse-transcription step. Rather, they were analyzed directly by PCR to control for DNA contamination in the immunoprecipitates. Lanes 1 and 4 (input) represent 1% of the RNA used in the immunoprecipitation. (G) Whole cell extract (WCE) from cells that were treated with either negative control siRNA (- CUGBP1 siRNA) or siRNA directed against CUGBP1 were applied to RNA affinity columns to which either the cSHMT 5'UTR or the cSHMT 3'UTR had been attached. Proteins that bound to the UTRs were eluted, separated by SDS-PAGE, and visualized by western blotting using antibodies against CUGBP1 or hnRNP H. For the WCE, equal protein loading was confirmed by using an an antibody against GAPDH. For the affinity column elutions, equal protein loading was confirmed by staining the gel with coomassie blue after transfer.

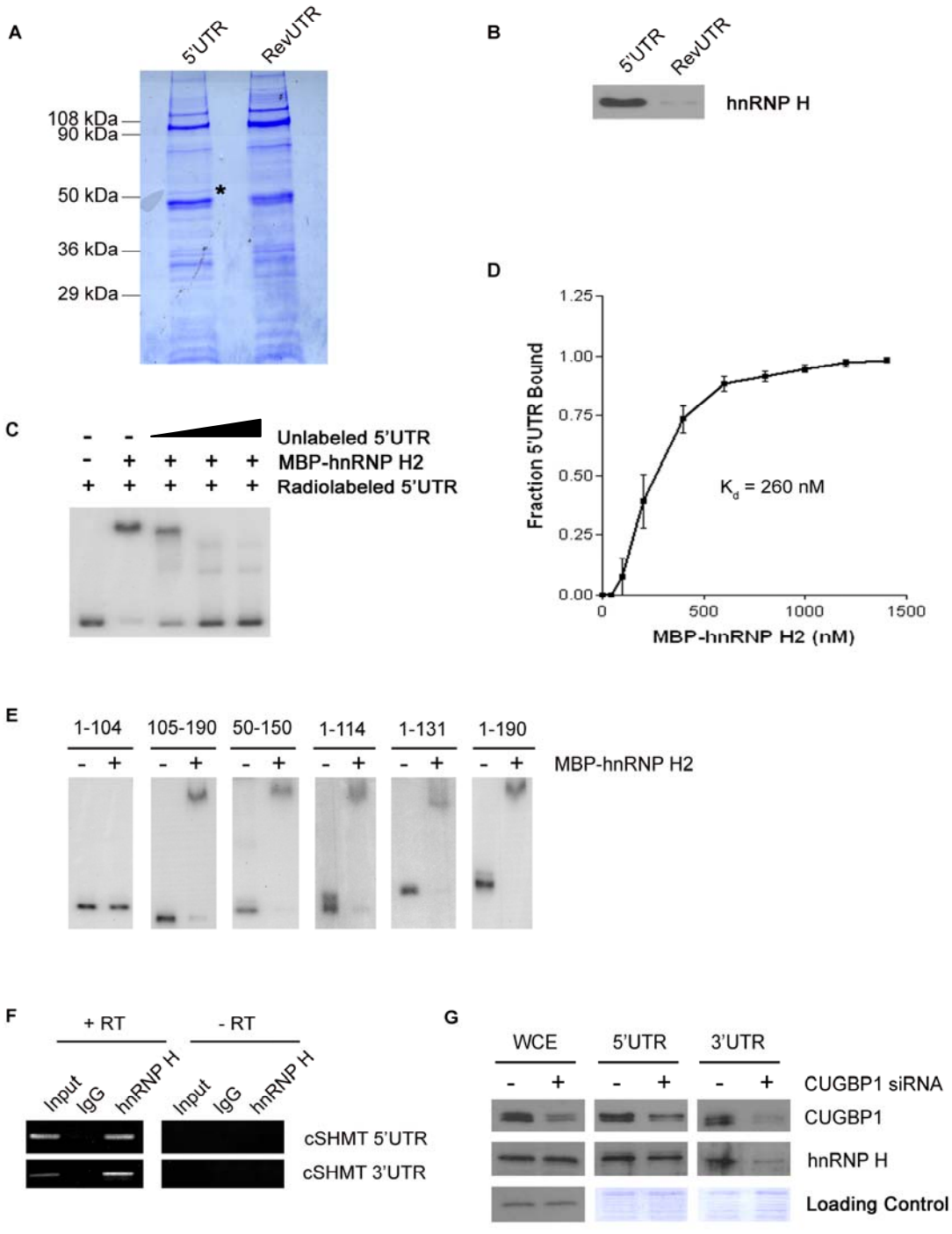
A
5'UTR
RevUTR
108 kDa
90 kDa
50 kDa
36 kDa
29 kDa
*
B
5'UTR
RevUTR
hnRNP H
C
Unlabeled 5'UTR
MBP-hnRNP H2
Radiolabeled 5'UTR
D
Fraction 5'UTR Bound
1.25
1.00
0.75
0.50
0.25
0.00
0
500
1000
1500
MBP-hnRNP H2 (nM)
K_d = 260 nM
E
1-104
105-190
50-150
1-114
1-131
1-190
MBP-hnRNP H2
F
+ RT
- RT
Input
IgG
hnRNP H
cSHMT 5'UTR
cSHMT 3'UTR
G
WCE
5'UTR
3'UTR
CUGBP1 siRNA
CUGBP1
hnRNP H
Loading Control

H2 binding site on the cSHMT 5'UTR. This region contains a run of Gs followed by a C (GGGGC), a sequence that has been shown to specifically promote hnRNP H1 and hnRNP H2 binding (34). RNA immunoprecipitation from UV-treated cells using an antibody against hnRNP H verified that the association between hnRNP H1/H2 and the cSHMT 5'UTR occurs *in vivo* (Figure 3.4F). It also revealed that hnRNP H2 interacts with the 3'UTR of cSHMT (Figure 3.4F), although it does not bind to the 3'UTR directly in EMSAs (data not shown). *In vitro,* the binding of hnRNP H2 to the 3'UTR decreases upon CUGBP1 depletion (Figure 3.4G). These results are consistent with a role for hnRNP H2 as the auxiliary factor that enables CUGBP1 to interact with the cSHMT 5'UTR.

hnRNP H2 interacts with CUGBP1. If hnRNP H2 indeed serves as the auxiliary factor for the interaction between CUGBP1 and the cSHMT 5'UTR, hnRNP H2 and CUGBP1 must physically interact. To test this hypothesis, a yeast two-hybrid analysis was performed. An hnRNP H2-GAL4 activating domain fusion and a CUGBP1-GAL4 DNA-binding domain fusion were expressed in the *Saccharomyces cerevisiae* strains Y187 and AH109, respectively. The mating of these strains activated the *HIS3* and *MEL1* reporter genes (as evidenced by the growth of blue colonies on SD/-Leu/-Trp/-His medium containing X-α-gal, data not shown), providing evidence that the two proteins interact. The results of the yeast two-hybrid were confirmed by both the coimmunoprecipitation of CUGBP1 with the hnRNP H antibody (Figure 3.5A), and the coimmunoprecipitation of hnRNP H with the CUGBP1 antibody (Figure 3.5B) from MCF-7 cell extracts. Although it has previously been reported that hnRNP H and CUGBP1 interact in an RNA-dependent manner in myoblasts (35), our data suggest that the interaction is RNA-independent, as the two proteins coimmunoprecipitated from a mixture containing only recombinant hnRNP H2 and recombinant CUGBP1 (Figure 3.5C and 3.5D).

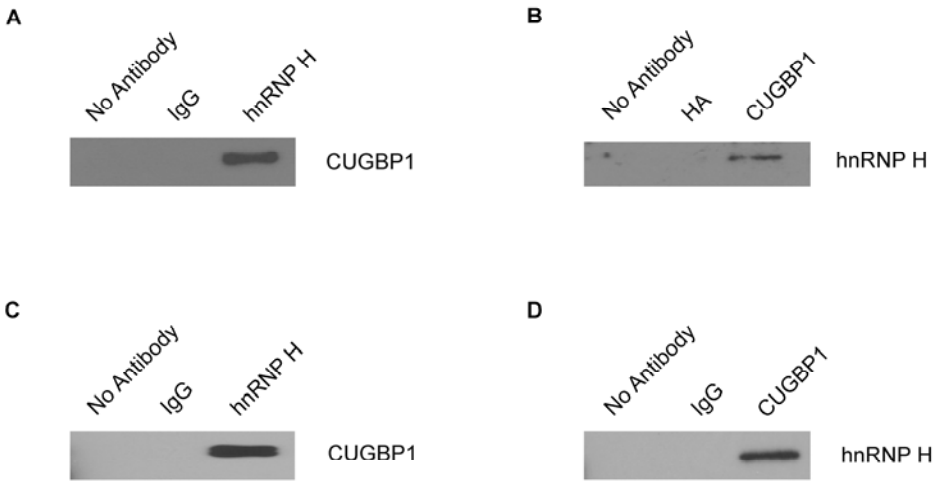

Figure 3.5. hnRNP H2 binds to CUGBP1 in an RNA-independent manner. CUGBP1 (A) and hnRNP H (B) were coimmunoprecipitated from MCF-7 whole cell extracts using antibodies against hnRNP H and CUGBP1, respectively. The no antibody, IgG, and HA coimmunoprecipitations serve as controls for non-specific binding. CUGBP1 (C) and hnRNP H (D) were coimmunoprecipitated from a mixture of recombinant hnRNP H2 and recombinant CUGBP1 using antibodies against hnRNP H and CUGBP1, respectively. The no antibody and IgG coimmunoprecipitations serve as controls for non-specific binding.

hnRNP H2 is a cSHMT ITAF. In order to determine if hnRNP H2 is involved in the IRES-mediated translation of cSHMT, siRNA was used to deplete hnRNP H2 protein levels in MCF-7 cells (Figure 3.6A). Following UV treatment, which activates the cSHMT IRES (Chapter 5), these cells were transfected with polyadenylated bicistronic mRNAs containing either the cSHMT 5'UTR or the cSHMT 5' and 3'UTRs. Although hnRNP H2 depletion had no effect on the IRES activity of the mRNA containing the 5'UTR alone, the IRES activity of the mRNA containing the 5' and 3'UTRs decreased 33% in hnRNP H2 siRNA-treated cells compared to control cells (Figure 3.6B). This reduction in IRES activity correlates with the decrease in cSHMT protein levels observed upon hnRNP H2 knockdown (Figure 3.6A). The stimulatory effect of hnRNP H2 on IRES activity was determined to be specific to cSHMT, as hnRNP H2 depletion had no significant effect on the IRES activity of the immunoglobulin heavy-chain binding protein (BiP) or the hepatits C virus (HCV) (Figure 3.6C).

Depletion of CUGBP1 or hnRNP H2 results in a decrease in the IRES-mediated translation of non-polyadenylated cSHMT mRNA. If an interaction between hnRNP H2 bound to the 5'UTR of the mRNA and CUGBP1 bound to the 3'UTR functions to circularize the cSHMT transcript, then removal of these factors from nuclease-treated rabbit reticulocyte lysate should reveal a requirement for the poly(A) tail. Indeed, the immunodepletion of CUGBP1 (Figure 3.7A) and hnRNP H2 (Figure 3.7B) reduced the IRES activity of the non-polyadenylated bicistronic mRNA containing the cSHMT 3'UTR to similar levels obtained when the IRES activity of the non-polyadenylated bicistronic mRNA lacking the 3'UTR was measured in rabbit reticulocyte lysate containing both factors. The immunodepletion of CUGBP1 and hnRNP H2 had no effect on the IRES activity of the non-polyadenylated bicistronic mRNA lacking the cSHMT 3'UTR. The addition of MBP-tagged recombinant protein

Figure 3.6. hnRNP H2 stimulates cSHMT IRES activity. (A) MCF-7 cells were treated with negative control siRNA or hnRNP H2 siRNA and subjected to western blot analysis using antibodies against hnRNP H2, cSHMT, and CUGBP1. GAPDH serves as a control for equal protein loading. (B) Control (white bars) and hnRNP H2 siRNA-treated cells (dark bars) were transiently transfected with bicistronic mRNAs with and without the cSHMT 3'UTR. The relative ratio of Fluc/Rluc for each bicistronic mRNA in the control cells was given a value of 1.0. The data represent the average of three independent experiments $\pm$ standard error. (C) Control (white bars) and hnRNP H2 siRNA-treated cells (dark bars) were transiently transfected with bicistronic mRNAs where the human cSHMT 5'UTR was replaced with either the BiP IRES or the HCV IRES. The relative ratio of Fluc/Rluc for each bicistronic mRNA in the control cells was given a value of 1.0. The data represent the average of three independent experiments $\pm$ standard error.

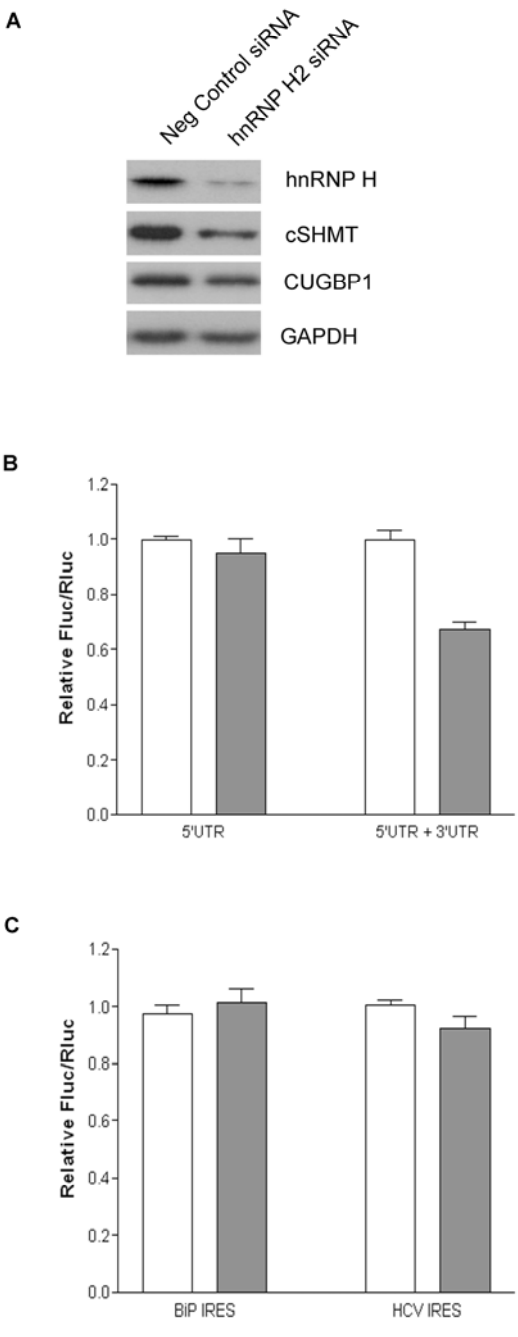
A
Neg Control siRNA
hnRNP H2 siRNA
hnRNP H
cSHMT
CUGBP1
GAPDH
B
Relative Fluc/Rluc
1.2
1.0
0.8
0.6
0.4
0.2
0.0
5'UTR
5'UTR + 3'UTR
C
Relative Fluc/Rluc
1.2
1.0
0.8
0.6
0.4
0.2
0.0
BiP IRES
HCV IRES

Figure 3.7. CUGBP1 and hnRNP H2 depletion result in a dependence on the poly(A) tail. CUGBP1 (A) and hnRNP H (B) were immunodepleted from rabbit reticulocyte lysate as described in Materials and Methods. The depletion of these proteins was confirmed by immunoblotting (right) using antibodies against CUGBP1 (A) and hnRNP H (B). GAPDH serves as a control for equal protein loading. The graphs on the left show the IRES activities of the bicistronic mRNAs containing a 30 nucleotide poly(A) tail (white bars) or lacking a poly(A) tail (dark bars) as measured in control rabbit reticulocyte, CUBBP1 (A) or hnRNP H (B)-depleted rabbit reticulocyte lysate, or immunodepleted lysate supplemented with recombinant CUGBP1 (A) or hnRNP H2 (B). The relative ratio of Fluc/Rluc for each bicistronic mRNA containing a poly(A) tail was given a value of 1.0. The data represent the average of three independent experiments $\pm$ standard error. (C) The 3'UTR of the bicistronic mRNA was truncated by removal of nucleotides from the 3' end, and the IRES activity of these truncation mutants was measured in rabbit reticulocyte lysate. The white bars represent the IRES activity of the truncated bicistronic mRNA containing a 30 nucleotide poly(A) tail, and the dark bars represent the IRES activity of the truncated bicistronic mRNA lacking a poly(A) tail. The relative ratio for each truncated bicistronic mRNA containing a poly(A) tail was given a value of 1.0. The data represent the average of three independent experiments $\pm$ standard error.

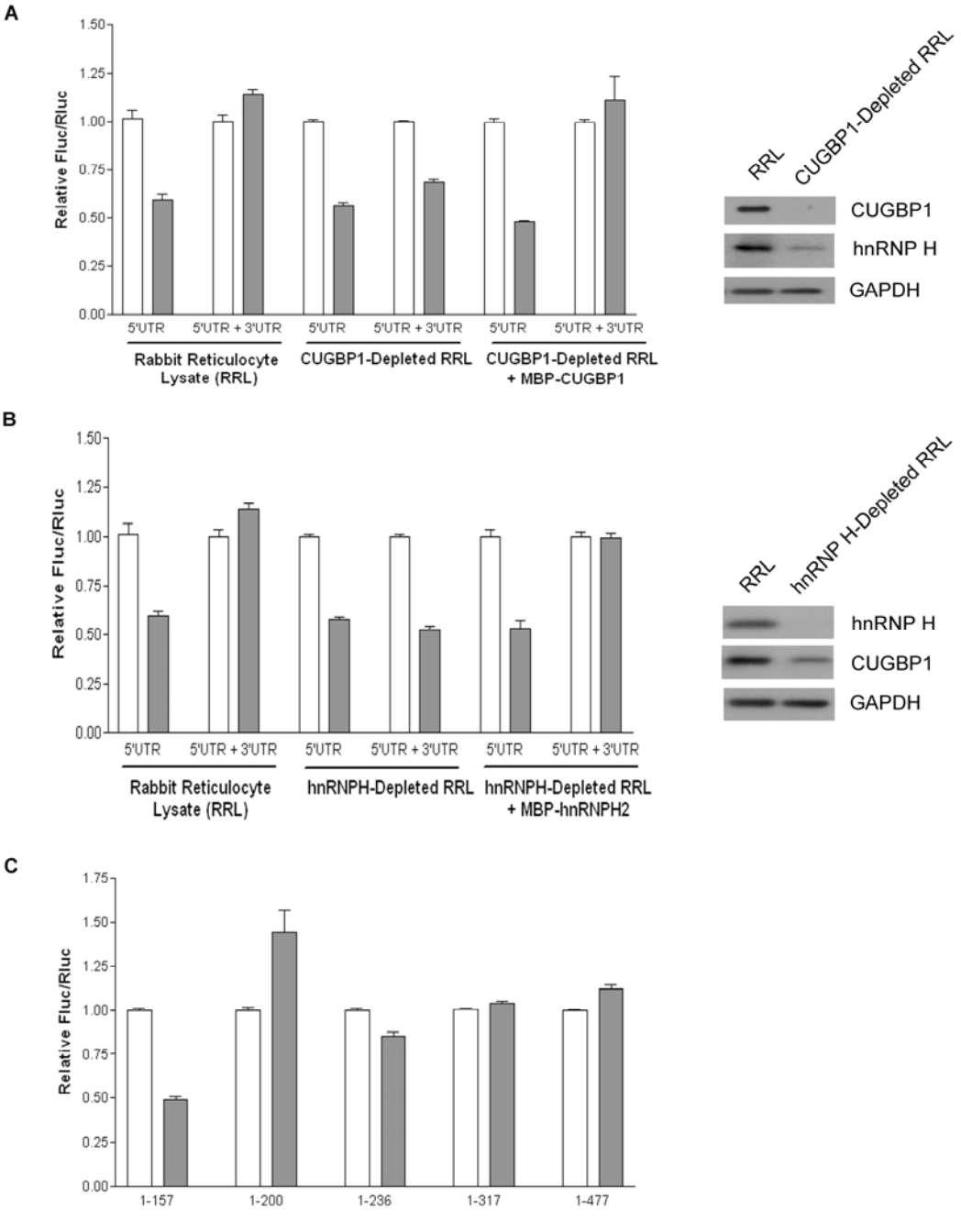
A
Relative Fluc/Rluc
1.50
1.25
1.00
0.75
0.50
0.25
0.00
5'UTR
5'UTR + 3'UTR
Rabbit Reticulocyte Lysate (RRL)
CUGBP1-Depleted RRL
CUGBP1-Depleted RRL + MBP-CUGBP1
RRL
CUGBP1-Depleted RRL
CUGBP1
hnRNP H
GAPDH
B
Relative Fluc/Rluc
Rabbit Reticulocyte Lysate (RRL)
hnRNPH-Depleted RRL
hnRNPH-Depleted RRL + MBP-hnRNPH2
RRL
hnRNP H-Depleted RRL
hnRNP H
CUGBP1
GAPDH
C
Relative Fluc/Rluc
1.75
1.50
1.25
1.00
0.75
0.50
0.25
0.00
1-157
1-200
1-236
1-317
1-477

(Figure 3.7A and 3.7B), but not MBP alone (data not shown), to the immunodepleted extracts restored the IRES activity of the non-polyadenylated bicistronic mRNA containing the cSHMT 3'UTR to the levels of its polyadenylated counterpart, demonstrating that the immunodepletion procedure did not completely remove any other factor required for cap-independent translation. However, consistent with an RNA-independent interaction between CUGBP1 and hnRNP H2, the immunodepletion of CUGBP1 did reduce the levels of hnRNP H present in the nuclease-treated rabbit reticulocyte lysate (Figure 3.7A) and vice versa (Figure 3.7B).

Like the immunodepletion of CUGBP1 from rabbit reticulocyte lysate, the deletion of all but the first 157 nucleotides from the cSHMT 3'UTR in the bicistronic mRNA resulted in a 50% decrease in the IRES activity of non-polyadenylated mRNA relative to that of its polyadenylated counterpart (Figure 3.7C). This requirement for the poly(A) tail was not observed when the cSHMT 3'UTR contained nucleotides 1-200, 1-236, 1-317, and 1-477 (Figure 3.7C). As only the 1-157 3'UTR truncation mutant is incapable of binding CUGBP1 (Figure 3.3D), these results further support a role for CUGBP1 in circularizing the cSHMT transcript.

The IRES-mediated translation of cSHMT involves ribosome scanning. Internal initiation has previously been shown to proceed by a "land and scan" mechanism, whereby the 40S ribosomal subunit binds upstream of the initiation codon and then migrates in a 5'-3' direction until AUG recognition occurs (36-38). Consistent with this mechanism, most cellular IRESes have been found to require eIF4A (7), a DEAD box helicase that unwinds mRNA secondary structure and thereby facilitates ribosome binding and scanning (39,40). To determine if ribosome scanning is involved in the IRES-mediated translation of cSHMT, cells were treated with hippuristanol, a small molecule inhibitor of the eIF4A helicase (41). As in previous reports (41), hippuristanol treatment did not reduce the IRES activity of HCV (Figure

3.8A) which is known to be eIF4A-independent (42). However, it did result in a significant decrease in the IRES-mediated translation of cSHMT (Figure 3.8B).

To locate the "landing" point of the ribosome within the cSHMT 5'UTR, a series of open reading frames (ORFs) were introduced throughout the IRES by site-directed mutagenesis of the bicistronic construct. A common stop codon (UAG) was placed at the 3' end of the IRES, but the locations of the start codon (AUG) varied. The ORFs were engineered within the 5'UTR so that they were out of frame with the downstream ORF of Fluc. All AUG codons were placed in a sequence context that is highly favorable for initiation (with a purine three nucleotides upstream of the AUG and a G in position +4) (43) in order to eliminate leaky scanning by the 40S ribosomal subunit (Figure 3.8C). It was anticipated that if the inserted ORFs are located downstream of the ribosome entry site, IRES activity would decrease. However, if the ORFs are located upstream of the ribosome entry site, IRES activity would be unaffected.

The mRNA produced from each mutated bicistronic construct was transiently transfected into MCF-7 cells, and IRES activity was measured and compared to wildtype (WT) and stop codon only controls (Figure 3.8D). The introduction of start codons at positions 52, 70, 82, and 103 resulted in similar reductions in IRES activity. However, the mutation of these AUGs to GUG or UUG also resulted in reduced IRES activity, indicating that mutations at these positions affect luciferase expression simply by perturbing the RNA structure. In contrast, the introduction of start codons at positions 118, 139, 151, and 169 resulted in reduced IRES activity that could be completely rescued by mutation of the AUGs to AUA or UUG, indicating that the 40S ribosomal subunit begins scanning between nucleotides 103 and 118 of the cSHMT 5'UTR. The gradual increase in IRES activity of the 118, 139, 151, and 169 AUG mutants is consistent with reinitiation, a process by which ribosomes remain

Figure 3.8. Ribosome scanning occurs between nucleotides 103 and 118 of the cSHMT 5'UTR. (A) MCF-7 cells were transiently transfected with polyadenylated bicistronic mRNAs containing the HCV IRES (A) or the cSHMT 5'UTR (B) and then treated with the indicated amount of hippuristanol. 11 h following treatment, Fluc (white bars) and Rluc (dark bars) expression was quantified as described in Materials and Methods. The relative luminosity in untreated cells was given a value of 1.0. The data represent the average of three independent experiments $\pm$ standard error. (C) The sequence of the cSHMT 5'UTR indicating the positions of the inserted open reading frames. The location of each start and stop codon is underlined, and the letters above the underlined nucleotides indicate changes to the wildtype sequence that were made by site directed mutagenesis. (D) MCF-7 cells were transiently transfected with bicistronic mRNAs containing the mutated cSHMT 5'UTRs. The number of each mutant represents the position of the A in the AUG or AUA, or the U in the UUG. The relative ratio of Fluc/Rluc for each the wildtype (WT) bicistronic mRNA was given a value of 100%. The data represent the average of at least three independent experiments $\pm$ standard error.

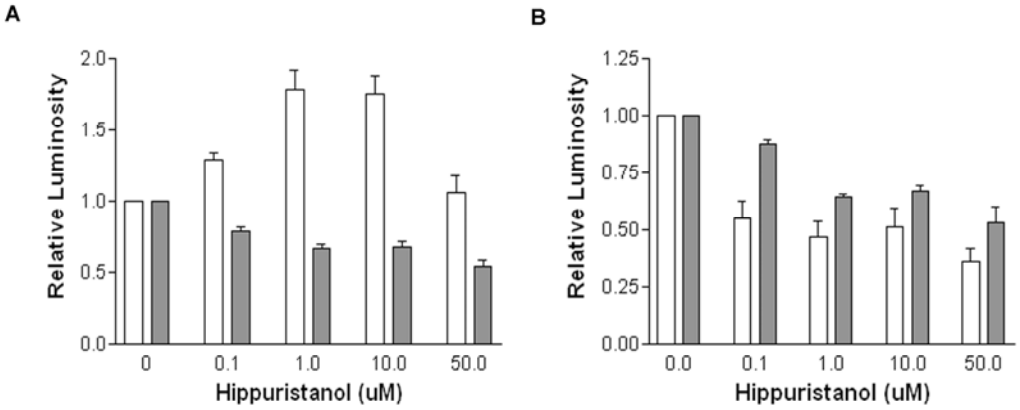

C

5'- GCCUGGCGCGCAGAGUGCACCUUCCUGAGCUCGAGCGGUCCAGCGCCAAG
AU AU A A
UUCGGGGUUUGGGGUUGGAGCGGCUGGUCACGUGGCUGGCCCGCGGCGG
A AU UG UG
UGCGCGGGGCGUUGGGUCAGCGGGUCUGGGACUGGUGGCACCGGCGGCG
A G G AU U
GCGUAGGACGGAGGCGUCGCUAGGCAGCUUCGAACCAGUGCA -3'

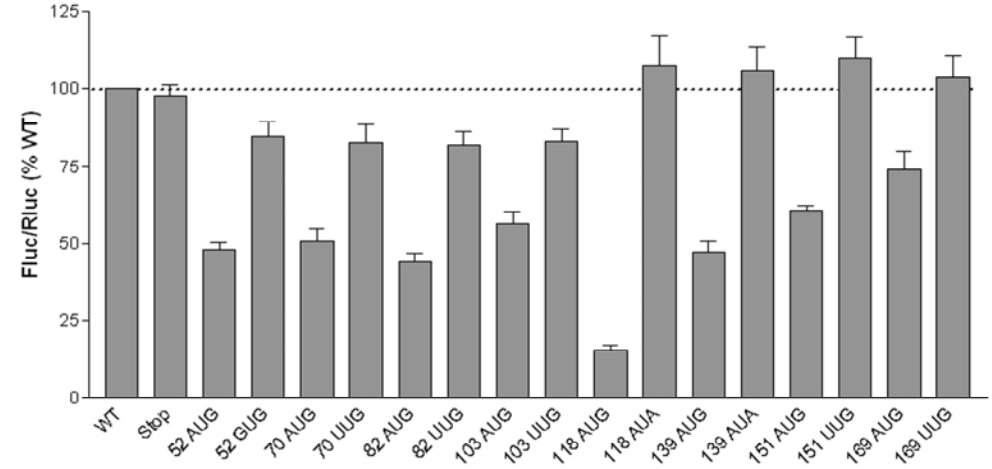

associated with the mRNA following the translation of an upstream ORF and then reinitiate at a downstream ORF. The shorter the upstream ORF, the greater the efficiency of reinitiation (44).

Discussion

There are few conserved properties shared among cellular IRESes in terms of their sequence, size, or structure, indicating that a universal mechanism for their mode of action is unlikely. This is evidenced by the growing list of ITAFs, many of which have only been implicated in the cap-independent translation of a small percentage of the known IRES-containing mRNA transcripts. In this study, we provided evidence that the IRES-mediated translation of cSHMT proceeds by a unique mechanism in that it involves two novel ITAFs, CUGBP1 and hnRNP H2, and does not require either the poly(A) tail or PABP.

The direct binding of hnRNP H2 to the cSHMT 5'UTR, the direct binding of CUGBP1 to the cSHMT 3'UTR, and the RNA-independent interaction between hnRNP H2 and CUGBP1 are all consistent with a model for the IRES-mediated translation of cSHMT whereby an hnRNP H2-CUGBP1 bridge results in the circularization of the mRNA. Formation of this bridge would replicate a function of the eIF4G/PABP/poly(A) tail interaction and would account for the finding that both the poly(A) tail and PABP are dispensable when the cSHMT 3'UTR, CUGBP1, and hnRNP H2 are present, but are required for maximal cSHMT IRES activity in the absence of any one of these factors. It would also explain the previously observed stimulatory effect of the cSHMT 3'UTR on IRES activity (25). Such a model of IRES-mediated translation is not unprecedented. The finding that several non-polyadenylated viral RNAs contain sequences in their 3'UTRs that are required for efficient IRES-mediated translation led to the hypothesis that an RNA/RNA or

RNA/protein bridge can be established between the IRES and the 3'UTR (23,45-47). However, this is the first report, to our knowledge, that demonstrates a cellular IRES/protein bridge experimentally.

Since endogenous cSHMT mRNA is polyadenylated and therefore can presumably bind PABP, why would it utilize an alternative set of factors to form a "closed loop"? One hypothesis comes from examining the CUGBP1 binding site on the 3'UTR. The data from this study indicate that CUGBP1 binds between nucleotides 157 and 200, which is more than 400 nucleotides upstream of the start of the poly(A) tail. Consequently, the interaction of CUGBP1 with the IRES would result in the formation of a much smaller "closed loop" than an interaction between PABP and the IRES. A smaller "closed loop" would likely increase the efficiency of 40S ribosomal subunit recycling.

It remains to be determined whether hnRNP H2 and CUGBP1 serve any additional role(s) in the IRES-mediated translation of cSHMT aside from circularizing the transcript. The proximity of the hnRNP H2 binding site (between nucleotides 105 and 114) and the 40S ribosomal subunit binding site (between nucleotides 103 and 118) on the cSHMT 5'UTR, combined with the previously reported association between CUGBP1 and the α and β subunits of eIF2 (48), raise the possibility that the ITAFs may physically recruit the translation initiation machinery to the 5'UTR. In support of this, preliminary results from our laboratory suggest that hnRNP H2 and CUGBP1 interact with eIF4A (data not shown). Further work is needed to investigate the requirement of the other canonical initiation factors in the IRES-mediated translation of cSHMT and to determine whether the essential initiation factors bind to the cSHMT ITAFs.

REFERENCES

1. Jang, S. K., Krausslich, H. G., Nicklin, M. J., Duke, G. M., Palmenberg, A. C., and Wimmer, E. (1988) *J Virol* **62**, 2636-2643
2. Pelletier, J., and Sonenberg, N. (1988) *Nature* **334**, 320-325
3. Hellen, C. U., and Sarnow, P. (2001) *Genes Dev* **15**, 1593-1612
4. Stoneley, M., and Willis, A. E. (2004) *Oncogene* **23**, 3200-3207
5. Johannes, G., Carter, M. S., Eisen, M. B., Brown, P. O., and Sarnow, P. (1999) *Proc Natl Acad Sci U S A* **96**, 13118-13123
6. Gallie, D. R. (1991) *Genes Dev* **5**, 2108-2116
7. Thoma, C., Bergamini, G., Galy, B., Hundsdoerfer, P., and Hentze, M. W. (2004) *Mol Cell* **15**, 925-935
8. Jacobson, A. (1996) in *Translational Control* (J.W.B. Hershey, M. B. M., and N. Sonenberg, ed), pp. 451-480, Cold Spring Harbor Laboratory Press, Cold Spring Harbor, NY
9. Munroe, D., and Jacobson, A. (1990) *Mol Cell Biol* **10**, 3441-3455
10. Sachs, A. B., and Davis, R. W. (1989) *Cell* **58**, 857-867
11. Sachs, A. B., and Varani, G. (2000) *Nat Struct Biol* **7**, 356-361
12. Svitkin, Y. V., Imataka, H., Khaleghpour, K., Kahvejian, A., Liebig, H. D., and Sonenberg, N. (2001) *Rna* **7**, 1743-1752
13. Tarun, S. Z., Jr., and Sachs, A. B. (1995) *Genes Dev* **9**, 2997-3007
14. Tarun, S. Z., Jr., Wells, S. E., Deardorff, J. A., and Sachs, A. B. (1997) *Proc Natl Acad Sci U S A* **94**, 9046-9051
15. Uchida, N., Hoshino, S., Imataka, H., Sonenberg, N., and Katada, T. (2002) *J Biol Chem* **277**, 50286-50292

16. Wells, S. E., Hillner, P. E., Vale, R. D., and Sachs, A. B. (1998) *Mol Cell* **2**, 135-140

17. Thoma, C., Fraterman, S., Gentzel, M., Wilm, M., and Hentze, M. W. (2008) *Rna* **14**, 1579-1589

18. Bonnal, S., Pileur, F., Orsini, C., Parker, F., Pujol, F., Prats, A. C., and Vagner, S. (2005) *J Biol Chem* **280**, 4144-4153

19. Giraud, S., Greco, A., Brink, M., Diaz, J. J., and Delafontaine, P. (2001) *J Biol Chem* **276**, 5668-5675

20. Hahm, B., Kim, Y. K., Kim, J. H., Kim, T. Y., and Jang, S. K. (1998) *J Virol* **72**, 8782-8788

21. Holcik, M., Gordon, B. W., and Korneluk, R. G. (2003) *Mol Cell Biol* **23**, 280-288

22. Komar, A. A., and Hatzoglou, M. (2005) *J Biol Chem* **280**, 23425-23428

23. Ito, T., Tahara, S. M., and Lai, M. M. (1998) *J Virol* **72**, 8789-8796

24. Herbig, K., Chiang, E. P., Lee, L. R., Hills, J., Shane, B., and Stover, P. J. (2002) *J Biol Chem* **277**, 38381-38389

25. Woeller, C. F., Fox, J. T., Perry, C., and Stover, P. J. (2007) *J Biol Chem* **282**, 29927-29935

26. Bensadoun, A., and Weinstein, D. (1976) *Anal Biochem* **70**, 241-250

27. Khaleghpour, K., Svitkin, Y. V., Craig, A. W., DeMaria, C. T., Deo, R. C., Burley, S. K., and Sonenberg, N. (2001) *Mol Cell* **7**, 205-216

28. Timchenko, L. T., Miller, J. W., Timchenko, N. A., DeVore, D. R., Datar, K. V., Lin, L., Roberts, R., Caskey, C. T., and Swanson, M. S. (1996) *Nucleic Acids Res* **24**, 4407-4414

29. Vlasova, I. A., Tahoe, N. M., Fan, D., Larsson, O., Rattenbacher, B., Sternjohn, J. R., Vasdewani, J., Karypis, G., Reilly, C. S., Bitterman, P. B., and Bohjanen, P. R. (2008) *Mol Cell* **29**, 263-270

30. Good, P. J., Chen, Q., Warner, S. J., and Herring, D. C. (2000) *J Biol Chem* **275**, 28583-28592

31. Kuyumcu-Martinez, N. M., Wang, G. S., and Cooper, T. A. (2007) *Mol Cell* **28**, 68-78

32. Roberts, R., Timchenko, N. A., Miller, J. W., Reddy, S., Caskey, C. T., Swanson, M. S., and Timchenko, L. T. (1997) *Proc Natl Acad Sci U S A* **94**, 13221-13226

33. Honore, B., Baandrup, U., and Vorum, H. (2004) *Exp Cell Res* **294**, 199-209

34. Caputi, M., and Zahler, A. M. (2001) *J Biol Chem* **276**, 43850-43859

35. Paul, S., Dansithong, W., Kim, D., Rossi, J., Webster, N. J., Comai, L., and Reddy, S. (2006) *Embo J* **25**, 4271-4283

36. Jopling, C. L., Spriggs, K. A., Mitchell, S. A., Stoneley, M., and Willis, A. E. (2004) *Rna* **10**, 287-298

37. Le Quesne, J. P., Stoneley, M., Fraser, G. A., and Willis, A. E. (2001) *J Mol Biol* **310**, 111-126

38. Mitchell, S. A., Spriggs, K. A., Coldwell, M. J., Jackson, R. J., and Willis, A. E. (2003) *Mol Cell* **11**, 757-771

39. Rogers, G. W., Jr., Richter, N. J., and Merrick, W. C. (1999) *J Biol Chem* **274**, 12236-12244

40. Svitkin, Y. V., Pause, A., Haghighat, A., Pyronnet, S., Witherell, G., Belsham, G. J., and Sonenberg, N. (2001) *Rna* **7**, 382-394

41. Bordeleau, M. E., Mori, A., Oberer, M., Lindqvist, L., Chard, L. S., Higa, T., Belsham, G. J., Wagner, G., Tanaka, J., and Pelletier, J. (2006) *Nat Chem Biol* **2**, 213-220

42. Pestova, T. V., Shatsky, I. N., Fletcher, S. P., Jackson, R. J., and Hellen, C. U. (1998) *Genes Dev* **12**, 67-83

43. Kozak, M. (1986) *Cell* **44**, 283-292

44. Luukkonen, B. G., Tan, W., and Schwartz, S. (1995) *J Virol* **69**, 4086-4094

45. Danthinne, X., Seurinck, J., Meulewaeter, F., Van Montagu, M., and Cornelissen, M. (1993) *Mol Cell Biol* **13**, 3340-3349

46. Meulewaeter, F., van Lipzig, R., Gultyaev, A. P., Pleij, C. W., Van Damme, D., Cornelissen, M., and van Eldik, G. (2004) *Nucleic Acids Res* **32**, 1721-1730

47. Wang, S., Browning, K. S., and Miller, W. A. (1997) *Embo J* **16**, 4107-4116

48. Timchenko, N. A., Wang, G. L., and Timchenko, L. T. (2005) *J Biol Chem* **280**, 20549-20557

CHAPTER 4

THE ROLE OF HEAVY CHAIN FERRITIN IN THE INTERNAL RIBOSOME ENTRY SITE-MEDIATED TRANSLATION OF CYTOPLASMIC SERINE HYDROXYMETHYLTRANSFERASE

Abstract

Heavy chain ferritin (H ferritin) is an iron chelator that has been shown to enhance the internal ribosome entry site (IRES)-mediated translation of the folate-dependent enzyme cytoplasmic serine hydroxymethyltransferase (cSHMT). Although it is well established that cells overexpressing H ferritin exhibit increased cSHMT IRES activity, and that mouse embryonic fibroblasts heterozygous for H ferritin expression display a reduction in IRES activity, the mechanism by which H ferritin acts has yet to be determined. In this study, the role of H ferritin in the IRES-mediated translation of cSHMT was investigated. We show that H ferritin does not participate directly in cSHMT IRES-mediated translation, nor does it stimulate cSHMT IRES activity by affecting cellular iron pools, altering the cytoplasmic levels of the IRES *trans*-acting factors (ITAFs), or activating the iron-loading protein poly r(C) binding protein 1 (PCBP1). Rather, H ferritin may function in the assembly of the ITAFs prior to the commencement of translation initiation.

Introduction

Ferritin is a multimeric protein composed of 24 heavy and light chain subunits, the ratio of which varies depending on cell type and function (1). Whereas the heavy chain subunit (H ferritin) sequesters iron through its ferroxidase active sites, the light chain subunit functions to mineralize the iron core of the ferritin polymer (2). Ferritin

plays a critical role in the regulation of intracellular iron homeostasis. When iron levels are low, Fe^{2+} is released from the protein so it can contribute to the labile iron pool; when iron levels are high, Fe^{2+} is oxidized to Fe^{3+} at the surface of the protein and deposited in the in the core of the ferritin polymer to prevent iron-mediated oxidative damage (1).

In agreement with results from clinical and epidemiological studies that suggest an interaction among iron status and folate (3-5), it has previously been shown that the expression of the H ferritin cDNA in cultured cells markedly elevates the expression of cytoplasmic serine hydroxymethyltransferase (cSHMT), an enzyme that regulates folate metabolism (6). The H ferritin-mediated stimulation of cSHMT expression occurs at the translational level through an internal ribosome entry site (IRES) located in the 5' untranslated region (UTR) of the cSHMT transcript (6,7). IRESes are *cis*-acting regulatory elements that allow for the cap-independent translation of an mRNA. With the aid of one or more IRES *trans*-acting factors (ITAFs), they recruit the 43S pre-initiation complex to a location close to or directly at the initiation codon. In doing so, they enhance the translation rates of transcripts that contain a long and/or structured 5'UTR and circumvent many of the controls that regulate cap-dependent translation (8-10).

Although the mechanism by which the majority of cellular IRESes function has yet to be explored, several recent studies have shed light on the mechanism of the IRES-mediated translation of cSHMT. It is now known that, in addition to H ferritin, cSHMT cap-independent translation involves the ITAFs CUG-binding protein 1 (CUGBP1) and heterogeneous nuclear ribonucleoprotein H2 (hnRNP H2). According to the present model, hnRNP H2 binds directly to the 5'UTR of the cSHMT mRNA and interacts with CUGBP1, which is bound directly to the 3'UTR. The interaction among hnRNP H2, CUGBP1, and the UTRs stimulates cSHMT IRES activity by

circularizing the transcript (Chapter 3). How H ferritin fits into this model is currently unknown. Because H ferritin can stimulate cSHMT IRES-activity in the absence of the 3'UTR of the transcript (7), and because it can interact with both CUGBP1(7) and hnRNP H2 (11), it has been hypothesized that H ferritin acts by binding directly to the 5'UTR of the cSHMT mRNA and indirectly to the 3'UTR through the auxiliary factor CUGBP1 (7). The following studies were conducted to test this hypothesis and to further investigate the role of H ferritin in cSHMT IRES-mediated translation.

Materials and Methods

Vectors- The generation of bicistronic DNA templates containing the cSHMT 5'UTR, the cSHMT 3'UTR, the reverse compliment of the cSHMT 5'UTR, and the reverse compliment of the cSHMT 3'UTR is described elsewhere (7). The H ferritin coding sequence (6) was subcloned into the pGEX4T-2 vector (GE Healthcare) using the primers 5'-TA**GGATCC**ATGACGACCGCGTCC-3' and 5'-TA**CTCGAG**TTAGCTTTCATTATCACTG-3' where the BamHI and XhoI restriction sites are shown in bold.

Purification of recombinant protein- BL21* cells were transformed with the H ferritin-pGEX vector and grown to mid-log phase. Protein synthesis was induced with isopropyl β-D-thiogalactopyranoside (final concentration 0.1 mM) for 16 h at 18^{o}C. The cells were lysed in B-PER (Pierce) followed by sonication on a Branson Digital Sonifier at 50% amplitude with intermittent icing. After removal of the insoluble material, the clarified supernatant was applied directly to a GST-Bind Resin (Novagen), and the protein was purified according to the manufacturer's protocol. The purity of the protein was determined by SDS-polyacrylamide gel electrophoresis, and its concentration was determined using the Lowry Assay as modified by Bensadoun (12).

In vitro transcription- DNA templates were linearized and purified using the Roche PCR clean-up column. The templates were transcribed using Ambion's MEGAscript kit (for uncapped mRNA) or mMESSAGE mMACHINE kit (for capped mRNA) according to the manufacturer's protocol. For preparation of radiolabeled mRNA for electrophoretic gel mobility shift assays, 50μCi of [α–^{32}P]-labeled rUTP (800Ci/mM, Perkin Elmer) was included in *in vitro* transcription reactions. The crude mRNA was treated with DNase I (Ambion) for 15 min at 40°C and precipitated in 2 M LiCl at -80°C. All RNA procedures were conducted under RNase-free conditions and all mRNA was stored with Recombinant RNasin® Ribonuclease Inhibitor (Promega). The mRNA was quantified by spectrophotometry and it's quality verified by electrophoresis.

RNA electrophoretic gel mobility shift assays- 20 nM [α–^{32}P]-labeled RNA and either the indicated amount of recombinant protein, 25 ng ferritin (type IV) from human liver (Sigma), or 25 ng ferritin (type VII) from human heart (Sigma) were added to binding buffer (20 mM Tris pH 7.5, 5 mM $MgCl_2$, 1 mM EDTA, 8 mM DTT, 2 μg BSA, 10% glycerol, 40 units Recombinant RNasin® Ribonuclease Inhibitor (Promega)) for a total volume of 10 μL. The binding reaction was incubated at 37^{o}C for 15 min and then run on a 4% native polyacrylamide gel at 32 mA. Electrophoresis buffer contained 25 mM Tris base, 0.2 M glycine, and 1 mM EDTA.

Cell culture and preparation of extracts- Mammary adenocarcinoma (MCF-7) cells were obtained from ATCC (HTB22). The generation of the stable cell lines expressing H ferritin cDNA is described elsewhere (7). All cells were cultured in α-MEM (Hyclone Laboratories) containing 11% fetal bovine serum (Hyclone Laboratories) at 37^{o}C and 5% CO_2. When the cells reached approximately 95% confluence, they were harvested by tripsinization and washed in phosphate-buffered saline. To obtain whole cell extract, cells were resuspended in lysis buffer (50 mM

Tris pH 7.5, 150 mM NaCl, 1% NP-40, 5 mM EDTA, 1 mM PMSF, 1:100 dilution of Sigma Protease Inhibitor Cocktail) and lysed on ice for 30 min. Nuclear and cytoplasmic extracts were obtained using the NE-PER Nuclear and Cytoplasmic Extraction Kit (Pierce) according to the manufacturer's protocol. The concentration of the protein in all the extracts was determined using the Lowry Assay as modified by Bensadoun (12).

RNA affinity chromatography- 1.0 nmol of the indicated *in vitro* transcribed mRNA (uncapped and polyadenylated) was incubated with 1.0 nmol biotinylated oligo (dT) probe (Promega) and 200 µl packed streptavidin agarose (Novagen) in TMK buffer (50 mM Tris pH 7.5, 10 mM $MgCl_2$, 150 mM KCl) for 1 h at 4^{o}C. After extensive washing with TMK buffer, the agarose was resuspended in TMK buffer containing 1.0 nmol of the corresponding *in vitro* transcribed reverse compliment UTR mRNA (competitor mRNA, uncapped and non-polyadenylated), 3.0 mg cell extract, 150 µg yeast tRNA (Ambion), and 600 units Recombinant RNasin® Ribonuclease Inhibitor (Promega). Following incubation for 1 h at 4^{o}C, the agarose was washed extensively with TMK buffer, and bound proteins were eluted in 2X SDS-PAGE sample buffer (160 mM Tris pH 6.8, 20 mM DTT, 4% SDS, 20% glycerol) at 95^{o}C for 5 min. The eluted proteins were separated by SDS-PAGE and subjected to western blot analysis. Equal loading was confirmed by staining the PVDF membrane with coomassie blue following protein transfer.

Western blotting- Proteins were separated by SDS-PAGE using a Tris-glycine gel and transferred to a PVDF membrane. The membrane was blocked with 5% non-fat dry milk in phosphate-buffered saline containing 1% NP-40 for 1 hour at room temperature, incubated with primary antibody overnight at 4^{o}C, and incubated with horseradish peroxidase-conjugated anti-IgG for 1-3 h at room temperature. After each incubation, the membrane was washed with phosphate-buffered saline/0.1% Tween20.

Proteins were visualized using Super Signal® substrate (Pierce) followed by autoradiography. When necessary, membranes were stripped with 0.2 M NaOH. Affinity purified sheep anti-H ferritin was used at a 1:500 dilution, mouse anti-CUGBP1 (3B1) (Santa Cruz Biotechnology) was used at a 1:10,000 dilution, sheep anti-human cSHMT was used at a 1:40,000 dilution, goat anti-hnRNP H (N-16, Santa Cruz Biotechnology) was used at a 1:500 dilution, rabbit anti-PCBP1 (Abcam) was used at a 1:1000 dilution, rabbit anti-Lamin A (H-102, Santa Cruz Biotechnology) was used at a 1:1000 dilution, and mouse anti-GAPDH (Novus Biologicals) was used at a 1:40,000 dilution. Goat anti-mouse IgG, rabbit anti-sheep IgG, and rabbit anti-goat IgG were all purchased from Pierce and used at a 1:5,000 dilution.

Polysome profile analysis- MCF-7 cells at approximately 80% confluence were washed twice with phosphate-buffered saline and then exposed to 10,000 μJ/cm^2 UV (254 nm) using the Stratagene UV Stratalinker 2400. The medium was then replaced and the cells cultured under normal conditions. 22 h following UV exposure, the cells were treated with 50 μg/mL cycloheximide (Sigma) for 30 min at 37^{o}C and 5% CO_2. The cells were scraped from the plate and then lysed in polysome extraction buffer (10 mM Tris pH 7.5, 10 mM NaCl, 1.5 mM $MgCl_2$, 1% Triton X-100, 1% deoxycholate, 2% Tween 20, 1000u Recombinant RNasin® Ribonuclease Inhibitor (Promega)) for 10 min on ice. Nuclei were pelleted by brief centrifugation and the resulting supernatant was fractionated through a 10-50% sucrose gradient by ultracentrifugation in a SW41-Ti rotor for 2 h at 36,000 rpm and 4^{o}C. 1 mL fractions were collected with a density gradient fractionation system (Brandel) and the absorbance at 254 nm was measured continuously as a function of gradient depth. Protein was isolated each fraction by TCA precipitation and analyzed by western blotting as described above.

Deferoxamine treatment- MCF-7 cells were grown in 6 well plates until approximately 50% confluent. Deferoxamine (Sigma) was then added to the cell

culture media at a final concentration of 12.5, 25, 50, or 100 μM. 24 or 48 h following treatment, the cells were either harvested and subjected to western blot analysis, or transfected with bicistronic mRNA as described below.

Ferric citrate treatment- MCF-7 cells were grown in 6 well plates until approximately 85% confluent. Ferric citrate (Sigma) was then added to the cell culture media at a final concentration of 0.1, 1 10, or 100 μM. 24 h following treatment, the cells were either harvested and subjected to western blot analysis, or transfected with bicistronic mRNA as described below.

mRNA transfections- MCF-7 cells were incubated in Opti-MEM (Invitrogen) containing a 1:100 dilution of DMRIE-C transfection reagent (Invitrogen) and 5 μg/mL mRNA (capped and polyadenylated) for 4 h at 37^{o}C and 5% CO_2. The Opti-MEM was then replaced with α-MEM and the cells incubated for an additional 6 h at 37^{o}C and 5% CO_2. Renilla and Firefly Luciferase expression was quantified on a Veritas Microplate Luminometer (Turner Biosystems) using the Dual-Glo Luciferase Assay System (Promega) according to the manufacturer's protocol. Where indicated, the cells were treated with 10,000 μJ/cm^2 UVC (254 nm) using the Stratagene UV Stratalinker 2400 12h prior to transfection.

siRNA transfections- MCF7 cells were grown to approximately 40% confluence and then transfected with 5 nM of either negative control siRNA (Ambion) or PCBP1 siRNA (Qiagen, sense strand: 5'-GGGAGAGUCAUGACCAUUCTT-3', antisense strand: 5'-GAAUGGUCAUGACUCUCCCTT-3') using the HiPerFect transfection reagent (Qiagen) according to the manufacturer's instructions. Following incubation with siRNA for approximately 50 h at 37^{o}C and 5% CO_2, some of the cells were harvested and subjected to western blot analysis to confirm PCBP1 knockdown. The remainder of were or transfected with bicistronic mRNA according to the protocol above.

Results

H ferritin does not bind to cSHMT mRNA. It has previously been suggested that H ferritin stimulates the IRES-mediated translation of cSHMT by binding directly to the 5'UTR of the transcript and interacting with the 3'UTR through the ITAF CUGBP1 (7). This proposal is based largely on the measurement of IRES-mediated translation in H ferritin overexpressing MCF-7 cell lines and *H ferritin* $^{+/-}$ mouse embryonic fibroblasts (MEFs) (7), and has not been verified by binding assays. In order to test the model, RNA electrophoretic mobility shift assays (EMSAs) were carried out using recombinant protein. Although the dissociation constants for the binding of the cSHMT ITAFs CUGBP1 and hnRNP H2 to the cSHMT UTRs are in the nanomolar range (Chapter 3), no binding to either the cSHMT 5'UTR or the cSHMT 3'UTR could be detected upon the addition of micromolar amounts of H ferritin (Figure 4.1A). The same results were obtained when EMSAs were carried out using ferritin isolated from human liver and heart (data not shown).

Since the EMSAs were performed in the absence of other proteins, the negative results of the experiment could indicate that H ferritin requires an auxiliary factor to interact with the cSHMT mRNA. However, when MCF-7 whole cell extract was applied to RNA affinity columns containing immobilized cSHMT 5' or 3'UTRs, no H ferritin binding could be detected (Figure 4.1B). The absence of H ferritin binding was not due to degradation of the protein during the course of the experiment, as H ferritin was detected in the flowthrough fraction (data not shown).

As an alternative to *in vitro* binding assays, the association of H ferritin with actively translating mRNAs within a cell was investigated by polysome profile analysis. Whereas CUGBP1and hnRNP H2 were observed in both monosomal and polysomal fractions, H ferritin was only present in the non-ribosomal fractions (Figure 4.1C). These results, combined with the data from the EMSAs and RNA affinity

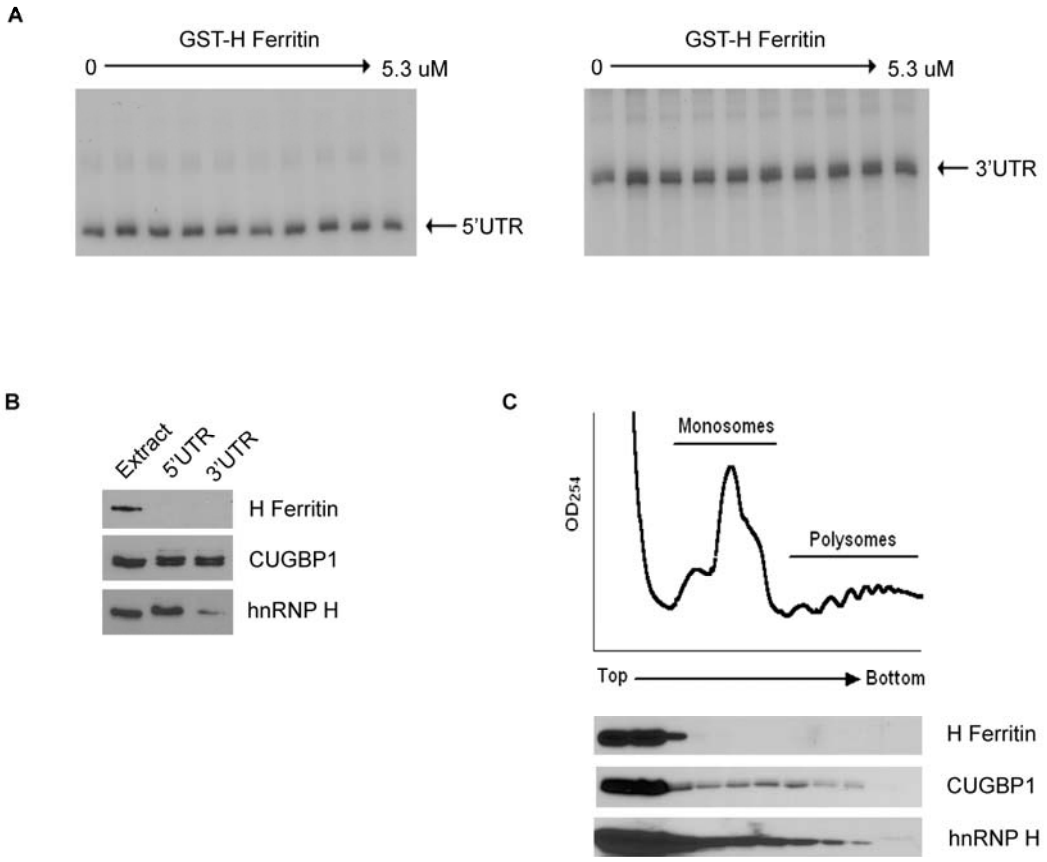

Figure 4.1. The interaction of H ferritin with the cSHMT UTRs. (A) Electrophoretic mobility shift assays were carried out using radiolabeled cSHMT 5'UTR *(left)* and cSHMT 3'UTR *(right)* and increasing concentrations of GST-tagged H ferritin. The arrows indicate the position of the unbound UTR. (B) MCF-7 whole cell extract was applied to RNA affinity columns to which either the cSHMT 5'UTR or the cSHMT 3'UTR had been attached. Proteins that bound to the UTRs were eluted and analyzed by western blotting using antibodies against H ferritin, CUGBP1, and hnRNP H. (C) Monosomal and polysomal fractions were separated from MCF-7 cells using a sucrose density gradient. Total protein was extracted from each fraction and subjected to western blot analysis using antibodies against H ferritin, CUGBP1, and hnRNP H.

columns, indicate that the role of H ferritin in the IRES-mediated translation of cSHMT is indirect. Rather than stimulating the cap-independent translation of cSHMT by binding to the cSHMT UTRs as previously proposed (7), H ferritin could exert its effect by causing changes in the labile iron pool, influencing the function CUGBP1 and/or hnRNP H2, or activating a novel cSHMT ITAF.

Neither ferric citrate nor iron chelators affect cSHMT IRES activity. Since H ferritin is an iron storage protein, a change in its concentration can have a dramatic effect on the labile iron pool within a cell. Thus, it is possible that the stimulation of cSHMT IRES activity observed upon H ferritin overexpression (7), and the decrease in cSHMT IRES activity seen in *H ferritin* $^{+/-}$ MEFs (7) is not caused by the H ferritin protein *per se*, but rather is due to H ferritin-induced changes in cellular iron status.

To mimic the decrease in the labile iron pool that occurs upon H ferritin overexpression (13,14), MCF-7 cells were treated with the iron chelator deferoxamine (DFO) for 24 or 48 h. Although H ferritin protein levels were not affected by DFO treatment, transferrin receptor (TfR) protein levels were elevated in DFO-treated cells (Figure 4.2A), indicating that iron depletion had occurred (15,16). DFO-treated cells were then transfected with bicistronic mRNA containing the cSHMT 5'UTR inserted between the Renilla luciferase (Rluc) and Firefly luciferase (Fluc) reporter genes, and the cSHMT 3'UTR 3' of the Fluc gene (Figure 4.2B). Whereas expression of the first cistron in this transcript (Rluc) is cap-dependent, expression of the second cistron (Fluc) is dependent on IRES activity. The results of the transfection experiments revealed that iron chelation by DFO does not affect cSHMT IRES activity, as quantified by the Fluc/Rluc ratio (Figure 4.2C). Similar data were obtained when mRNA transfections were performed using a bicistronic mRNA that lacks the cSHMT 3'UTR (Figures 4.2B and 4.2D). In agreement with the IRES activity measurements, cSHMT protein levels remained unchanged following DFO treatment (Figure 4.2A).

Figure 4.2. The effect of DFO on cSHMT IRES activity. (A) MCF-7 cells were treated with the indicated amounts of the iron chelator DFO. 24 or 48 h following treatment, total protein lysates were prepared and resolved by SDS-PAGE. Protein levels were determined by immunoblotting using antibodies against H ferritin, TfR, and cSHMT. GAPDH serves as a control for equal protein loading. (B) The two bicistronic mRNAs used to quantify cSHMT IRES activity. Both consist of (in the 5' to 3' direction) a cap analog, the Renilla luciferase (Rluc) reporter gene followed by three sequential in-frame stop codons, the human cSHMT 5'UTR which contains the IRES element, the Firefly luciferase (Fluc) reporter gene, and a 30 nucleotide poly(A) tail. The bicistronic mRNA on the left also contains the human cSHMT 3'UTR inserted between Fluc and the poly(A) tail (C) MCF-7 cells were transfected with bicistronic mRNA containing the cSHMT 3'UTR 24 h (white) or 48 h (grey) following DFO treatment. Fluc and Rluc activities were then quantified as described in Materials and Methods. The ratio of total Fluc activity divided by total Rluc activity in untreated cells was given a value of 1.0. The data represent the average of three independent experiments $\pm$ standard error. (D) The IRES activity of bicistronic mRNAs lacking the cSHMT 3'UTR as measured in MCF-7 cells 24 h (striped bars) or 48 h (black bars) following DFO treatment. The ratio of Fluc/Rluc in untreated cells was given a value of 1.0. The data represent the average of three independent experiments $\pm$ standard error.

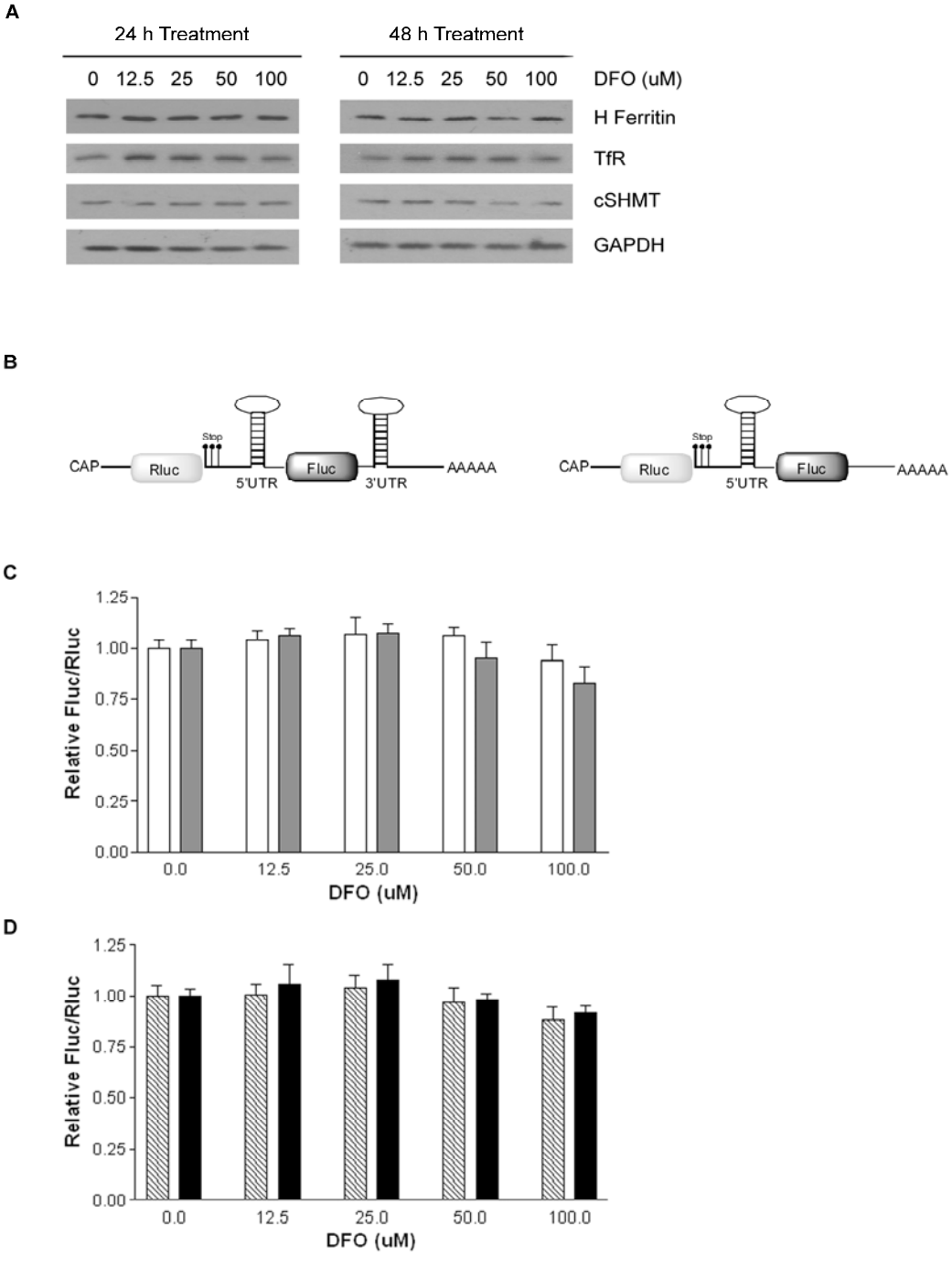
A
24 h Treatment
48 h Treatment
0 12.5 25 50 100
0 12.5 25 50 100
DFO (uM)
H Ferritin
TfR
cSHMT
GAPDH
B
CAP
Rluc
Stop
5'UTR
Fluc
3'UTR
AAAAA
C
Relative Fluc/Rluc
1.25
1.00
0.75
0.50
0.25
0.00
0.0
12.5
25.0
50.0
100.0
DFO (uM)
D
Relative Fluc/Rluc
DFO (uM)

To mimic the increased iron availability that occurs upon decreased H ferritin expression, MCF-7 cells were cultured with supplemental ferric citrate for 24 h. As expected based on previous findings (15), H ferritin protein levels exhibited a concentration-dependent increase following ferric citrate addition to the cell culture media (Figure 4.3A). However, consistent with earlier reports (6), cSHMT protein levels remained unchanged (Figure 4.3A). Treatment with ferric citrate also did not have a significant effect on cSHMT IRES activity, regardless of whether the 3'UTR was present (Figure 4.3B) or absent (Figure 4.3C) from the transcript. Taken together, the data from the DFO and ferric citrate studies suggest that H ferritin does not stimulate the IRES-mediated translation of cSHMT by altering the labile iron pool.

H ferritin does not affect CUGBP1 or hnRNP H2 protein levels or cellular localization. Because it is well established that the stimulation of many cellular IRESes depends on an increase in concentration and/or cytoplasmic localization of ITAFs (17), we next investigated the effect of H ferritin on CUGBP1 and hnRNP H2 protein levels and cellular compartmentation. Whole cell, cytoplasmic, and nuclear extract were isolated from three MCF-7cell lines that had been stably transfected with H ferritin cDNA, and two control MCF-7cell lines. The cell lines expressing the H ferritin cDNA had been analyzed previously and found to exhibit a 3.4 to 4-fold increase in H ferritin protein levels compared to control cells (7). Clones 1 and 2 also displayed a statistically significant increase in cSHMT IRES activity (7). However, none of the three clonal cell lines tested showed an increase in the overall levels of CUGBP1 or hnRNP H2, or the relocalization of these factors from the nucleus, where they primarily reside under normal cellular conditions (18,19), to the cytoplasm, where translation occurs (Figure 4.4).

Depletion of PCBP1 does not affect cSHMT IRES activity. Since the above results suggest that H ferritin does not stimulate cSHMT IRES activity indirectly by

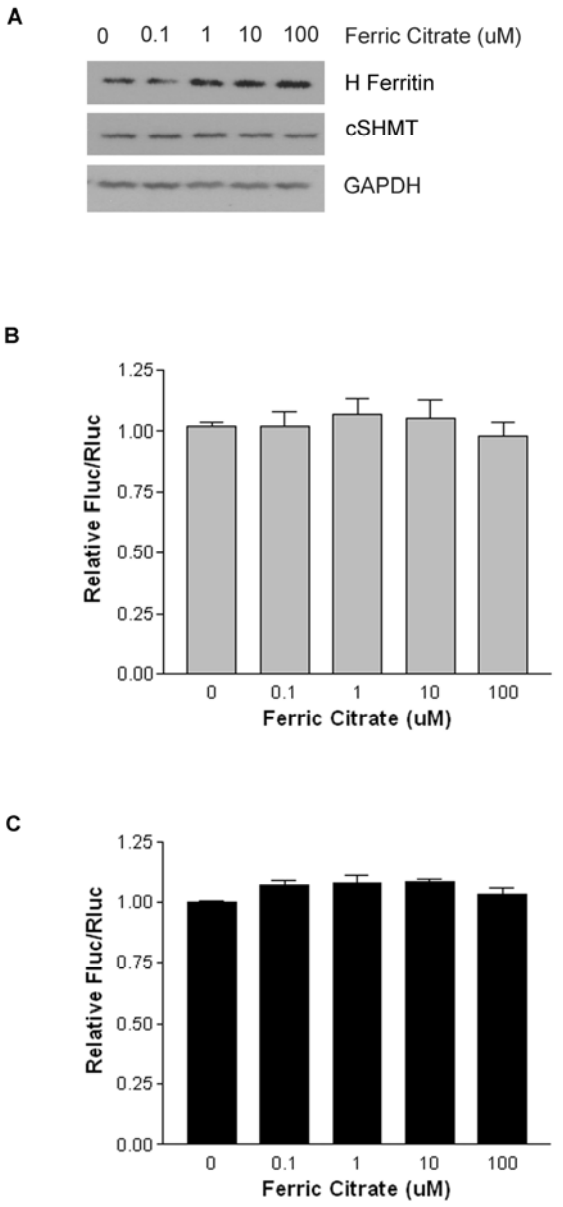

Figure 4.3. The effect of ferric citrate on cSHMT IRES activity. (A) MCF-7 cells were treated with the indicated amounts of ferric citrate. 24 h following treatment, total protein lysates were prepared and resolved by SDS-PAGE. Protein levels were determined by immunoblotting using antibodies against H ferritin and cSHMT. GAPDH serves as a control for equal protein loading. (B and C) MCF-7 cells that had been incubated with the indicated amount of ferric citrate for 24 h were transfected with bicistronic mRNA containing (B) or lacking (C) the cSHMT 3'UTR, and the ratio of Fluc to Rluc activity was measured. The Fluc/Rluc value in untreated cells was given a value of 1.0. The data represent the average of three independent experiments $\pm$ standard error.

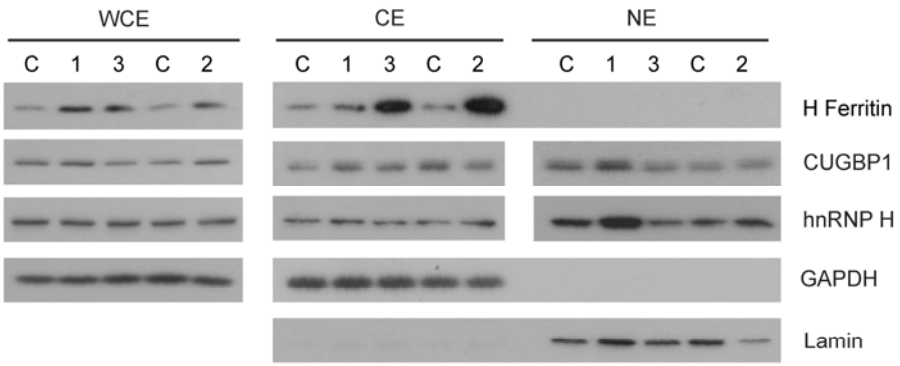

Figure 4.4. CUGBP1 and hnRNP H2 protein levels and localization in H ferritin overexpressing cell lines. (A) Nuclear (NE) and cytoplasmic (CE) extracts were isolated from three MCF-7cell lines that had been stably transfected with H ferritin cDNA (1, 2, and 3), and two control MCF-7cell lines (C). Whole cells extracts (WCE) were also obtained from the same cell lines. All extracts were subjected to immunoblotting using an anti-H ferritin, anti-CUGBP1, or anti-hnRNP H antibody. GAPDH is shown as a control to demonstrate that the nuclear fractions are free of cytoplasmic contamination. Lamin A is shown as a control to demonstrate that the cytoplasmic fractions are free of nuclear contamination. Both GAPDH and Lamin A serve as controls for protein loading.

increasing the cytoplasmic concentrations of the two known cSHMT ITAFs, it is possible that it exerts its effect through a currently unidentified cSHMT ITAF. The best candidate for this novel ITAF is poly r(C) binding protein 1 (PCBP1). PCBP1 was recently identified as an iron chaperone that delivers iron to H ferritin (20). It is also an RNA-binding protein that has been implicated in the IRES-mediated translation of several transcripts (21-23). To determine if PCBP1 plays a role in the IRES-mediated translation of cSHMT, siRNA was used to knockdown PCBP1 protein levels in MCF-7 cells, and IRES activity was measured using the bicistronic constructs. Although PCBP1 protein levels were reduced by at least 50% compared to cells treated with negative control siRNA (Figure 4.5A), cSHMT IRES activity remained unchanged (Figure 4.5B), even when the cells were exposed to UV radiation, which is known to activate the cSHMT IRES (Chapter 5).

Discussion

The experiments described in this report were conducted to determine the mechanism by which H ferritin stimulates the IRES-mediated translation of cSHMT. Although they all produced negative results, they did succeed in casting doubt on many of the possible roles of H ferritin in cap-independent translational regulation. H ferritin's effect on cSHMT IRES-mediated translation appears to be unrelated to its catalytic activity. Alterations in the labile iron pool induced upon the addition of ferric citrate and the iron chelator DFO had no effect on cSHMT IRES activity, although we cannot rule out the possibility that Fe^{2+} bound to the outer surface of the ferritin molecule affects IRES stimulation by H ferritin. PCBP1, the iron chaperone that delivers iron to H ferritin, likewise does not play a role in the IRES-mediated translation of cSHMT.

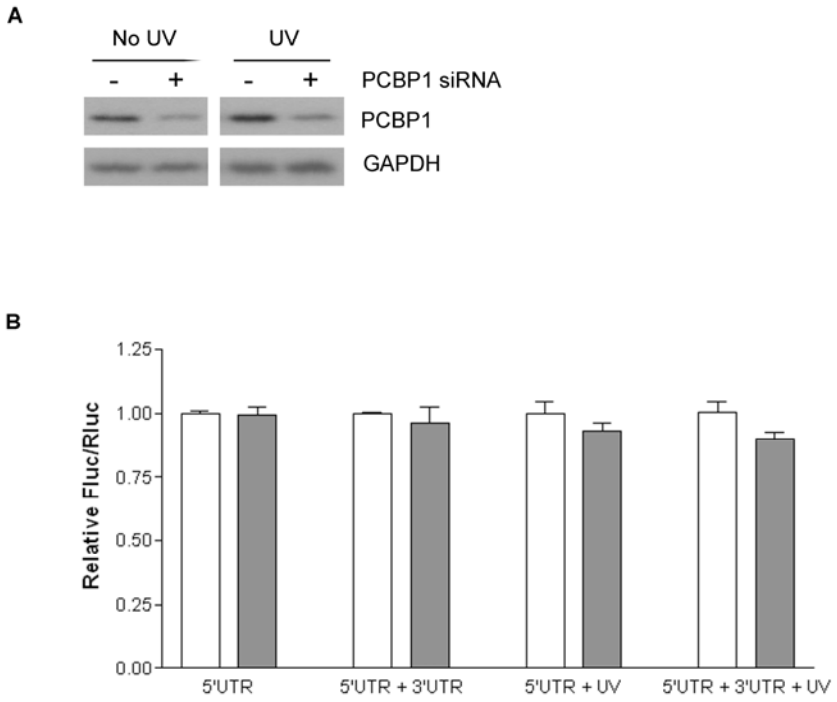

Figure 4.5. PCBP1 does not affect cSHMT IRES activity. (A) MCF-7 cells were transfected with negative control siRNA (- PCBP1 siRNA) or PCBP1 siRNA and then treated with UV. 22 h after UV treatment, PCBP1 knockdown was confirmed by western blotting. GAPDH serves as a control for equal protein loading. (B) The activity of the cSHMT IRES was quantified as the Fluc/Rluc ratio in MCF-7 cells treated with negative control siRNA (white bars) or PCBP1 siRNA (grey bars). Cells were transfected with the biscistronic mRNAs described in Figure 4.2B containing or lacking the cSHMT 3'UTR in the presence and absence of UVC exposure. For each experimental condition, values obtained from negative control siRNA-treated cells were given a value of 1.0. The data represent the average of two independent experiments $\pm$ standard error.

Previous studies have shown that CUGBP1 and hnRNP H2 are ITAFS that stimulate cSHMT IRES activity by binding to the 5' and 3'UTRs of the transcript, respectively (Chapter 3) (7). CUGBP1 and hnRNP H2 physically interact, and their interaction functions to circularize the cSHMT mRNA, thereby facilitating the recycling and/or recruitment of the translation initiation complex (Chapter 3). Both of these ITAFs have been shown to interact with H ferritin in immunoprecipitation experiments and yeast two-hybrid assays (7,11), but surprisingly, the results of this study demonstrate that the interactions among CUGBP1, hnRNP H2, and H ferritin do not play a direct role in cSHMT IRES-mediated translation. H ferritin is not present with CUGBP1 and hnRNP H2 in polysomes that contain actively translating mRNA and it does not bind to the cSHMT 5'UTR or 3'UTR *in vitro*. H ferritin also does not influence IRES activity by altering the cellular levels or localization of CUGBP1 or hnRNP H2. However, it is still possible H ferritin functions to facilitate the assembly of the CUGBP1-hnRNP H2 complex prior to the binding of the translation initiation machinery. This would be consistent with an indirect role of H ferritin in cSHMT IRES-mediated translation, and would fit nicely into the previously determined model of cSHMT IRES activation. Further work is needed to test the influence of H ferritin on the CUGBP1-hnRNP H2 interaction.

REFERENCES

1. Munro, H. N., and Linder, M. C. (1978) *Physiol Rev* **58**(2), 317-396
2. Levi, S., Luzzago, A., Cesareni, G., Cozzi, A., Franceschinelli, F., Albertini, A., and Arosio, P. (1988) *J Biol Chem* **263**(34), 18086-18092
3. Westerman, D. A., Evans, D., and Metz, J. (1999) *Br J Haematol* **107**(3), 512-515
4. Lagarde, S., Jovenin, N., Diebold, M. D., Jaussaud, R., Cahn, V., Bertin, E., Jolly, D., Thiefin, G., and Cadiot, G. (2006) *Gastroenterol Clin Biol* **30**(11), 1245-1249
5. Suh, J. R., Herbig, A. K., and Stover, P. J. (2001) *Annu Rev Nutr* **21**, 255-282
6. Oppenheim, E. W., Adelman, C., Liu, X., and Stover, P. J. (2001) *J Biol Chem* **276**(23), 19855-19861
7. Woeller, C. F., Fox, J. T., Perry, C., and Stover, P. J. (2007) *J Biol Chem* **282**(41), 29927-29935
8. Hellen, C. U., and Sarnow, P. (2001) *Genes Dev* **15**(13), 1593-1612
9. Martinez-Salas, E., Lopez de Quinto, S., Ramos, R., and Fernandez-Miragall, O. (2002) *Biochimie* **84**(8), 755-763
10. Stoneley, M., and Willis, A. E. (2004) *Oncogene* **23**(18), 3200-3207
11. Fox, J. T., and Stover, P. J. (Unpublished Results)
12. Bensadoun, A., and Weinstein, D. (1976) *Anal Biochem* **70**(1), 241-250
13. Picard, V., Epsztejn, S., Santambrogio, P., Cabantchik, Z. I., and Beaumont, C. (1998) *J Biol Chem* **273**(25), 15382-15386
14. Picard, V., Renaudie, F., Porcher, C., Hentze, M. W., Grandchamp, B., and Beaumont, C. (1996) *Blood* **87**(5), 2057-2064
15. Ponka, P. (1999) *Kidney Int Suppl* **69**, S2-11

16. Rao, K. K., Shapiro, D., Mattia, E., Bridges, K., and Klausner, R. (1985) *Mol Cell Biol* **5**(4), 595-600

17. Lewis, S. M., and Holcik, M. (2008) *Oncogene* **27**(8), 1033-1035

18. Michalowski, S., Miller, J. W., Urbinati, C. R., Paliouras, M., Swanson, M. S., and Griffith, J. (1999) *Nucleic Acids Res* **27**(17), 3534-3542

19. Timchenko, L. T., Miller, J. W., Timchenko, N. A., DeVore, D. R., Datar, K. V., Lin, L., Roberts, R., Caskey, C. T., and Swanson, M. S. (1996) *Nucleic Acids Res* **24**(22), 4407-4414

20. Shi, H., Bencze, K. Z., Stemmler, T. L., and Philpott, C. C. (2008) *Science* **320**(5880), 1207-1210

21. Nishimura, K., Ueda, K., Guwanan, E., Sakakibara, S., Do, E., Osaki, E., Yada, K., Okuno, T., and Yamanishi, K. (2004) *Virology* **325**(2), 364-378

22. Pickering, B. M., Mitchell, S. A., Evans, J. R., and Willis, A. E. (2003) *Nucleic Acids Res* **31**(2), 639-646

23. Spangberg, K., and Schwartz, S. (1999) *J Gen Virol* **80 (Pt 6)**, 1371-1376

CHAPTER 5

A UV-RESPONSIVE INTERNAL RIBOSOME ENTRY SITE ENHANCES CYTOPLASMIC SERINE HYDROXYMETHYLTRANSFERASE EXPRESSION FOR DNA DAMAGE REPAIR

Abstract

Thymidine nucleotides are required for faithful DNA synthesis and repair, and their de novo biosynthesis is regulated by cytoplasmic serine hydroxymethyltransferase (cSHMT). The cSHMT transcript contains a heavy chain ferritin (H ferritin), heterogeneous nuclear ribonucleoprotein H2 (hnRNP H2), and CUG-Binding Protein 1 (CUGBP1)-responsive internal ribosome entry site (IRES) that regulates cSHMT translation. In this study, a non-lethal dose of UVC is shown to increase cSHMT IRES activity and cSHMT protein levels. The mechanism for the UV-induced activation of the cSHMT IRES involves an increase in H ferritin and hnRNP H2 expression and the translocation of CUGBP1 from the nucleus to the cytoplasm. The UV-induced increase in cSHMT translation is accompanied by an increase in the Small Ubiquitin-Like Modifier (SUMO)-dependent nuclear localization of the *de novo* thymidylate biosynthesis pathway and a decrease in DNA strand breaks, indicating a role for cSHMT and nuclear folate metabolism in DNA repair.

Introduction

UV radiation is mutagenic and damages cellular macromolecules, including proteins, lipids and DNA. Thymine bases within DNA are sensitive to UV-induced damage, forming cyclobutane-type pyrimidine dimers and (6-4)-photoproducts (2). These lesions hinder RNA polymerase processivity and thus inhibit transcription (3).

In mammalian cells, cyclobutane-type pyrimidine dimers and (6-4)-photoproducts are repaired by nucleotide excision repair (NER). NER involves the removal of approximately 30 nucleotides surrounding the damage site, resulting in a single-strand gap that requires DNA synthesis and ligation to complete the repair process (4).

Thymidine triphosphate is required for faithful DNA synthesis. Insufficient pools of thymidine nucleotides during DNA replication and NER result in elevated rates of uracil misincorporation into DNA, which ultimately leads to DNA strand breaks and genome instability (7). Thymidine nucleotides can either be synthesized through a salvage pathway or can be synthesized *de novo* through folate-mediated one-carbon metabolism (Figure 5.1). In the *de novo* biosynthetic pathway, 5,10-methylenetetrahydrofolate (5,10-methyleneTHF) provides the activated one-carbon units and reducing equivalents for the thymidylate synthase (TS)-catalyzed conversion of deoxyuridine monophosphate (dUMP) to thymidylate. 5,10-methyleneTHF can be generated by two alternative pathways: the reduction of 10-formylTHF, or through the activity of cytoplasmic serine hydroxymethyltransferase (cSHMT), which catalyzes the conversion of THF and serine to glycine and 5,10-methyleneTHF.

The cSHMT enzyme is a key regulator of *de novo* thymidylate biosynthesis and is poised to play a role in the repair of UV-induced DNA damage. In addition to providing one-carbon units for the synthesis of thymidylate, cSHMT-derived 5,10-methyleneTHF can be reduced by methyleneTHF reductase (MTHFR) to form 5-methylTHF, a cofactor utilized in the remethylation of homocysteine to methionine (Figure 5.1). The concentration of free folate in the cell is negligible, and therefore TS and MTHFR compete for limiting pools of the 5,10-methyleneTHF cofactor (8-11). Several studies have demonstrated that whereas the majority of 5,10-methyleneTHF derived from the reduction of 10-formylTHF is directed toward the synthesis of methionine (12,13), cSHMT-derived 5,10-methyleneTHF is partitioned to TS (14)

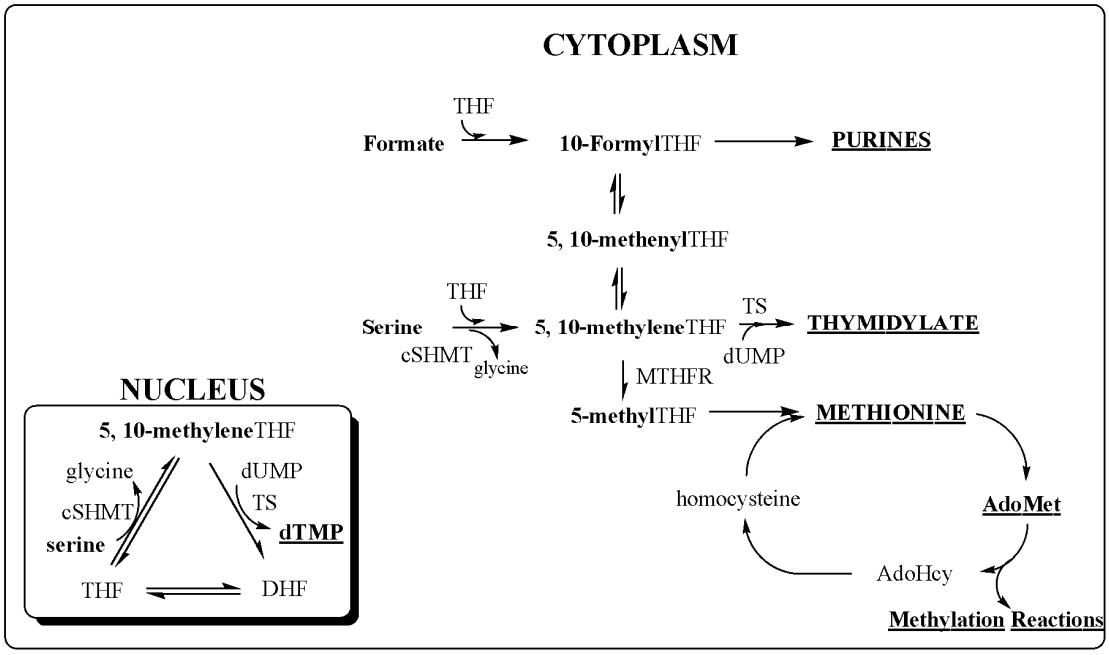

Figure 5.1. Folate-mediated one-carbon metabolism. Folate-mediated one-carbon metabolism is required for the *de novo* synthesis of purines and thymidylate and for the remethylation of homocysteine to methionine. Mitochondrial-derived formate can enter the cytoplasm and function as a one-carbon donor through the conversion of tetrahydrofolate (THF) to 10-formylTHF. 5,10-methyleneTHF, which can be generated through the reduction of 10-formylTHF or through the catalytic activity of cytoplasmic serine hydroxymethyltransferase (cSHMT), provides the one-carbon units for the thymidylate synthase (TS)-catalyzed conversion of deoxyuridine monophosphate (dUMP) to thymidylate. It also serves as a substrate for methyleneTHF reductase (MTHFR), which reduces 5,10-methyleneTHF to ultimately form S-adenosylmethionine (AdoMet), the one-carbon donor in numerous cellular methylation reactions. *De novo* thymidylate biosynthesis also occurs in the nucleus through the SUMO-dependent import of the thymidylate synthesis pathway during S-phase.

through the cell cycle-dependent and Small Ubiquitin-Like Modifier (SUMO)-mediated nuclear localization of the thymidylate biosynthesis pathway (15,16) (Figure 5.1).

The DNA damage caused by UV radiation evokes adaptive cellular responses which include cell cycle arrest (17) and changes in transcription (18,19) and translation. At the translational level, UV radiation inhibits global cap-dependent protein synthesis by inducing the phosphorylation of eukaryotic initiation factor (eIF) 2α (5,20,21) and thereby preventing the recycling of the ternary complex (eIF2-GTP-Met-tRNAi) (22). Despite the reduction in cap-dependent translation, several mRNAs whose protein products are essential for the UV-induced stress response (for example p53 (23) and Apaf-1 (24)) have evolved alternative mechanisms of protein synthesis that allow for their continued expression following exposure to UV. One such mechanism involves ribosome recruitment to an internal ribosome entry site (IRES) located within the 5'untranslated region (UTR) of the transcript (25,26).

We have previously shown that the cSHMT 5'UTR contains an IRES whose activity is stimulated by heavy chain ferritin (H ferritin) (1) and the IRES *trans*-acting factors (ITAFs) heterogeneous nuclear ribonucleoprotein H2 (hnRNP H2) and CUG-Binding Protein 1 (CUGBP1) (Chapter 3) (1). However, the responsiveness of the IRES to stress stimuli that inhibit cap-dependent translation has not been explored. In the present study, we demonstrate the role of the cSHMT IRES and folate-dependent nuclear thymidylate biosynthesis in the provision of one-carbon units during UV-induced DNA damage repair.

Materials and Methods

Cell culture- Human MCF-7 mammary adenocarcinoma cells (HTB22), HeLa cells (CCL2), and pagetoid sarcoma skin fibroblasts (CRL-7677) were obtained from

ATCC. The human SH-SY5Y neuroblastoma, a subline of the SK-N-SH neuroblastoma, was obtained from June Biedler (Fordham University). MCF-7, HeLa, and SH-SY5Y cells were cultured in α-MEM (Hyclone Laboratories) containing 11% fetal bovine serum (Hyclone Laboratories). Pagetoid sarcoma skin fibroblasts were cultured in DMEM (Gibco) containing 11% fetal bovine serum (Hyclone Laboratories). All cells were maintained at 37^{o}C and 5% CO_2.

Treatment and preparation of cell extracts- MCF-7 cells at 30% confluence were arrested at the G2/M phase of the cell cycle by treatment with 60 ng/mL nocodazole (Calbiochem) for 24 h. Cell cycle analysis was carried out by fluorescence-activated cell sorting using 3 mM sodium citrate containing 1% Triton X-100 and 50 ng/mL propidium iodide as the lysis/DNA binding reagent. For experiments involving UV treatment, cells at 95% confluence were washed twice with phosphate-buffered saline and then exposed to 10,000 μJ/cm^2 UV (254 nm) using the Stratagene UV Stratalinker 2400. The medium was then replaced and the cells cultured under normal conditions. At the indicated time intervals following treatment, the cells were harvested by trypsinization and washed in phosphate-buffered saline. To obtain whole cell extracts, the cells were resuspended in lysis buffer (50 mM Tris pH 7.5, 150 mM NaCl, 1% NP-40, 5 mM EDTA, 1 mM PMSF, 1:100 dilution of Sigma Protease Inhibitor Cocktail, 10 mM N-ethylmalemide) and lysed on ice for 30 min. Nuclear and cytoplasmic extracts were obtained using the NE-PER Nuclear and Cytoplasmic Extraction Kit (Pierce) according to the manufacturer's protocol. The protein concentration of all extracts was determined using the Lowry Assay as modified by Bensadoun (27).

Trypan Blue Exclusion- MCF-7 cells were treated with UV according to the protocol above. 24 h after UV exposure, the cells were harvested by trypsinization, pelleted by centrifugation, and then resuspended in serum-free α-MEM. The

suspension was then diluted 1:1 with 0.4% Trypan Blue (Invitrogen), and the viable and non-viable cells were counted using a hemocytometer.

Metabolic labeling- Control and UV-irradiated cells were labeled with 100 μCi/mL EasyTag^{TM} EXPRESS ^{35}S Protein Labeling Mix (Perkin Elmer, 1175 Ci/mmol) for 30 min in methionine/cysteine-free DMEM (Sigma). Cells were then harvested and lysed as described above. The protein concentration of all extracts was determined using the Lowry Assay as modified by Bensadoun (27), and equal amounts of extract were separated by 12% SDS-PAGE. The gel was stained with Coomassie Blue (R-250), dried, and autoradiographed. To quantify the amount of ^{35}S incorporation, equal amounts of protein were precipitated with TCA, and radioactivity was quantified in a LS 6500 Multi-Purpose Scintillation Counter (Beckman Coulter).

Western blotting- Proteins were separated by SDS-PAGE using a Tris-glycine gel and transferred to a PVDF membrane. The membrane was blocked with 5% non-fat dry milk in phosphate-buffered saline containing 1% NP-40 for 1 h at room temperature, incubated with primary antibody overnight at 4^{o}C, and then incubated with horseradish peroxidase-conjugated anti-IgG for 1-3 h at room temperature. After each incubation, the membrane was washed with phosphate-buffered saline/0.1% Tween 20. Proteins were visualized using Super Signal® substrate (Pierce) followed by autoradiography. Mouse anti-phospho-p53 (Ser15, Cell Signaling) was used at a 1:1000 dilution, rabbit anti-phospho-eIF2α (Ser51, Cell Signaling) was used at a 1:1000 dilution, affinity purified sheep anti-human cSHMT was used at a 1:40,000 dilution, sheep anti-TS (Abcam) was used at a 1:2000 dilution, mouse anti-CUGBP1 (3B1, Santa Cruz Biotechnology) was used at a 1:10,000 dilution, affinity purified sheep anti-H ferritin was used at a 1:500 dilution, goat anti-hnRNP H (N-16, Santa Cruz Biotechnology) was used at a 1:1000 dilution, rabbit anti-SUMO-1 (Active Motif) was used at a 1:1000 dilution, rabbit anti-p53 (Active Motif) was used at a

1:1000 dilution, goat anti-eIF2α (Santa Cruz Biotechnology) was used at a 1:1000 dilution, rabbit anti-Lamin A (H-102, Santa Cruz Biotechnology) was used at a 1:1000 dilution, and mouse anti-GAPDH (Novus Biologicals) was used at a 1:40,000 dilution. Goat anti-mouse IgG, rabbit anti-sheep IgG, rabbit anti-goat IgG, and goat anti-rabbit IgG were all purchased from Pierce and used at a 1:5,000 dilution. When necessary, membranes were stripped with 0.2 M sodium hydroxide.

Real time PCR- RNA was extracted from cells using Trizol (Invitrogen) according to the manufacturer's protocol. After incubating with DNaseI for 1 h at 37^{o}C to remove any residual DNA, the RNA was purified using the RNeasy Mini Kit (Qiagen) and reverse transcribed into cDNA using the High Capacity cDNA Reverse Transcription Kit (Applied Biosystems). The PCR was carried out using either the 2X Taqman Universal PCR mix and FAM-labeled Taqman probes complimentary to cSHMT (Hs00541038_m1) and GAPDH (Hs99999905_m1), or the QuantiFast SYBR Green PCR Kit (Qiagen) and primers complimentary to Fluc (5'-ATTTATCGGAGTTGCAGTTGCGCC-3'; 5'-GCTGCGAAATGCCCATACTGTTGA-3') and Rluc (5'-AACGCGGCCTCTTCTTATTT-3'; 5'-ATTTGCCTGATTTGCCCATA-3'). PCR products were quantified using the Applied Biosystems 7500 Real-Time PCR System.

Polysome profile analysis- MCF-7 cells at approximately 80% confluence were treated with UVC following the protocol above. 22 h following UV exposure, the cells were treated with 50 μg/mL cycloheximide (Sigma) for 30 min at 37^{o}C and 5% CO_2. The cells were scraped from the plate and then lysed in polysome extraction buffer (10 mM Tris pH 7.5, 10 mM NaCl, 1.5 mM $MgCl_2$, 1% Triton X-100, 1% deoxycholate, 2% Tween 20, 1000u Recombinant RNasin® Ribonuclease Inhibitor (Promega)) for 10 min on ice. Nuclei were pelleted by brief centrifugation and the resulting supernatant was fractionated through a 10-50% sucrose gradient by

ultracentrifugation in a SW41-Ti rotor for 2 h at 36,000 rpm and 4^{o}C. 1 mL fractions were collected with a density gradient fractionation system (Brandel) and the absorbance at 254 nm was measured continuously as a function of gradient depth. RNA was isolated by phenol-chloroform extraction, treated with DNaseI for 1 h at 37^{o}C, and then reverse transcribed using the SuperScriptIII First-Strand Synthesis System (Invitrogen) according to the manufacturer's protocol. The PCR was carried out using primers specific to cSHMT (Fwd = 5'-ATGCCCTACAAGGTGAACCCAGAT-3' and Rev = 5'-ACCACATGGCAGTGTTCAAATGGG-3'), CUGBP1 (Fwd= 5'-TCACTTGGAGCCCTGCAGACATTA-3' and Rev=5'-AGCAGCATATTGCTGGATACCCGA-3'), and ATF4 (Fwd= 5'-CCAACAACAGCAAGGAGGATGCCTTCTC-3' and Rev= 5'-GGATCATGGCAACGTAAGCAGTGTAGTC-3').

Generation of capped bicistronic mRNA for use in MCF-7 cell transfections- The generation of pSP64 polyA DNA templates containing the Renilla and Firefly luciferase reporter genes and either the cSHMT 5'UTR, cSHMT 5'UTR and 3'UTR, the reverse complement of the cSHMT 5'UTR (Rev UTR), or the mouse cSHMT 5'UTR is described elsewhere (1). The DNA templates were linearized with EcoRI and purified using the Roche PCR clean-up column. The templates were transcribed using the T7 mMESSAGE mMACHINE kit (Ambion) according to the manufacturer's protocol. The crude mRNA was treated with DNaseI (Ambion) for 15 min at 40°C and precipitated in 2 M LiCl at -80°C. All RNA procedures were conducted under RNase-free conditions and all mRNA was stored with Recombinant RNasin® Ribonuclease Inhibitor (Promega). The mRNA was quantified by spectrophotometry and its quality verified by electrophoresis.

mRNA transfections- Cells were cultured in 6-well plates and then treated with UVC or nocodazole according to the protocol above. 12 h after UV treatment or 24 h after nocodazole treatment, the cells were incubated in Opti-MEM (Invitrogen) containing a 1:100 dilution of DMRIE-C transfection reagent (Invitrogen), and 5 μg/mL bicistronic mRNA (capped and polyadenylyated) for 4 h at 37°C and 5% CO_2. The Opti-MEM was then replaced with α-MEM or DMEM and the cells incubated for an additional 6 h at 37°C and 5% CO_2. Renilla and Firefly Luciferase activity was quantified on a Veritas Microplate Luminometer (Turner Biosystems) using the Dual-Glo Luciferase Assay System (Promega) according to the manufacturer's protocol.

siRNA transfections- MCF-7 cells were grown to approximately 40% confluence in 6-well plates. The cells were transfected with 5 nM of either negative control siRNA (Ambion), CUGBP1 siRNA (Qiagen, sense: r(GGAACUCUUCGAACAGUAU)dTdT, antisense: r(AUACUGUUCGAAGAGUUCC)dCdG), or cSHMT siRNA (Qiagen, sense: r(CUAGGCUCUUGCUUAAAUA)dTdT, antisense: r(UAUUUAAGCAAGAGCCUAG)dGdG) using the HiPerFect transfection reagent (Qiagen) according to the manufacturer's instructions. Following incubation with siRNA for 48-55 h at 37° C and 5% CO_2, the cells were treated with UVC according to the protocol above. At the indicated time following UV treatment, the cells were lysed and subjected to SDS-PAGE/immunoblot analysis to determine knockdown efficiency.

Immunofluorescence- MCF-7 cells were grown on sterile coverslips to approximately 30% confluence and then exposed to 10,000 μJ/cm^2 UV (254 nm) according to the protocol above. 22 h following UV treatment, the coverslips were incubated in phosphate-buffered saline containing 10 μM DRAQ5 (Biostatus Limited) for 5 min at room temperature and then fixed with 100% methanol for 5 min. After a

brief wash in phosphate-buffered saline, the coverslips were blocked with phosphate-buffered saline containing 2% bovine serum albumen and 0.1% Triton X-100. After 2 h, the blocking solution was removed and the coverslips incubated in phosphate-buffered saline containing 2% bovine serum albumen and a 1:250 dilution of mouse anti-CUGBP1 (3B1, Santa Cruz Biotechnology) for 2 h at room temperature. Following extensive washing with phosphate-buffered saline, the coverslips were incubated in phosphate-buffered saline containing 2% bovine serum albumen and a 1:500 dilution of an Alexa-Fluor 488-conjugated goat anti-mouse IgG secondary antibody (Invitrogen) for 1 hour. The coverslips were then washed extensively with phosphate-buffered saline and mounted to slides using Fluoromount-G (Southern Biotech). The cells were visualized using a Leica TCS SP2 confocal microscope at the Cornell University Microscopy and Imaging Facility.

Comet assay- MCF-7 cells were treated with either negative control siRNA or cSHMT siRNA and then exposed to 10,000 μJ/cm^2 UVC according to the protocol above. At the indicated times following UV treatment, the cells were scraped from the plate. Half of the cells were subjected to western blot analysis to confirm cSHMT knockdown. The other half were resuspended in α-MEM (Hyclone Laboratories) supplemented with 10% DMSO and 20 mM EDTA pH 7.5, dispensed into cryogenic tubes, frozen in liquid nitrogen, and stored at -80^{o}C.

The cryopreserved cells from above were thawed at room temperature and then diluted to a final concentration of 10^5 cells/mL with phosphate-buffered saline, pH 7.4. The diluted cells were then combined 1:10 with 1% low-melting point agarose and dispensed onto a CometSlide (Trevigen). After the agarose solidified, the slides were immersed in lysis solution (10% DMSO, 1% Triton X-100, 2.5 M NaCl, 100 mM EDTA, 10 mM Tris pH 10.2) for 1-3 h at 4^{o}C. Following a 10 min incubation in 0.4 M Tris pH 7.5, the slides were placed in an electrophoresis tank and incubated in

alkaline (pH 13) electrophoresis buffer (0.3M NaOH, 1 mM EDTA pH 8.0) for 20 min at 4^{o}C to allow for the unwinding of supercoiled DNA. Electrophoresis was carried out at 27 V for 40 min at 4^{o}C. The slides were then incubated in 0.4 M Tris pH 7.5 for 15 min, washed for 5 min in 100% ethanol, and dried overnight. To assess DNA damage, the dried slides were flooded with SYBR Gold^{TM} (Invitrogen) and then visualized at 20X magnification using a fluorescent microscope (Olympus BX-50) at the Cornell University Microscopy and Imaging Facility. Cells were photographed using a QImaging Retiga EXi cooled CCD camera and analyzed using Komet 5.5 Software (Andor Technology). The parameters analyzed included % tail DNA (the proportion of DNA that has migrated from the nucleoid core), tail length (the distance (microns) of DNA migration from the nucleoid core), extent tail moment (% tail DNA x tail length/100), and olive tail moment ([tail center of gravity – head center of gravity] x % tail DNA/100). The olive tail moment value captures both the smallest detectable size of migrating DNA (which is quantified in the comet tail length) and the number of strand breaks (quantified by the intensity of DNA in the tail). The mean value from 75 scored cells was taken as an index of damage for a given sample. Sensitivity of the assay was established by incubating untreated MCF-7 cells in 0, 50, 100, or 200 μM hydrogen peroxide for 15 min prior to lysis and then quantifying the resulting comets as stated above. The concordance of each measured parameter in relation to hydrogen peroxide concentration (R^2) ranged from 0.92 to 0.96.

MTT Assay - MCF-7 cells were treated with either negative control siRNA or cSHMT siRNA and then exposed to 10,000 μJ/cm^2 UVC according to the protocol above. 24 h following UV treatment, MTT (thiazolyl blue tetrazolium bromide; Sigma) was added to the media (final concentration of MTT = 0.5 mg/mL). After a 1 h incubation at 37^{o}C/5% CO_2, the media was removed from the cells and the insoluble formazan (formed by the reduction of MTT by living mitochondria) was resuspended

in DMSO. The absorbance at 550 nm was measured using a Dynex MRXTC II microplate reader.

Immunoprecipitations- MCF-7 whole cell extracts were incubated for 2 h at 4ºC with 40µL of protein A/G conjugated agarose beads (Pierce) to remove nonspecific matrix-binding proteins. The precleared extracts were incubated with 10 µg of either sheep IgG (Pierce), affinity purified sheep anti-human cSHMT antibody, or sheep-anti-human TS antibody (Abcam) overnight at 4ºC. 40µL of the protein A/G agarose beads was then added and the reaction was allowed to incubate for 2 h at 4^{o}C. The beads were collected and washed 5 times with lysis buffer (50 mM Tris pH 7.5, 150 mM NaCl, 1% NP-40, 5 mM EDTA, 1 mM PMSF, 1:100 dilution of Sigma Protease Inhibitor Cocktail), and bound proteins were eluted in 2X SDS-PAGE sample buffer (160 mM Tris pH 6.8, 20 mM DTT, 4% SDS, 20% glycerol) at 95^{o}C for 10 min. The samples were analyzed by western blotting as described above, except that TrueBlot™ (eBioscience, 1:1000 dilution) was used as the secondary antibody to eliminate IgG contamination.

Results

The expression of cSHMT is induced by UV radiation. Previously, we have shown that cSHMT is rate-limiting for *de novo* thymidylate biosynthesis during DNA replication in MCF-7 cells (28), and that mice lacking cSHMT exhibit elevated levels of uracil in their DNA (29). In this study, the effect of UV radiation on cSHMT protein levels was examined to investigate the regulation of nuclear thymidylate biosynthesis during DNA repair. MCF-7 cells were treated with 10,000 µJ/cm^2 UVC (254 nm). This dose of UV was not lethal, as 90% of treated cells remained viable 24 hours after UV exposure compared to 97% of untreated cells (Figure 5.2). However, the dose was sufficient to evoke a stress response. As anticipated based on previous

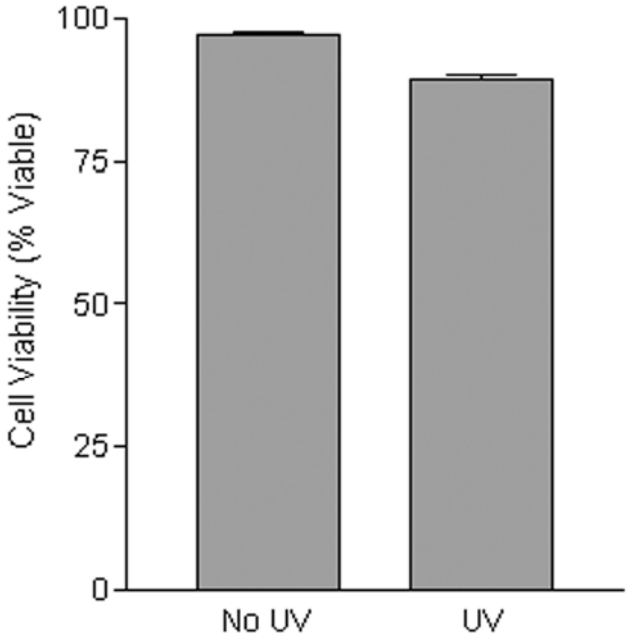

Figure 5.2. MCF-7 cells remain viable following UV treatment. The % viability of untreated and UV-treated MCF-7 cells was determined by trypan blue exclusion 24 h following UV exposure. The data represent the average of three independent experiments ± standard error.

studies (5,20,21,30-32), global protein synthesis was impaired (Figures 5.3A and 5.3B), p53 protein levels increased (Figure 5.4A), and both p53 and eIF2α became phosphorylated in a time-dependent manner following UV exposure (Figure 5.4A), indicating that DNA damage had occurred and that cap-dependent protein synthesis was suspended. Western blot analysis of cSHMT protein levels revealed that despite the cessation of cap-dependent translation, cSHMT protein levels were increased 12 and 24 hours following UV treatment (Figure 5.4A). The increase in cSHMT protein levels in response to UV exposure was not specific to MCF-7 cells, as similar results were obtained with cervical cancer (HeLa) cells (Figure 5.4B), transformed skin fibroblasts (Figure 5.4C) and neuroblastoma (SH-SY5Y) cells (Figure 5.4D).

The cSHMT IRES is UV responsive. CSHMT mRNA levels did not increase following UV treatment (Figure 5.5), indicating that the increase in cSHMT protein levels may be due to elevated rates of translation. Consistent with this hypothesis, the polysome analysis of untreated (Figure 5.6A) and UV-treated (Figure 5.6B) MCF-7 cells revealed that cSHMT mRNA continued to be actively translated following UV exposure. Because cellular IRESes are typically responsive to stress stimuli that inhibit global cap-dependent translation (25), the effect of UV treatment on cSHMT IRES activity was investigated. Following UV treatment, MCF-7 cells, HeLa cells, transformed skin fibroblasts, and SH-SY5Y cells were transfected with bicistronic mRNAs containing the cSHMT 5'UTR inserted between the Renilla luciferase (Rluc) and Firefly luciferase (Fluc) reporter genes, and the cSHMT 3'UTR located 3' of the Fluc gene (Figure 5.7A). Whereas expression of the first cistron in this transcript (Rluc) is cap-dependent, expression of the second cistron (Fluc) is dependent on IRES activity. The activity of the cSHMT IRES increased significantly in all UV-exposed cells compared to unexposed cells as quantified by the Fluc/Rluc ratio (Figure 5.7B). Bicistronic mRNAs containing either the reverse (Rev) complement of the cSHMT

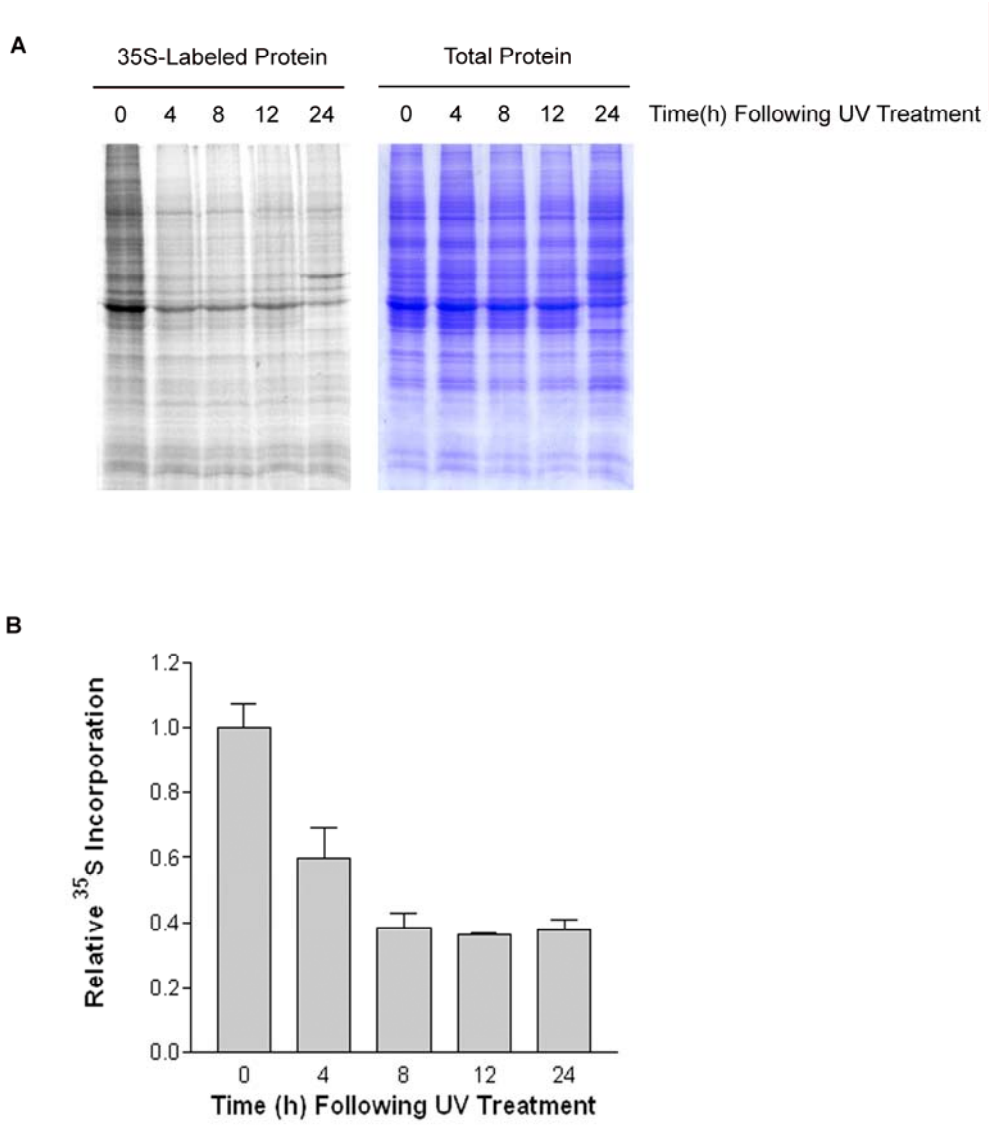

Figure 5.3. Nascent protein synthesis decreases following UV treatment. (A) MCF-7 cells were treated with 10,000 μJ/cm^2 UVC (254 nm). At the indicated times following UV treatment, the cells were pulse-labeled with [^{35}S]Met/Cys, and total cell extracts were resolved by SDS-PAGE. The gel was then stained with Coomassie Blue (*right panel*) to visualize total proteins, followed by autoradiography (*left pane*l) to detect newly synthesized proteins. (B) Equal amounts of protein from (A) were precipitated with TCA, and ^{35}S incorporation was quantified in a scintillation counter. The counts per minute recorded for the 0 h sample was given a value of 1.0. The data represent the average of three independent TCA precipitations ± standard error.

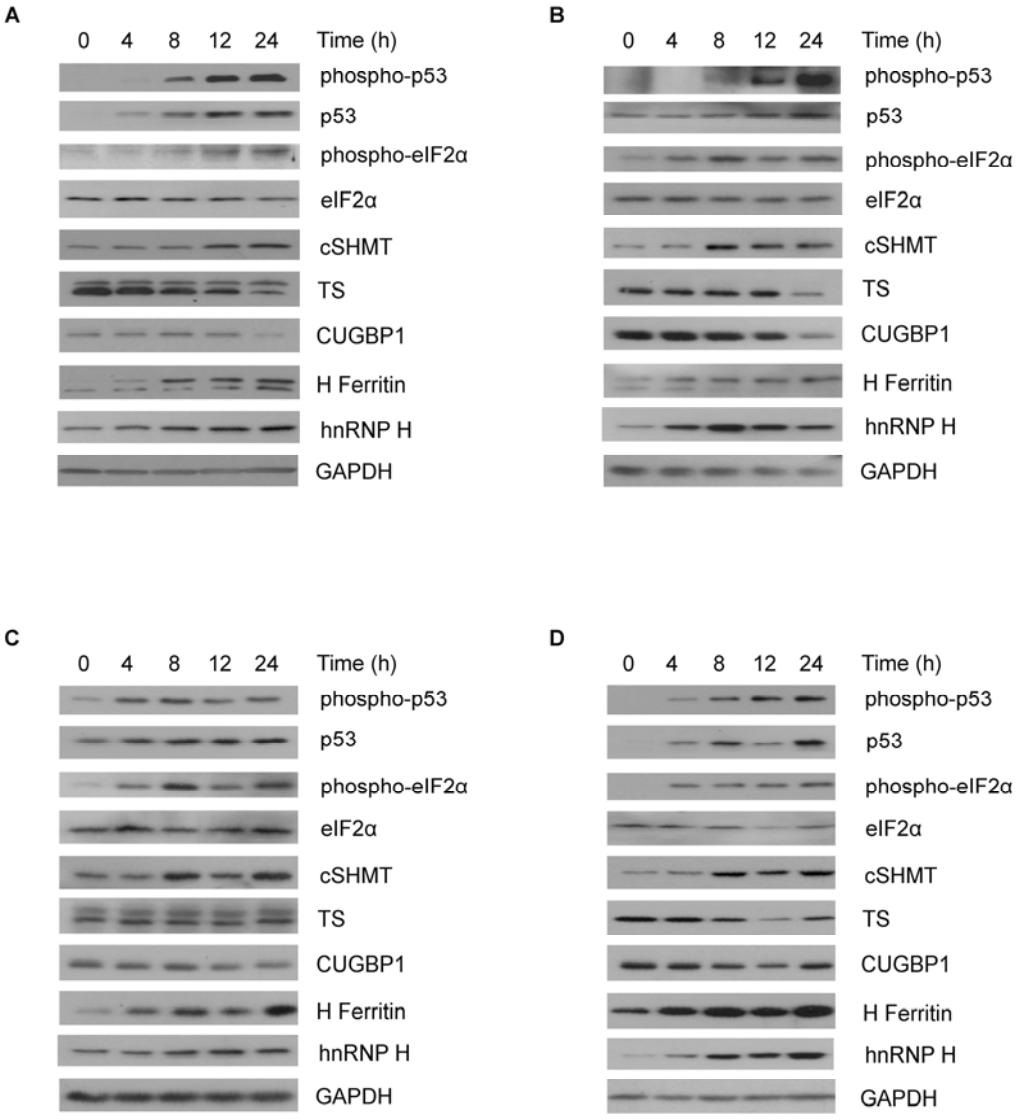

Figure 5.4. Effect of UVC on protein levels. (A) MCF-7 cells, (B) HeLa cells, (C) transformed skin fibroblasts, and (D) SH-SY5Y cells were treated with 10,000 μJ/cm^2 UVC (254 nm). At the indicated times following UV treatment, total protein lysates were prepared and resolved by SDS-PAGE. Protein levels were determined by immunoblotting using antibodies against phosphorylated p53, p53, phosphorylated eIF2α, eIF2α, cSHMT, TS, CUGBP1, H ferritin, and hnRNP H. GAPDH serves as a control for equal protein loading.

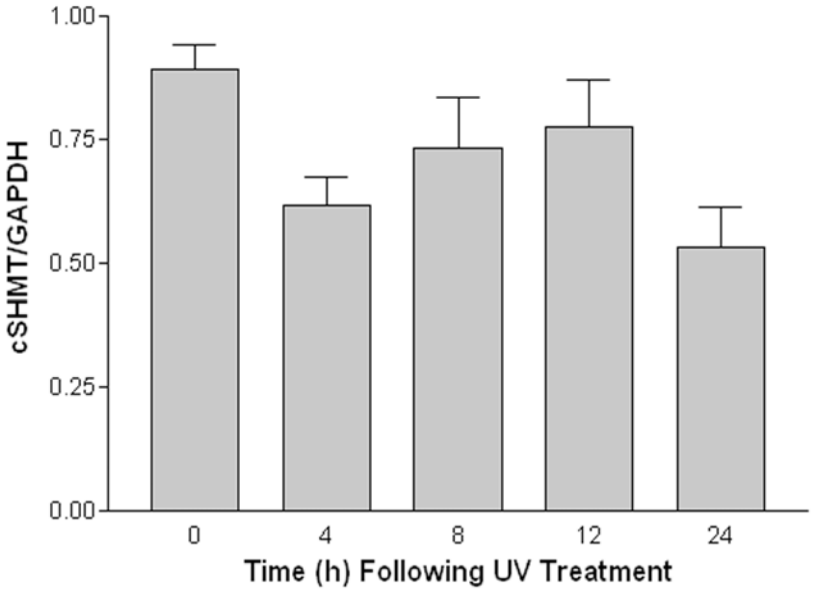

Figure 5.5. UV treatment does not increase cSHMT mRNA levels. MCF-7 cells were treated with 10,000 μJ/cm^2 UVC (254 nm). At the indicated times following UV treatment, total RNA was extracted from the cells and reverse transcribed into cDNA. Relative cSHMT and GAPDH mRNA levels were determined by real time PCR. The data represent the average of three independent experiments $\pm$ standard error.

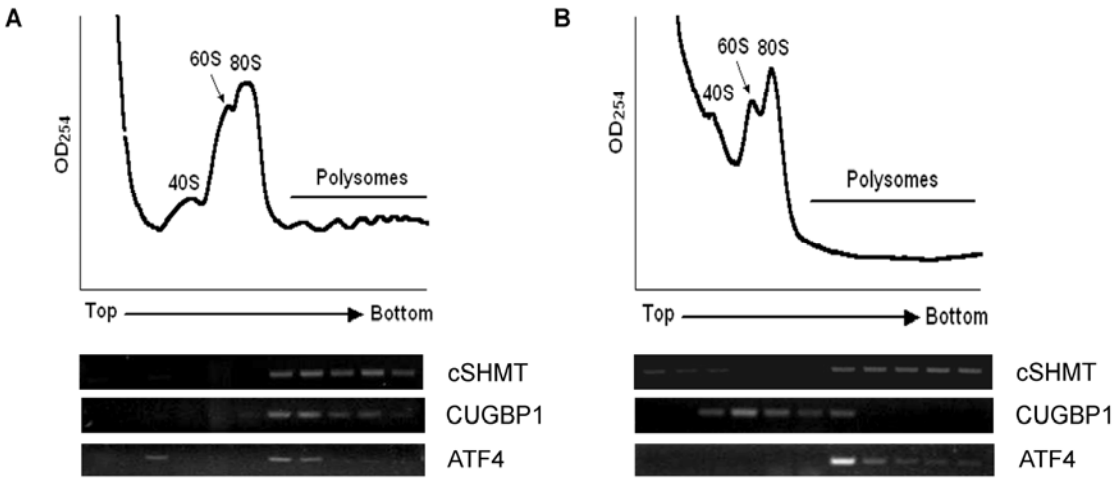

Figure 5.6. cSHMT mRNA remains associated with polysomes following UV exposure. The polysome profile of (A) untreated and (B) UV-irradiated MCF-7 cells was recorded 22 h following UV treatment. The positions of different ribosomal species, as determined by the optical density (OD) at 254 nm, are indicated. Total RNA was extracted from each fraction, and cSHMT mRNA was detected by reverse-transcription PCR. CUGBP1 mRNA, which is not known to contain an IRES, and ATF4 mRNA, which is known to be translated under conditions that induce eIF2α phosphorylation (5,6), are shown for comparison.

Figure 5.7. UV treatment results in an increase in cSHMT IRES activity. (A) The bicistronic construct used to quantify cSHMT IRES activity. It consists of (in the 5' to 3' direction) a cap analog, the Renilla luciferase (Rluc) reporter gene followed by three sequential in-frame stop codons, the human cSHMT 5'UTR which contains the IRES element, the Firefly luciferase (Fluc) reporter gene, the human cSHMT 3'UTR which was shown to stimulate cSHMT IRES activity (1), and a 30 nucleotide poly(A) tail. (B) Untreated (light bars) and UV-treated (dark bars) cells were transiently transfected with the bicistronic construct in (A). 22 h following treatment, Fluc and Rluc activities were quantified. The relative ratio of total Fluc activity divided by total Rluc activity in untreated cells was given a value of 1.0. The data represent the average of three independent experiments $\pm$ standard error. (C) Untreated (light bars) and UV-treated (dark bars) MCF-7 cells were transiently transfected with either the bicistronic construct containing the human cSHMT 5'UTR or bicistronic constructs where the human cSHMT 5'UTR was replaced with either the reverse (Rev) complement of the human cSHMT 5'UTR or the mouse cSHMT 5'UTR. None of the bicistronic constructs used in this experiment contained the cSHMT 3'UTR. IRES activity is reported as the ratio of total Fluc activity divided by total Rluc activity as measured 22 h after UV treatment. The data represent the average of three independent experiments $\pm$ standard error. (D) MCF-7 cells were treated with 10,000 $\mu J/cm^2$ UVC and transiently transfected with the bicistronic mRNA in (A). 22 h following UV treatment, total RNA was extracted from the cells and reverse transcribed into cDNA. Rluc and Fluc mRNA levels were determined by real time PCR. The data represent the average of three independent experiments $\pm$ standard error.

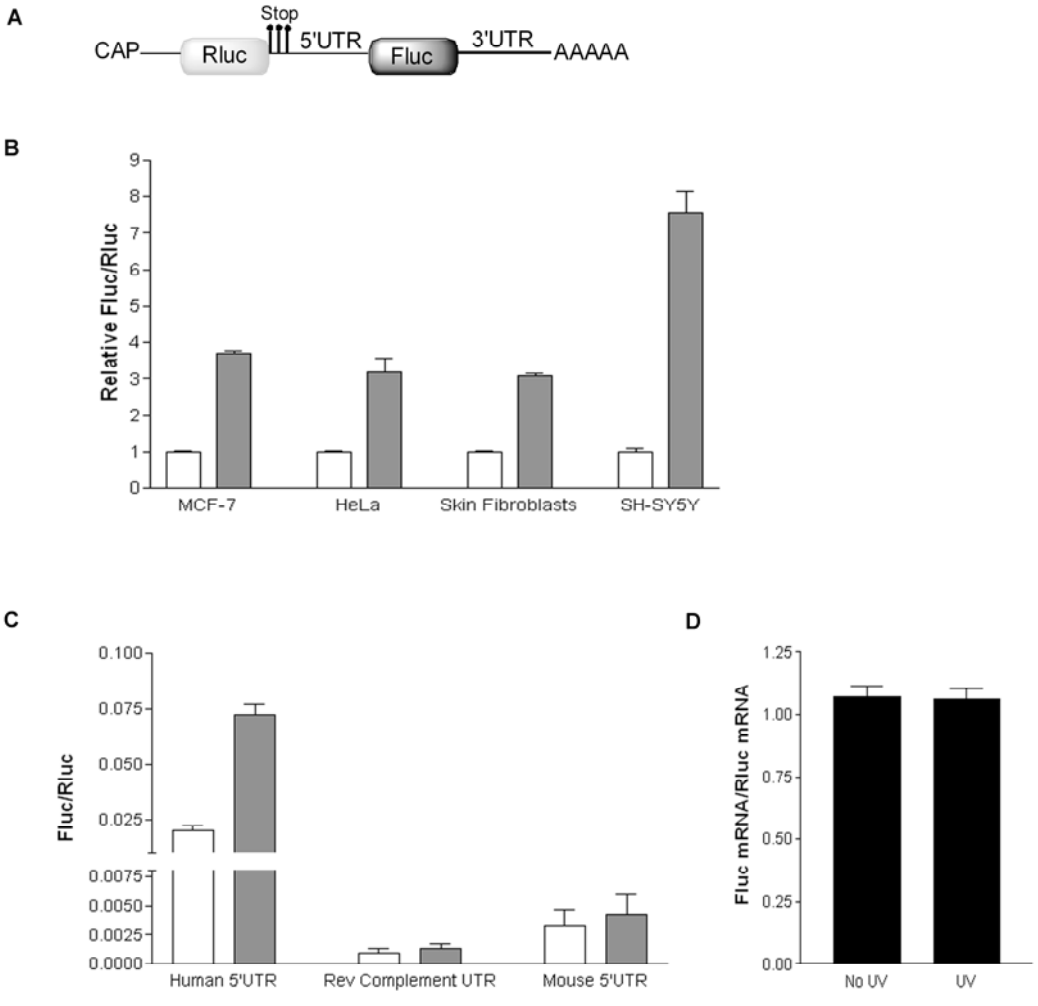
A
Stop
CAP
Rluc
5'UTR
Fluc
3'UTR
AAAAA
B
Relative Fluc/Rluc
9
8
7
6
5
4
3
2
1
0
MCF-7
HeLa
Skin Fibroblasts
SH-SY5Y
C
Fluc/Rluc
0.100
0.075
0.050
0.025
0.0075
0.0050
0.0025
0.0000
Human 5'UTR
Rev Complement UTR
Mouse 5'UTR
D
Fluc mRNA/Rluc mRNA
1.25
1.00
0.75
0.50
0.25
0.00
No UV
UV

5'UTR or the mouse cSHMT 5'UTR, both of which have been shown previously to lack IRES activity (1), were not stimulated by UV exposure (Figure 5.7C). The results from these control bicistronic mRNAs demonstrate that cSHMT IRES activity is associated only with the human 5'UTR, and indicate that ribosomal re-initiation cannot account for the induction of Fluc translation following UV exposure. Real time PCR analysis of Fluc and Rluc RNA levels following the transfections revealed that degradation of the bicistronic construct is likewise not responsible for the induction of Fluc translation upon UV treatment (Figure 5.7D).

The UV-induced increase in cSHMT IRES activity is mediated by H ferritin, hnRNP H2, and CUGBP1. CSHMT IRES activity has previously been shown to be mediated by H ferritin (1) the ITAFs hnRNP H2 (Chapter 3) and CUGBP1 (1). It is known that the regulation of many cellular IRESes during stress conditions depends on a change in concentration and/or subcellular location of ITAFs. For example, during apoptosis, an increase in polypyrimidine tract binding protein levels correlates with the activity of apoptotic IRESes (33); the genotoxic-stress-induced IRES-mediated translation of BAG-1 results from the relocalization of the BAG-1 ITAFs from the nucleus to the cytoplasm (34); and the relocalization of hnRNPA1 from the nucleus to the cytoplasm following osmotic shock inhibits XIAP IRES activity (35). Thus, given the significant role that H ferritin, hnRNP H2, and CUGBP1 play in the stimulation of cSHMT IRES activity, their concentration and/or subcellular localization following UV treatment was investigated.

Several transcription factors are activated by UV-induced DNA damage. Among them is NFκB (36), a known activator of H ferritin expression (37). In agreement with the UV-induced activation of NFκB, western blot analysis of H ferritin protein levels in MCF-7 cells, HeLa cells, transformed skin fibroblasts, and

SH-SY5Y cells revealed a time-dependent increase following UV treatment (Figure 5.4A-D).

Western blot analysis of hnRNP H1/H2 protein levels in all four cell lines also revealed a time-dependent increase following UV treatment (Figure 5.4A-D). The increase in hnRNP H2 protein levels occurred primarily in the cytoplasm (Figure 5.8A). This finding is consistent with the previously reported results of siRNA knockdown experiments, which showed that hnRNP H2 is essential for IRES activation by UV (Chapter 3, Figure 3.6).

In contrast to H ferritin and hnRNP H2, CUGBP1 protein levels decreased following UV exposure in the majority of the cell types tested (Figure 5.4A-D). However, given that CUGBP1 is primarily a nuclear protein under normal cellular conditions (38,39), we hypothesized that CUGBP1 cellular localization changes, thereby enabling increased cSHMT IRES activity following UV treatment. To test this hypothesis, we determined the nuclear versus cytoplasmic distribution of CUGBP1 in MCF-7 cells by western blot analysis (Figure 5.8A) and immunofluorescence (Figure 5.8B) 22h following UV exposure. Both methods showed that CUGBP1 protein levels increase in the cytoplasm and decrease in the nucleus following UV treatment. CUGBP1 was also shown to be essential for IRES activation by UV. Treatment of MCF-7 cells with CUGBP1 siRNA depleted CUGBP1 protein levels by 90% compared to cells treated with negative control siRNA (Figure 5.8C), and reduced cSHMT protein levels (Figure 5.8C) and IRES activity (Figure 5.8D) in UV-treated cells by 50% compared to levels in cells treated with negative control siRNA. CUGBP1 depletion had the greatest impact on UV-activated IRES activity when the cSHMT 3'UTR was present in the bicistronic construct (Figure 5.8D). Previously, we have shown that the cSHMT 3'UTR is required for CUGBP1 activation of the IRES (1). These data indicate that the increase in H ferritin and hnRNP H2 expression,

Figure 5.8. Exposure to UV radiation results in the cytoplasmic accumulation of CUGBP1. (A) Nuclear (NE) and cytoplasmic (CE) extracts were isolated from untreated and UV-treated MCF-7 cells 22 h after UV exposure. Whole cells extracts (WCE) were also obtained from the same samples. All extracts were run side-by-side on an SDS gel and subjected to immunoblotting using an anti-CUGBP1, anti-H ferritin, or anti-hnRNP H antibody. p53 is shown as a control for UV treatment. GAPDH is shown as a control to demonstrate that the nuclear fractions are free of cytoplasmic contamination. Lamin A is shown as a control to demonstrate that the cytoplasmic fractions are free of nuclear contamination. Both GAPDH and Lamin A serve as controls for equal protein loading. (B) Immunofluorescence was used to determine CUGBP1 localization in untreated and UV-treated MCF-7 cells 22 h after UV exposure. CUGBP1 was visualized with Alexa Fluor 488 (green), and the nucleus was visualized with DRAQ5 (red). The right column is a merge of the green and red channels. (C) MCF-7 cells were transfected with negative control siRNA or CUGBP1 siRNA and then treated with UV. 22 h after UV treatment, CUGBP1, cSHMT, H ferritin, and hnRNP H protein levels were visualized by western blotting. GAPDH serves as a control for equal protein loading. (D) The activity of the cSHMT IRES was quantified as the Fluc/Rluc ratio in MCF-7 cells treated with negative control siRNA (light bars) or CUGBP1 siRNA (dark bars). Cells were transfected with biscistronic mRNA containing or lacking the cSHMT 3'UTR in the presence or absence of UVC exposure. For each experimental condition, values obtained from negative control siRNA-treated cells were given a relative value of 1.0. The data represent the average of three independent experiments $\pm$ standard error. The * and ** represent statistical significance ($p= 0.04$ and $p=0.002$, respectively) as determined by Student's t-test.

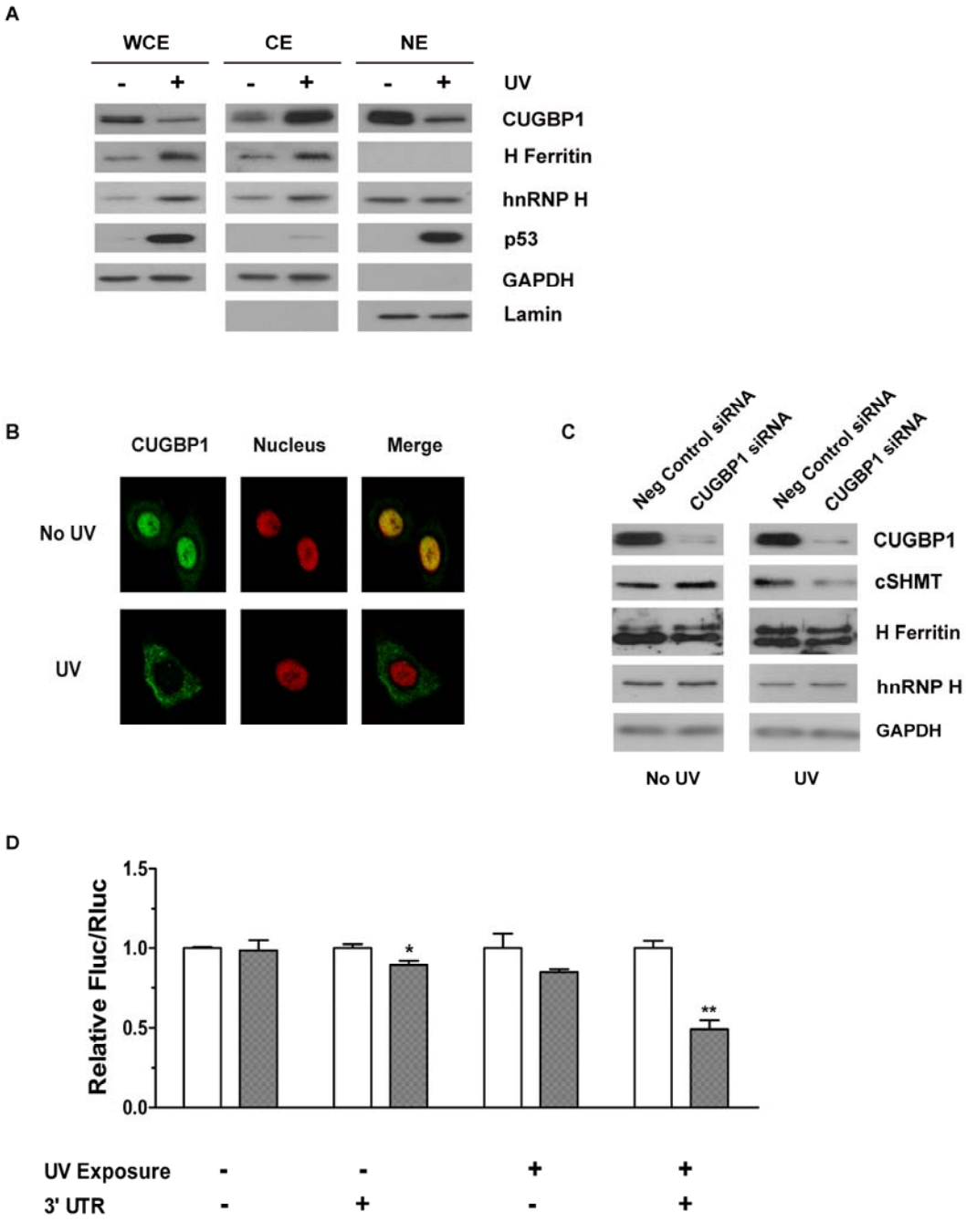
A
WCE
CE
NE
- + - + - +
UV
CUGBP1
H Ferritin
hnRNP H
p53
GAPDH
Lamin
B
CUGBP1
Nucleus
Merge
No UV
UV
C
Neg Control siRNA
CUGBP1 siRNA
Neg Control siRNA
CUGBP1 siRNA
CUGBP1
cSHMT
H Ferritin
hnRNP H
GAPDH
No UV
UV
D
Relative Fluc/Rluc
1.5
1.0
0.5
0.0
*
**
UV Exposure - - + +
3' UTR - + - +

combined with the relocalization of CUGBP1 to the cytoplasm, are responsible for the UV-mediated increase in cSHMT IRES activity.

The increase in cSHMT levels is independent of cell cycle. The increase in cSHMT IRES activity could result directly from UV exposure, or result from UV-induced inhibition of the cell cycle. Indeed, 24 hours following UV exposure, MCF-7 cells exhibited cell cycle arrest in the G2/M phase (compare Figures 5.9A and 5.9B). Many cellular IRESes are known to be activated during G2/M when cap-dependent translation is inhibited (40-42). To determine if the enhanced levels of cSHMT protein resulted directly from UV treatment or resulted from a UV-induced G2/M cell cycle block, MCF-7 cells were treated with nocodazole, and changes in cSHMT IRES activity, protein expression, and protein localization were monitored. Like UV, nocodazole arrests cells in the G2/M phase of the cell cycle; but whereas UV acts by causing DNA damage, nocodazole acts by disrupting microtubules. Following nocodazole treatment, 74% of the cells were arrested in the G2/M phase of the cell cycle (Figure 5.9C) compared to 24% following UV treatment (Figure 5.9B). However, nocodazole treatment did not affect cSHMT IRES activity (Figure 5.10A), or cSHMT, H ferritin, or hnRNP H protein levels (Figure 5.10B). As in the case with UV-treatment, CUGBP1 protein levels decreased in response to nocodazole treatment (Figure 5.10B), but there was no relocalization from the nucleus to the cytoplasm (Figure 5.10C). These results demonstrate that the increase in cSHMT protein levels following UV treatment was not the result of cell-cycle arrest at G2/M and raised the possibility that cSHMT, through its involvement in *de novo* thymidylate biosynthesis, plays a role in the DNA synthesis step of NER.

cSHMT enhances genome stability following UV exposure. To test the hypothesis that cSHMT is involved in the repair of UV-induced DNA damage, we determined the impact of cSHMT depletion (Figure 5.11A) on genome stability

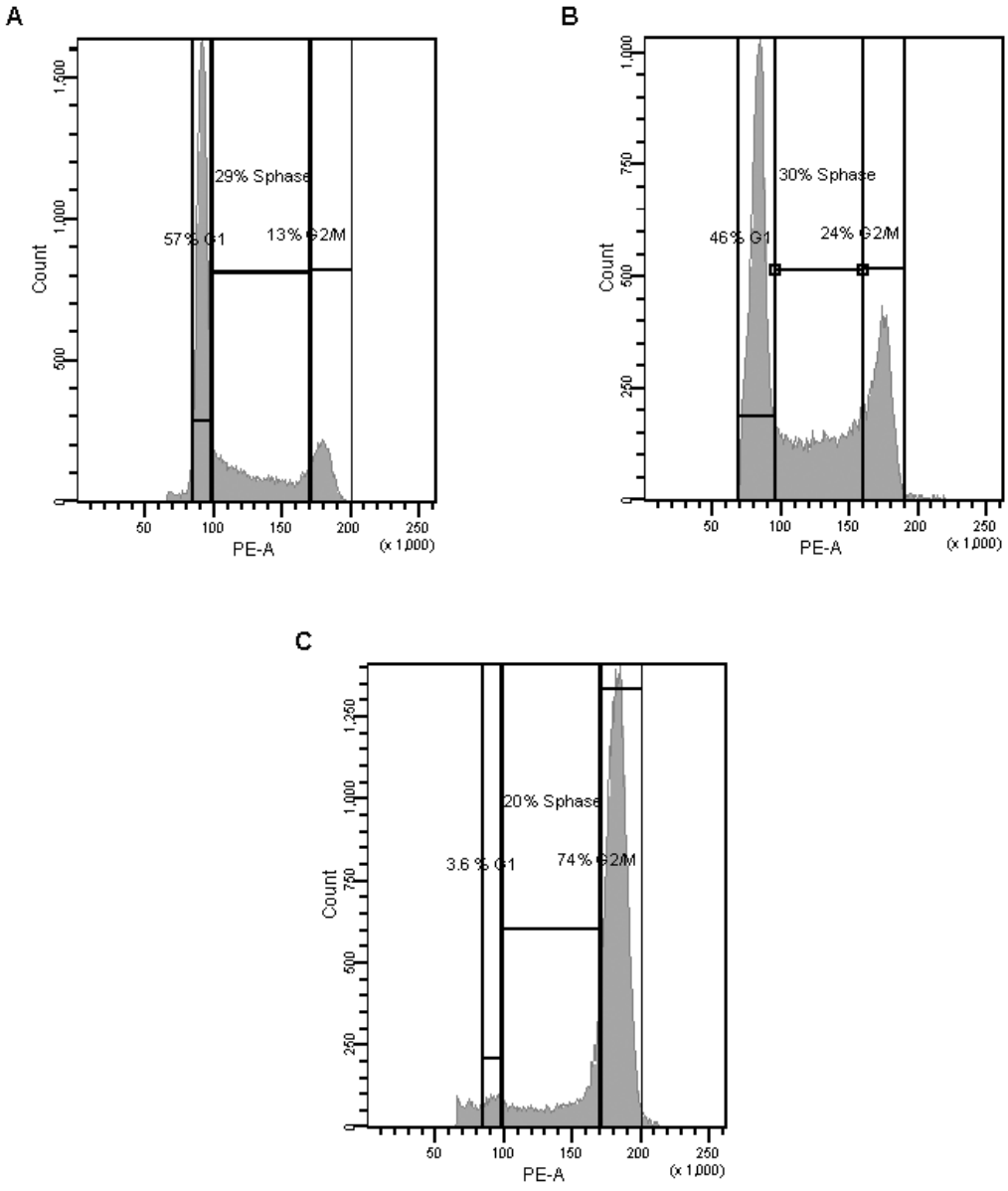

Figure 5.9. Cell cycle profile of UV and nocodazole-treated cells. MCF-7 cells were treated with either 10,000 μJ/cm^2 UVC (254 nm) or 60 ng/mL nocodazole. 24 h following treatment, cell cycle analysis was carried out by fluorescence-activated cell sorting as described in Materials and Methods. (A) Untreated cells. (B) UVC-treated cells. (C) Nocodazole-treated cells.

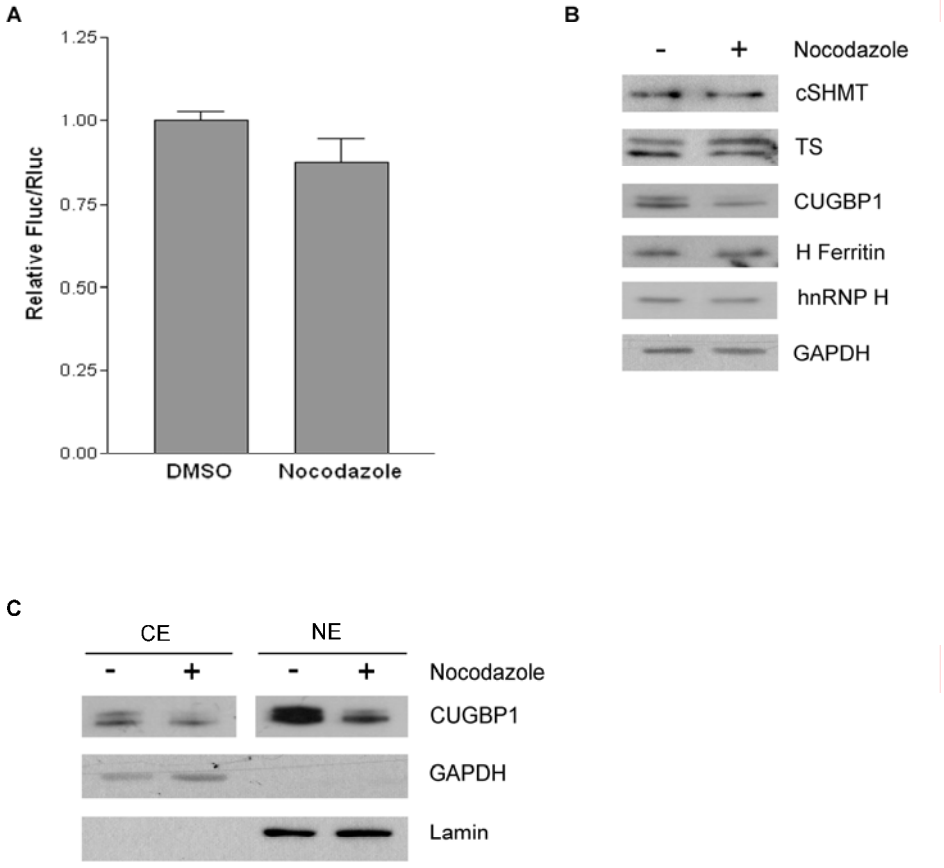

Figure 5.10. Nocodazole treatment does not produce the same effects as UV radiation. (A) MCF-7 cells were treated with either vehicle (DMSO) or 60 ng/mL nocodazole for 24 h and then transiently transfected with the bicistronic mRNA in Figure 5.7A. The ratio of Fluc/Rluc in DMSO-treated cells was given a value of 1.0. The data represent the average of three independent experiments $\pm$ standard error. (B) Total protein lysates were prepared from untreated and nocodazole-treated cells and resolved by SDS-PAGE. Protein levels were determined by immunoblotting using antibodies against cSHMT, TS, CUGBP1, H ferritin, and hnRNP H. GAPDH serves as a control for equal protein loading. (C) Nuclear (NE) and cytoplasmic (CE) fractions were also isolated from these cells and subjected to immunoblotting using an anti-CUGBP1 antibody. GAPDH is shown as a control to demonstrate that the nuclear fractions are free of cytoplasmic contamination. Lamin A is shown as a control to demonstrate that the cytoplasmic fractions are free of nuclear contamination. Both GAPDH and Lamin A serve as controls for equal protein loading.

Figure 5.11. CSHMT is involved in the repair of UV-induced DNA damage. MCF-7 cells were treated with negative control siRNA (light bars) or cSHMT siRNA (dark bars) for 55 h and then exposed to UV radiation (245 nm). At the indicated times following UV treatment, the cells were harvested and divided into two samples. One sample was used for immunoblotting to ensure the knockdown of cSHMT, and the other sample was used in the comet assay to determine DNA damage, or in the MTT assay to determine cell viability. (A) A representative western blot showing cSHMT and TS protein levels in cells treated with either the negative control siRNA or the cSHMT siRNA. GAPDH serves as a control for equal protein loading. (B) For the comet assay, single cells were embedded in agarose, lysed, and subjected to electrophoresis. The DNA content of each cell was visualized using SYBR Gold. The panels are representative images of (from left to right) a cell with little DNA damage, a cell with an intermediate amount of DNA damage, and a cell with extensive DNA damage. (C-F) The DNA content of the cells was quantified using Komet 5.5 Software. The data represent the average of three independent experiments $\pm$ standard error. Each experiment was performed in duplicate, and 75 cells were analyzed per experiment per time point. The * represents statistical significance ($p<0.05$) at a given time point as determined by Student's t-test. (C) % tail DNA=the proportion of DNA that has migrated from the nucleoid core (D) extent tail moment=% tail DNA x tail length/100 (E) olive tail moment =(tail center of gravity – head center of gravity) x % tail DNA/100 (F) tail length=the distance (microns) of DNA migration from the nucleoid core. (G) For the MTT assay, the production of formazan by living mitochondria was measured in negative control siRNA-treated cells (light bars) and cSHMT siRNA-treated cells (dark bars) 24 h following UV treatment by recording the absorbance at 550 nm. The absorbance from non-irradiated, negative control siRNA-treated cells was given a value of 100%. The results represent the average of four independent experiments $\pm$ standard error. The * indicates statistical significance ($p=0.0002$) as determined by Student's t-test.

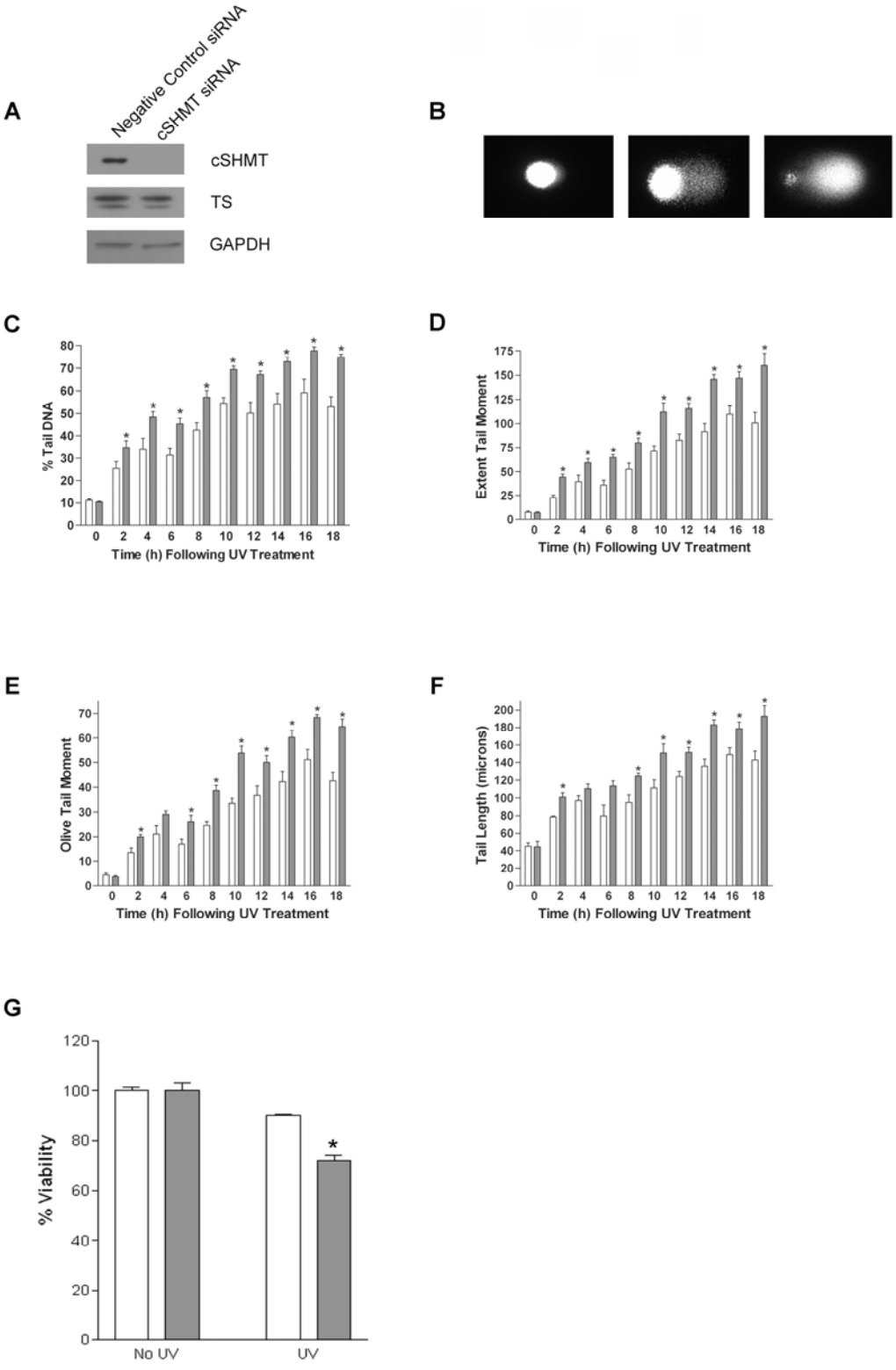
A
Negative Control siRNA
cSHMT siRNA
cSHMT
TS
GAPDH
B
C
% Tail DNA
Time (h) Following UV Treatment
D
Extent Tail Moment
Time (h) Following UV Treatment
E
Olive Tail Moment
Time (h) Following UV Treatment
F
Tail Length (microns)
Time (h) Following UV Treatment
G
% Viability
No UV
UV

following UV treatment using the comet assay. The assay involves the use of electrophoresis to separate intact DNA from damaged DNA, which forms a "comet" (Figure 5.11B). The head of the comet represents intact DNA, and DNA containing strand breaks comprises the comet tail. Four different parameters were calculated for each comet as defined in Materials and Methods: % tail DNA, extent tail moment, olive tail moment, and tail length. All parameters are directly proportional to the number of DNA strand breaks. Prior to UV treatment, cSHMT depletion did not affect any of the comet assay parameters, indicating that cSHMT did not influence DNA integrity prior to UV exposure. Following UV exposure, cSHMT depletion resulted in increased levels of DNA damage compared to the control cells for each comet assay parameter measured (Figure 5.11C-F). The increased amount of DNA damage in the cSHMT depleted cells correlates with the reduced viability of these cells relative to control cells following UV treatment (Figure 5.11G), and supports a role for cSHMT in the repair of UV-induced DNA damage.

cSHMT and TS localize to the nucleus in response to UV treatment. *De novo* thymidylate biosynthesis occurs in both the cytoplasm and the nucleus (Figure 5.1). Nuclear thymidylate biosynthesis is enabled by the SUMO-dependent nuclear import of cSHMT and TS (15,16). An increase in SUMOylation in response to UV treatment has previously been reported for several proteins involved in the cellular stress response including TIP60 (43), XPC (44) and DJ-1 (45). Immunoprecipitation of cSHMT and TS from untreated and UV-treated MCF-7 whole cell extract revealed that the SUMOylation of these proteins is likewise increased in response to UV radiation (Figures 5.12A and 5.12B). These findings are supported by an increase in the amount of cSHMT and TS in the nucleus of UV-treated cells (Figure 5.12C). In the case of TS, increased nuclear concentration occurs despite an overall decrease in protein levels (Figure 5.4A and Figure 5.12C).

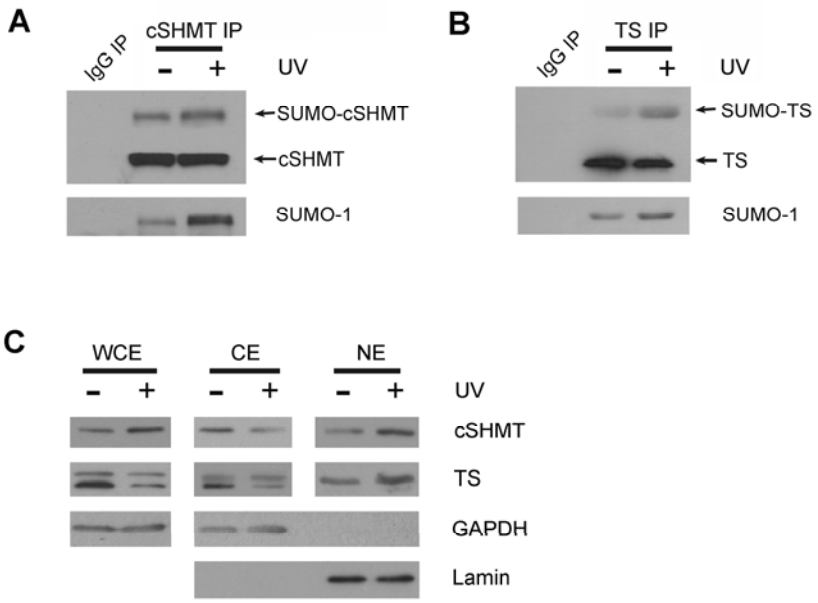

Figure 5.12. CSHMT and TS SUMOylation and nuclear localization increase in response to UV treatment. (A) cSHMT and (B) TS were immunoprecipitated from untreated and UV-treated MCF-7 whole cell extracts 22 h after UV exposure. Immunoblotting was performed on the immunoprecipitates using antibodies against SUMO-1, cSHMT, and TS. The IgG IP (lane 1) serves as control for non-specific binding. (C) Whole cell (WCE), nuclear (NE), and cytoplasmic (CE) fractions were isolated from untreated and UV-treated MCF-7 cells 22 h after UV exposure. All extracts were resolved by SDS-PAGE and subjected to immunoblotting using an anti-cSHMT or anti-TS antibody. GAPDH is shown as a control to demonstrate that the nuclear fractions are free of cytoplasmic contamination. Lamin A is shown as a control to demonstrate that the cytoplasmic fractions are free of nuclear contamination. Both GAPDH and Lamin A serve as controls for equal protein loading.

Discussion

The results from this study demonstrate a role for cSHMT and nuclear folate-dependent thymidylate biosynthesis in the repair of UV-induced DNA damage. Previous studies have demonstrated that cSHMT activity is rate limiting in thymidylate biosynthesis in MCF-7 cells. Overexpression of cSHMT in MCF-7 cells not only favors the partitioning of folate-derived one-carbon units to thymidylate biosynthesis, but also enhances the efficiency of *de novo* thymidylate biosynthesis relative to synthesis through the salvage pathway (14). Unlike the other enzymes involved in folate-mediated one-carbon metabolism, cSHMT expression is not ubiquitous. Although it is expressed primarily in the liver and kidney (46), significant amounts of the cSHMT transcript are present in exposed tissues of the body such as the eyes and skin (UniGene, National Center for Biotechnology Information; Figure 5.4C), which are highly susceptible to UV-induced DNA damage.

The UV-responsive IRES located within the 5'UTR of the cSHMT transcript enables cSHMT to escape the control mechanisms that repress cap-dependent translation during cellular stress and to function in DNA repair. CSHMT is not the only protein whose expression is activated by a UV-responsive IRES. It was recently shown that lethal doses of UVC result in an increase in both the IRES activity and protein levels of the pro-apoptotic factor Apaf-1 (24). However, this is the first report, to our knowledge, of a UV-responsive IRES that regulates the translation of a protein involved in DNA repair. Whereas the mechanism responsible for the UV-induced activation of the Apaf-1 IRES has yet to be determined, we have shown that an increase in the concentration of H ferritin and hnRNP H2 and a change the localization of CUGBP1 enables the UV-induced IRES-mediated translation of cSHMT.

H ferritin has previously been proposed to play an important role in protecting cells from UV-induced DNA damage. By sequestering free iron, it prevents the

conversion of UV-generated reactive oxygen species to even more damaging hydroxyl radicals via the Fenton reaction (47,48). Based on the results of this study, we can now ascribe an additional role to H ferritin in the DNA damage response, as it increases cSHMT expression for NER by stimulating the IRES-mediated translation of cSHMT.

The mechanisms by which hnRNP H2 protein levels increase and CUGBP1 relocalizes to the cytoplasm following UV treatment remain to be determined. Because global protein synthesis decreases upon UV exposure and because hnRNP H2 mRNA is not known to contain an IRES, changes in transcription or protein stability most likely contribute to the accumulation of hnRNP H2. Several studies have shown that changes in the phosphorylation status of a protein can alter its cellular localization (49-52). As it is known that CUGBP1 is phosphorylated *in vivo* (53), it is interesting to speculate that a UV-responsive kinase is responsible for the translocation of CUGBP1 from the nucleus to the cytoplasm.

The involvement of cSHMT in DNA repair is supported by the increase in cSHMT and TS SUMOylation and nuclear compartmentation in response to UV radiation. Nuclear cSHMT and TS form a complex with Proliferating Cell Nuclear Antigen (PCNA), the processivity factor for the NER polymerase (54). Although thymidylate generated in the cytoplasm can freely diffuse into the nucleus, production of this deoxyribonucleotide directly at the site of DNA repair may allow for more rapid DNA synthesis and enhance the fidelity of the repair polymerase by decreasing uracil misincorporation. As uracil misincorporation can ultimately result in DNA strand breaks (7), this would account for the decrease in DNA damage observed in UV-treated control cells compared to those depleted of cSHMT (Figure 5.11C-F).

In mice, such a response to UV-induced DNA damage is not possible as the 5'UTR of the murine cSHMT transcript, which shares only 42% sequence identity

with the human cSHMT 5'UTR, lacks IRES activity (1). The species specificity of the UV-inducible cSHMT IRES suggests that it may have evolved as an adaptive response to protect the skin from UV damage.

REFERENCES

1. Woeller, C. F., Fox, J. T., Perry, C., and Stover, P. J. (2007) *J Biol Chem* **282**(41), 29927-29935
2. Ravanat, J. L., Douki, T., and Cadet, J. (2001) *J Photochem Photobiol B* **63**(1-3), 88-102
3. Tornaletti, S., and Hanawalt, P. C. (1999) *Biochimie* **81**(1-2), 139-146
4. de Laat, W. L., Jaspers, N. G., and Hoeijmakers, J. H. (1999) *Genes Dev* **13**(7), 768-785
5. Deng, J., Harding, H. P., Raught, B., Gingras, A. C., Berlanga, J. J., Scheuner, D., Kaufman, R. J., Ron, D., and Sonenberg, N. (2002) *Curr Biol* **12**(15), 1279-1286
6. Vattem, K. M., and Wek, R. C. (2004) *Proc Natl Acad Sci U S A* **101**(31), 11269-11274
7. Hori, T., Ayusawa, D., Shimizu, K., Koyama, H., and Seno, T. (1984) *Cancer Res* **44**(2), 703-709
8. Scott, J. M., and Weir, D. G. (1981) *Lancet* **2**(8242), 337-340
9. Suh, J. R., Herbig, A. K., and Stover, P. J. (2001) *Annu Rev Nutr* **21**, 255-282
10. Schirch, V., and Strong, W. B. (1989) *Arch Biochem Biophys* **269**(2), 371-380
11. Strong, W. B., Tendler, S. J., Seither, R. L., Goldman, I. D., and Schirch, V. (1990) *J Biol Chem* **265**(21), 12149-12155
12. Reed, M. C., Nijhout, H. F., Neuhouser, M. L., Gregory, J. F., 3rd, Shane, B., James, S. J., Boynton, A., and Ulrich, C. M. (2006) *J Nutr* **136**(10), 2653-2661
13. Green, J. M., MacKenzie, R. E., and Matthews, R. G. (1988) *Biochemistry* **27**(21), 8014-8022

14. Herbig, K., Chiang, E. P., Lee, L. R., Hills, J., Shane, B., and Stover, P. J. (2002) *J Biol Chem* **277**(41), 38381-38389
15. Woeller, C. F., Anderson, D. D., Szebenyi, D. M., and Stover, P. J. (2007) *J Biol Chem* **282**(24), 17623-17631
16. Anderson, D. D., Woeller, C. F., and Stover, P. J. (2007) *Clin Chem Lab Med* **45**(12), 1760-1763
17. Laiho, M., and Latonen, L. (2003) *Ann Med* **35**(6), 391-397
18. Fritz, G., and Kaina, B. (1999) *Mol Cell Biol* **19**(3), 1768-1774
19. Bender, K., Blattner, C., Knebel, A., Iordanov, M., Herrlich, P., and Rahmsdorf, H. J. (1997) *J Photochem Photobiol B* **37**(1-2), 1-17
20. Jiang, H. Y., and Wek, R. C. (2005) *Biochem J* **385**(Pt 2), 371-380
21. Wu, S., Hu, Y., Wang, J. L., Chatterjee, M., Shi, Y., and Kaufman, R. J. (2002) *J Biol Chem* **277**(20), 18077-18083
22. Gebauer, F., and Hentze, M. W. (2004) *Nat Rev Mol Cell Biol* **5**(10), 827-835
23. Mazan-Mamczarz, K., Galban, S., Lopez de Silanes, I., Martindale, J. L., Atasoy, U., Keene, J. D., and Gorospe, M. (2003) *Proc Natl Acad Sci U S A* **100**(14), 8354-8359
24. Ungureanu, N. H., Cloutier, M., Lewis, S. M., de Silva, N., Blais, J. D., Bell, J. C., and Holcik, M. (2006) *J Biol Chem* **281**(22), 15155-15163
25. Holcik, M., Sonenberg, N., and Korneluk, R. G. (2000) *Trends Genet* **16**(10), 469-473
26. Spriggs, K. A., Stoneley, M., Bushell, M., and Willis, A. E. (2008) *Biol Cell* **100**(1), 27-38
27. Bensadoun, A., and Weinstein, D. (1976) *Anal Biochem* **70**(1), 241-250
28. Oppenheim, E. W., Adelman, C., Liu, X., and Stover, P. J. (2001) *J Biol Chem* **276**(23), 19855-19861

29. MacFarlane, A. J., Liu, X., Perry, C. A., Flodby, P., Allen, R. H., Stabler, S. P., and Stover, P. J. (2008) *J Biol Chem* **283**(38), 25846-25853
30. Shieh, S. Y., Ikeda, M., Taya, Y., and Prives, C. (1997) *Cell* **91**(3), 325-334
31. Latonen, L., Taya, Y., and Laiho, M. (2001) *Oncogene* **20**(46), 6784-6793
32. Maltzman, W., and Czyzyk, L. (1984) *Mol Cell Biol* **4**(9), 1689-1694
33. Bushell, M., Stoneley, M., Kong, Y. W., Hamilton, T. L., Spriggs, K. A., Dobbyn, H. C., Qin, X., Sarnow, P., and Willis, A. E. (2006) *Mol Cell* **23**(3), 401-412
34. Dobbyn, H. C., Hill, K., Hamilton, T. L., Spriggs, K. A., Pickering, B. M., Coldwell, M. J., de Moor, C. H., Bushell, M., and Willis, A. E. (2007) *Oncogene*
35. Lewis, S. M., Veyrier, A., Hosszu Ungureanu, N., Bonnal, S., Vagner, S., and Holcik, M. (2007) *Mol Biol Cell* **18**(4), 1302-1311
36. Legrand-Poels, S., Schoonbroodt, S., Matroule, J. Y., and Piette, J. (1998) *J Photochem Photobiol B* **45**(1), 1-8
37. Pham, C. G., Bubici, C., Zazzeroni, F., Papa, S., Jones, J., Alvarez, K., Jayawardena, S., De Smaele, E., Cong, R., Beaumont, C., Torti, F. M., Torti, S. V., and Franzoso, G. (2004) *Cell* **119**(4), 529-542
38. Timchenko, L. T., Miller, J. W., Timchenko, N. A., DeVore, D. R., Datar, K. V., Lin, L., Roberts, R., Caskey, C. T., and Swanson, M. S. (1996) *Nucleic Acids Res* **24**(22), 4407-4414
39. Michalowski, S., Miller, J. W., Urbinati, C. R., Paliouras, M., Swanson, M. S., and Griffith, J. (1999) *Nucleic Acids Res* **27**(17), 3534-3542
40. Cormier, P., Pyronnet, S., Salaun, P., Mulner-Lorillon, O., and Sonenberg, N. (2003) *Prog Cell Cycle Res* **5**, 469-475
41. Pyronnet, S., and Sonenberg, N. (2001) *Curr Opin Genet Dev* **11**(1), 13-18

42. Sachs, A. B. (2000) *Cell* **101**(3), 243-245

43. Cheng, Z., Ke, Y., Ding, X., Wang, F., Wang, H., Ahmed, K., Liu, Z., Xu, Y., Aikhionbare, F., Yan, H., Liu, J., Xue, Y., Powell, M., Liang, S., Reddy, S. E., Hu, R., Huang, H., Jin, C., and Yao, X. (2007) *Oncogene*

44. Wang, Q. E., Zhu, Q., Wani, G., El-Mahdy, M. A., Li, J., and Wani, A. A. (2005) *Nucleic Acids Res* **33**(13), 4023-4034

45. Shinbo, Y., Niki, T., Taira, T., Ooe, H., Takahashi-Niki, K., Maita, C., Seino, C., Iguchi-Ariga, S. M., and Ariga, H. (2006) *Cell Death Differ* **13**(1), 96-108

46. Girgis, S., Nasrallah, I. M., Suh, J. R., Oppenheim, E., Zanetti, K. A., Mastri, M. G., and Stover, P. J. (1998) *Gene* **210**(2), 315-324

47. Balla, G., Jacob, H. S., Balla, J., Rosenberg, M., Nath, K., Apple, F., Eaton, J. W., and Vercellotti, G. M. (1992) *J Biol Chem* **267**(25), 18148-18153

48. Stohs, S. J., and Bagchi, D. (1995) *Free Radic Biol Med* **18**(2), 321-336

49. Habelhah, H., Shah, K., Huang, L., Ostareck-Lederer, A., Burlingame, A. L., Shokat, K. M., Hentze, M. W., and Ronai, Z. (2001) *Nat Cell Biol* **3**(3), 325-330

50. Xie, J., Lee, J. A., Kress, T. L., Mowry, K. L., and Black, D. L. (2003) *Proc Natl Acad Sci U S A* **100**(15), 8776-8781

51. Zhou, B. P., Liao, Y., Xia, W., Spohn, B., Lee, M. H., and Hung, M. C. (2001) *Nat Cell Biol* **3**(3), 245-252

52. van der Houven van Oordt, W., Diaz-Meco, M. T., Lozano, J., Krainer, A. R., Moscat, J., and Caceres, J. F. (2000) *J Cell Biol* **149**(2), 307-316

53. Timchenko, N. A., Wang, G. L., and Timchenko, L. T. (2005) *J Biol Chem* **280**(21), 20549-20557

54. Anderson, D. D., and Stover, P. J. (Unpublished Results)

CHAPTER 6

CONCLUSIONS AND FUTURE DIRECTIONS

Part I: Abstract

Cytoplasmic serine hydroxymethyltransferase (cSHMT) is a key regulator of folate-mediated one-carbon metabolism. By preferentially directing one-carbon units toward the synthesis of thymidylate and inhibiting methionine synthesis, cSHMT decreases uracil content in DNA and impairs cellular methylation reactions. The 5' untranslated region (UTR) of the cSHMT transcript contains an internal ribosome entry site (IRES) that regulates cSHMT expression. Although it had previously been shown that the cSHMT 3'UTR and the proteins CUG-binding protein 1 (CUGBP1) and heavy chain ferritin (H ferritin) influence the IRES-mediated translation of cSHMT, the mechanism by which they act and the biological function of the cSHMT IRES had not yet been determined. The studies conducted in Chapters 3-5 were designed to 1) elucidate the interactions among the 5'UTR, 3'UTR, poly(A) tail, 40S ribosomal subunit, and CUGBP1 that contribute to cSHMT IRES activity, 2) investigate the role of H ferritin in cSHMT IRES-mediated translation, and 3) determine physiological significance of the cSHMT IRES. The following chapter provides a comprehensive summary of the data generated from these studies and proposes a model for the UV-induced IRES-mediated translation of cSHMT that is consistent with the experimental results. It also discusses the knowledge gaps that still remain in our understanding of the mechanism and physiological function of cSHMT IRES activity and suggests experiments that can be conducted to address them.

Part II: Summary of Results

CUGBP1 and hnRNP H2 are cSHMT ITAFs

The data presented here expand upon the previously reported finding that CUGBP1 stimulates IRES activity when the 3'UTR of cSHMT is present in the transcript (1) by investigating the interaction between CUGBP1 and the cSHMT mRNA. CUGBP1 is shown to bind directly to the 3'UTR of cSHMT both *in vitro* and in UV-treated cells. Evidence generated through the use of 3'UTR truncation mutants indicates that this binding occurs between nucleotides 157 and 200. CUGBP1 is also shown to interact with the cSHMT 5'UTR both *in vitro* and in UV-treated cells, although in this case, the interaction occurs via an auxiliary factor rather then direct mRNA binding. The results of the binding studies, combined with those from the functional experiments (1), enable CUGBP1 to be classified as a novel IRES *trans*-acting factor (ITAF).

The experiments in this report also identify and characterize a second novel ITAF, heterogeneous nuclear ribonucleoprotein H2 (hnRNP H2). hnRNP H2 interacts with CUGBP1 in an RNA-independent manner. It binds directly to the 5'UTR of cSHMT both *in vitro* and in UV-treated cells, and interacts with the 3'UTR of cSHMT in the presence of CUGBP1. Evidence generated through the use of truncation mutants indicates that the binding of hnRNP H2 to the 5'UTR occurs between nucleotides 105 and 114. Like CUGBP1, hnRNP H2 stimulates the IRES-mediated translation of cSHMT only when the 3'UTR is included in the transcript.

CUGBP1 and hnRNP H2 Functionally Replace the Poly(A) Tail of the Transcript

Translation, both cap-dependent and IRES-mediated, is thought to occur by a "closed loop" mechanism whereby interactions between eIF4G, poly(A)-binding

protein (PABP), and the poly(A) tail result in circularization of the transcript (reviewed in (2)). However, the studies presented here provide compelling evidence that both the poly(A) tail and PABP are dispensable for cSHMT IRES-mediated translation when the cSHMT 3'UTR, CUGBP1, and hnRNP H2 are present. In the absence of any one of these factors, PABP-depletion or the removal of the poly(A) tail of the mRNA results in an approximately 50% decrease in the IRES-mediated translation of cSHMT.

cSHMT IRES-Mediated Translation Proceeds by a "Land and Scan" Mechanism

While the mechanism of the IRES-mediated translation of cSHMT is unique in that it does not require either PABP or the poly(A) tail for maximal activity, the recruitment of the 40S ribosomal subunit to the initiation codon proceeds in a more conventional manner. Consistent with a "land and scan" mechanism whereby the 40S ribosomal subunit binds upstream of the initiation codon and then migrates in a 5'-3' direction until AUG recognition occurs, the data presented here show that ribosome scanning begins between nucleotides 103 and 118 of the cSHMT 5'UTR and requires the helicase eIF4A.

H Ferritin is Not a cSHMT ITAF, but it Regulates IRES Activity

It had previously been suggested that there is another cSHMT ITAF in addition to CUGBP1 and hnRNP H2– heavy chain ferritin (H ferritin) (1). However, the results from these studies do not support this hypothesis. H ferritin does not bind to either of the cSHMT UTRs *in vitro* and cannot be detected in polysomal fractions. Although H ferritin does not function as an ITAF, it does stimulate the IRES mediated translation of cSHMT in an indirect manner. The indirect effect of H ferritin on IRES activity does not involve the poly r(C) binding protein, changes in the labile iron pool,

or changes in CUGBP1 or hnRNP H2 protein levels or nuclear localization. Rather, H ferritin interacts with both CUGBP1 (1) and hnRNP H2 (18) and may function in the assembly of the initiation complex.

Tbe cSHMT IRES and the Factors that Influence its Activity are UV-Responsive

Cellular IRESes allow for the continued expression of a protein during certain physiological or stress conditions that inhibit cap-dependent translation (3). The data presented here indicate that for cSHMT, one of these conditions is exposure to UV radiation. UV radiation is shown to increase cSHMT protein levels despite a significant reduction in global protein synthesis. Although this increase could potentially be due in part to enhanced protein stability, the finding that cSHMT mRNA remains associated with polysomes following UV treatment argues that translation also plays a role. In agreement with this, cSHMT IRES activity is shown to increase approximately four-fold upon UV exposure.

cSHMT is not the only protein whose expression is elevated following treatment with UV radiation. H ferritin protein levels also increase as do the cytoplasmic concentrations of the ITAFs hnRNP H2 and CUGBP1, both of which are primarily located in the nucleus under normal cellular conditions. In the case of CUGBP1, the increase in the cytoplasmic levels of the protein is concurrent with a large reduction in the amount of CUGBP1 in the nucleus, resulting in an overall decrease in protein abundance.

UV Increases the SUMOylation and Nuclear Localization of cSHMT and TS

cSHMT is post-translationally modified by the small ubiquitin-like modifier (SUMO) (4). The SUMOylation of cSHMT results in its import into the nucleus (4) where it forms a complex with SUMOylated thymidylate synthase (TS) and

proliferating cell nuclear antigen (PCNA) at the site of DNA replication or repair (5). The experiments conducted in this report show that cSHMT and TS SUMOylation are enhanced following UV exposure, and that there is an increase in the amount of both proteins in the nucleus of UV-treated cells.

cSHMT Reduces the Levels of UV-Induced DNA Damage

Thymidine nucleotides are required for faithful DNA repair. Because cSHMT had previously been shown to regulate *de novo* thymidylate synthesis (6,7), and because the data presented here show that cSHMT expression is UV-responsive, experiments were conducted to determine the contribution of cSHMT to the repair of UV-induced DNA damage. The results show that upon the siRNA-mediated knockdown of cSHMT there is an increase in the number of UV-induced DNA strand breaks and a parallel decrease in cell viability.

Part III: Model for the UV-Induced IRES-Mediated Translation of cSHMT

Collectively, the results of the studies presented here allow for the formulation of a model for the UV-induced IRES-mediated translation of cSHMT (Figure 6.1). Under normal cellular conditions, cSHMT translation proceeds primarily by the canonical cap-dependent ribosome scanning mechanism. This is due to the fact that CUGBP1 resides almost exclusively in the nucleus and that there is little hnRNP H2 present in the cytoplasm. Following UV exposure, which damages DNA and globally inhibits cap-dependent translation, the concentrations of H ferritin and hnRNP H2 increase, and CUGBP1 relocalizes to the cytoplasm. hnRNP H2 binds directly to the 5'UTR of the cSHMT transcript, and, with the aid of H ferritin, interacts with CUGBP1, which binds directly to the 3'UTR of the transcript. The interaction between the two cSHMT ITAFs results in the formation of a closed loop and thereby

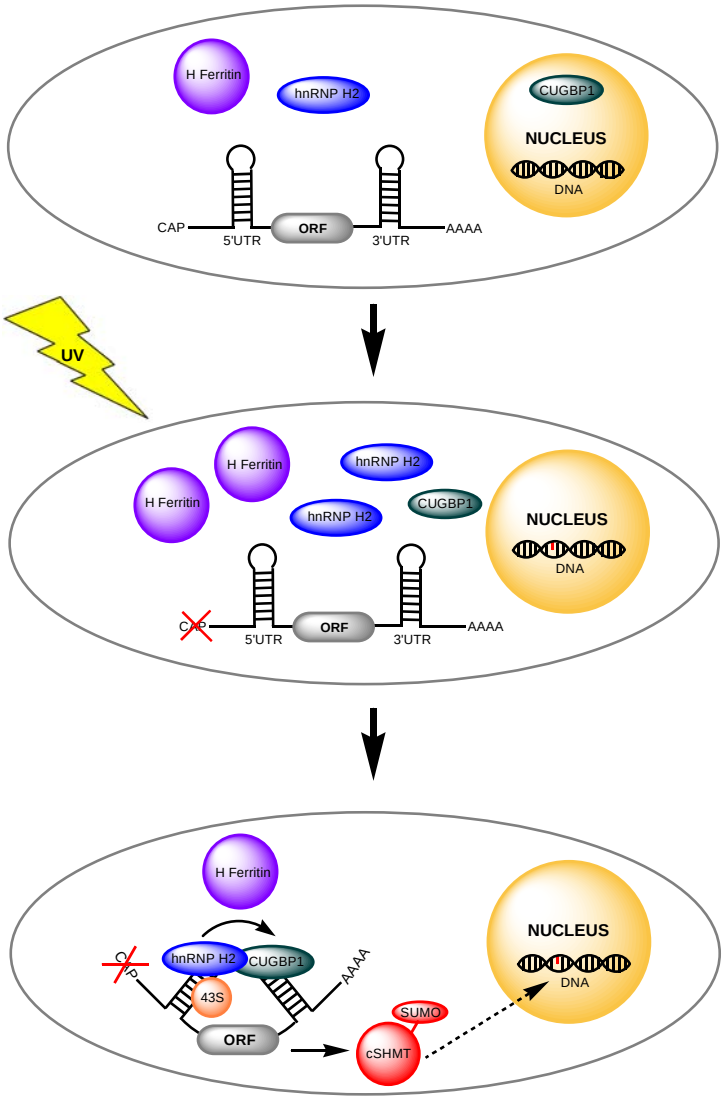

Figure 6.1. Model for the IRES-mediated translation of cSHMT following exposure to UV radiation. Exposure to UV radiation results in the formation of DNA lesions, the inhibition of cap-dependent protein synthesis, the cytoplasmic accumulation of hnRNP H2 and H ferritin, and the relocalization of CUGBP1 from the nucleus to the cytoplasm. hnRNP H2 binds to the 5'UTR of cSHMT and CUGBP1 binds to the 3'UTR of cSHMT. The interaction of hnRNP H2 with CUGBP1, which may be mediated by H ferritin, circularizes the cSHMT transcript and in doing so enhances the rate of IRES-mediated translation. The protein produced from the IRES activity of cSHMT is imported into the nucleus in a SUMO-dependent manner where it functions to provide the thymidine nucleotides necessary for the repair of UV-induced DNA damage.

eliminates the need for the eIF4G-PABP-poly(A) tail interaction. The 40S ribosomal subunit is then recruited to the 5'UTR of cSHMT. It binds between nucleotides 103 and 118, and then scans through the remainder of the 5'UTR until the initiation codon is reached. The 60S ribosomal subunit then joins the 40S subunit, and the ribosome translates the cSHMT open reading frame. Once the cSHMT protein is synthesized, it becomes SUMOylated, as does TS, and both proteins translocate into the nucleus. In the nucleus, cSHMT and TS interact with PCNA, the processivity factor for the nucleotide excision repair (NER) polymerase (5). This allows for thymidylate production directly at the site of DNA repair.

Part III: Future Directions

Verifying the Model

Although the above is an attractive model for the UV-induced IRES-mediated translation of cSHMT, there are a few details that still need to be verified. The first is that the interactions among hnRNP H2, CUGBP1, and the cSHMT UTRs do indeed form a closed loop. Reconstitution experiments can be carried out using recombinant hnRNP H2 and CUGBP1 and *in vitro* transcribed cSHMT mRNA, and the resulting complex can be visualized by atomic force microscopy. Such a procedure has been used previously to demonstrate the circularization of mRNA by eIF4E, eIF4G, and PABP (8).

The second hypothesis that needs to be addressed is that H ferritin facilitates the interaction between hnRNP H2 and CUGBP1. This can be tested by fluorescence resonance energy transfer (FRET). WT cells, H ferritin-overexpressing cells, and H ferritin knockdown cells can be co-transfected with CFP-tagged hnRNP H2 and YFP-tagged CUGBP1. Upon CFP excitation, YFP emission will be detected if the two

proteins interact. The amount of YFP emission can then be quantified. If H ferritin does indeed assist in bringing the two cSHMT ITAFs together, the H ferritin overexpressing cells will produce the greatest FRET signal while the H ferritin knockdown cells will produce the least.

Mechanism of CUGBP1 Relocalization and hnRNP H2 Upregulation Following UV Exposure

As discussed in Chapter 5, the mechanisms by which hnRNP H2 protein levels increase and CUGBP1 relocalizes to the cytoplasm following UV treatment remain to be determined. However, it is hypothesized that changes in transcription or protein stability contribute to the accumulation of hnRNP H2, and that changes in phosphorylation status alter the cellular location of CUGBP1. Protein stability and hnRNP H2 mRNA levels can be ascertained by carrying out pulse-chase and real-time PCR experiments, respectively. Insight into the contribution of phosphorylation status to CUGBP1 relocalization can be gained by immunoprecipitating CUGBP1 from the nuclear and cytoplasmic fractions of untreated and UV-treated cells and conducting an immunoblot analysis using antibodies specific for phosphorylated serine, threonine, and tyrosine residues. If it is found that transcriptional upregulation and kinase activation do indeed play a role, candidate transcription factors and kinases can then either be over-expressed in untreated cells or knocked down in UV-treated cells to determine which are responsible for the increase in hnRNP H2 protein levels and CUGBP1 relocalization.

Canonical Initiation Factor Requirements and Recruitment

The canonical initiation factors necessary for IRES-mediated translation vary from transcript to transcript. The IRES-mediated translation of the

encephalomyocarditis virus requires all of the canonical initiation factors except eIF4E (9,10); the IRES-mediated translation of L-myc involves the entire eIF4F complex (composed of eIF4E, eIF4A, and eIF4G) as well as eIF3 and the ternary complex (composed of eIF2, GTP, and the initiator Met-tRNA) (11); and the IRES-mediated translation of the hepatitis C and cricket paralysis viruses is eIF-independent (12-14). Although it has been demonstrated that the IRES-mediated translation of cSHMT can function in the absence of eIF4E binding (1) but not upon the inhibition of eIF4A, it is not known if eIF4G, eIF3, and eIF2 are necessary for the cap-independent translation of this transcript. The requirement for eIF4G can be tested by reducing eIF4G protein levels using an RNAi approach. Cells in which eIF4G has been knocked down can then be transfected with RNAi-resistant eIF4G which harbors a mutation in its eIF3-binding site to determine the need for eIF3. A dominant negative mutant of eIF2α and/or salubrinal, a selective inhibitor of complexes that dephosphorylate eIF2α, can be used to probe the involvement of the ternary complex. Since the cSHMT IRES has been shown to be active under conditions where eIF2α is phosphorylated, it is hypothesized that neither the dominant negative mutant nor salubrinal will have an effect on IRES-mediated translation.

Once it is revealed what canonical initiation factors play a role in the IRES-mediated translation of cSHMT, the next step will be to determine how these factors are recruited to the 5'UTR. As discussed in Chapter 3, the finding that the ribosome scanning start site (between nucleotides 103 and 118) overlaps with the hnRNP H2 binding site (between nucleotides 105 and 114) suggests that the hnRNP H2-CUGBP1 complex may serve as a guide to recruit the initiation complex. It could do so either by interacting with one or more of the canonical initiation factors or by acting as a chaperone to expose the RNA structure to ribosome binding. To test the hypothesis that the hnRNP H2-CUGBP1 complex is recruiting the ribosome to the cSHMT

5'UTR, the hnRNP H2 binding site can be shifted from nucleotides 105-114 to a position near one of the upstream engineered AUGs in Figure 3.8C (for example between nucleotides 55 and 64). The experiment used to locate the "landing" spot of the ribosome within the cSHMT 5'UTR (Chapter 3) can then be repeated to determine if moving the hnRNP H2 binding site also shifts the point of ribosome entry.

The Physiological Significance of Small Changes in cSHMT Protein Levels

One criticism of the data presented here has been that none of the results show large changes in cSHMT expression and thus may have little physiological impact. For example, when H ferritin (1), CUGBP1, or hnRNP H2 protein levels are reduced by 50%, 90%, and 80%, respectively, cSHMT protein levels and IRES activity only decrease by approximately 30%, 50%, and 33%, respectively. Although this may be partially due to the fact that all three factors were never knocked down concurrently, UV-treated cells, which have increased concentrations of H ferritin, CUGBP1, and hnRNP H2 in the cytoplasm, exhibit, on average, only a four-fold increase in cSHMT protein levels.

In rebuttal to this criticism, recent studies have shown that small changes in the expression of cSHMT can have significant physiological consequences. *SHMT1* $^{+/-}$ embryos from dams fed a folate- and choline-deficient diet exhibit exencephaly, a fatal neural tube defect (NTD) characterized by the absence of the cranial bones and protrusion of the brain. When combined with the *splotch* mutation, which is known to cause the NTD spina bifida, the disruption of a single *SHMT1* allele significantly exacerbates NTD frequency and severity (15). The livers of *SHMT1* $^{+/-}$ mice also show increased levels of uracil misincorporation into their DNA (16). Although this alone does not produce a phenotype, the disruption of a single *SHMT1* allele significantly increases the occurrence of intestinal and colorectal tumors when

combined with either a mutation in the *APC* gene or exposure to the carcinogen azoxymethane (17). Additional experiments are currently underway to determine the physiological impact of small changes in cSHMT expression in response to UV radiation. Hairless WT and *SHMT1*$^{+/-}$ mice will be exposed to UV and monitored for tumor formation. It is hypothesized that the *SHMT1*$^{+/-}$ mice will exhibit increased cancer incidence compared to their irradiated WT counterparts.

The Physiological Significance of Small Changes in cSHMT Nuclear Localization

In addition to the reported changes in cSHMT protein levels, concerns have also been raised about the impact of the small (approximately 2-fold) increase in the SUMOylation and nuclear localization of cSHMT that was observed following UV treatment. To address these concerns, work is currently underway to produce a mouse which harbors K38R and K39R mutations in the cSHMT enzyme. These mutations have previously been shown to inhibit cSHMT SUMOylation and decrease the nuclear localization of the protein *in vitro* and in cell culture models (4,5). Hairless WT and *SHMT1*$^{+/K38R, K39R}$ mice can then be exposed to UV radiation and monitored for the development of skin cancer.

The Physiological Significance of Small Changes in cSHMT IRES Activity

Although transgenic mice are useful in determining the physiological relevance of small changes in cSHMT protein levels and nuclear localization in response to UV-induced DNA damage, they cannot directly address the biological significance of changes in IRES-mediated translation because murine cSHMT lacks IRES activity (1). In the human population, there are two single nucleotide polymorphisms (SNPs), one at nucleotide 47 (rs3783) and one at nucleotide 412 (rs9902011), that exist in linkage disequilibrium within the 3'UTR of cSHMT. cSHMT transcripts that contain a C at

nucleotide 46 and a G at nucleotide 412 exhibit a 60% reduction in UV-induced IRES-mediated translation compared to transcripts that contain a G at nucleotide 47 and an A at nucleotide 412 (18). Although the mechanism by which these SNPs affect IRES activity is not known, the SNPs can be exploited to investigate the contribution of cSHMT cap-independent translation to protection against skin cancer. A case-control study can be conducted using healthy individuals and those that have been diagnosed with skin cancer. The 3'UTRs of all participants in the study can be genotyped and the odds ratio calculated to assess the correlation between the SNPs and UV-induced malignancies.

REFERENCES

1. Woeller, C. F., Fox, J. T., Perry, C., and Stover, P. J. (2007) *J Biol Chem* **282**, 29927-29935
2. Jacobson, A. (1996) in *Translational Control* (J.W.B. Hershey, M. B. M., and N. Sonenberg, ed), pp. 451-480, Cold Spring Harbor Laboratory Press, Cold Spring Harbor, NY
3. Spriggs, K. A., Stoneley, M., Bushell, M., and Willis, A. E. (2008) *Biol Cell* **100**, 27-38
4. Woeller, C. F., Anderson, D. D., Szebenyi, D. M., and Stover, P. J. (2007) *J Biol Chem* **282**, 17623-17631
5. Anderson, D. D., and Stover, P. J. (Unpublished Results)
6. Herbig, K., Chiang, E. P., Lee, L. R., Hills, J., Shane, B., and Stover, P. J. (2002) *J Biol Chem* **277**, 38381-38389
7. Oppenheim, E. W., Adelman, C., Liu, X., and Stover, P. J. (2001) *J Biol Chem* **276**, 19855-19861
8. Wells, S. E., Hillner, P. E., Vale, R. D., and Sachs, A. B. (1998) *Mol Cell* **2**, 135-140
9. Pestova, T. V., Hellen, C. U., and Shatsky, I. N. (1996) *Mol Cell Biol* **16**, 6859-6869
10. Pestova, T. V., Shatsky, I. N., and Hellen, C. U. (1996) *Mol Cell Biol* **16**, 6870-6878
11. Spriggs, K. A., Cobbold, L. C., Jopling, C. L., Cooper, R. E., Wilson, L. A., Stoneley, M., Coldwell, M. J., Poncet, D., Shen, Y. C., Morley, S. J., Bushell, M., and Willis, A. E. (2009) *Mol Cell Biol* **29**, 1565-1574

12. Ji, H., Fraser, C. S., Yu, Y., Leary, J., and Doudna, J. A. (2004) *Proc Natl Acad Sci U S A* **101**, 16990-16995

13. Otto, G. A., and Puglisi, J. D. (2004) *Cell* **119**, 369-380

14. Pestova, T. V., Shatsky, I. N., Fletcher, S. P., Jackson, R. J., and Hellen, C. U. (1998) *Genes Dev* **12**, 67-83

15. Beaudin, A. E., Noden, D. M., Perry, C. A., Chu, S., Stabler, S. A., Allen, R. H., and Stover, P. J. (2009) *Submitted*

16. MacFarlane, A. J., Liu, X., Perry, C. A., Flodby, P., Allen, R. H., Stabler, S. P., and Stover, P. J. (2008) *J Biol Chem* **283**, 25846-25853

17. MacFarlane, A. J., and Stover, P. J. (Unpublished Results)

18. Fox, J. T., and Stover, P. J. (Unpublished Results)